Institute of Clinical Pharmacology and Toxicology
Pharmacology for Pharmacists
University Medical Center Hamburg-Eppendorf

The role of the transcriptional coactivator CRTC1 in the development of cardiac hypertrophy in mice

Dissertation
Submitted to the Department of Chemistry
Faculty of Mathematics, Informatics, and Natural Sciences
University of Hamburg
for the degree of
Doctor of Natural Sciences

by
Karoline Morhenn

Hamburg 2016

August 2013 - December 2016

Date of the oral defense: March, 24th 2017

Date of approval for publication: March, 31st 2017

1. Referee: Prof. Dr. med. Elke Oetjen

2. Referee: Prof. Dr. rer. nat. Viacheslav Nikolaev

Der Beginn aller Wissenschaft ist das Erstaunen,
dass die Dinge sind, wie sie sind.

Aristoteles

Table of contents

List of figures

List of tables

List of abbreviations

A	Angiotensin II
A_{600}	Absorption at 600 nm
aa	Amino acids
ABC	Ammonium bicarbonate
AC	Adenylyl cyclase
ACE	Angiotensin converting enzyme
Acta1	α-skeletal actin
AKAP	A-kinase anchoring proteins
AMVM	Adult mouse ventricular myocytes
ANOVA	Analysis of variances
ANP	Atrial natriuretic peptide
AP-1	Activator protein-1
APS	Ammonium persulfate
Ara-C	Cytosine β-D-arabinofuranoside
ATF1	Activating transcription factor
ATP	Adenosine triphosphate
AU	Arbitrary unit
AWTh	Anterior wall thickness
BCA	Bicinchoninic acid
BDM	2,3-Butanedione monoxime
BDNF	Brain-derived neurotrophic factor
β-MHC	β-myosin heavy chain
BNP	Brain natriuretic peptide
bp	Base pairs

bpm	Beats per minute
BS	Bluescript
BSA	Bovine serum albumin
BW	Body weight
Ca^{2+}	Calcium - cation
cAMP	Cyclic adenosine monophosphate
CBD	CREB binding domain
CBP	CREB binding protein
CCD	Charge coupled device
cDNA	Complementary DNA
Chad	Chondroadherin - murine gene
ChIP	Chromatin immunoprecipitation
cm	Centimeter
CMV	Cytomegalovirus
cMybpC	Cardiac myosin binding protein C
CO	Cardiac output
Col1a1	Collagen 1α1 - murine gene
Col3a1	Collagen 3α1 - murine gene
CRE	cAMP response element
CREB	CRE binding protein
CREM	cAMP response element modulator
Crtc	cAMP regulated transcriptional coactivator - murine gene
CRTC	cAMP regulated transcriptional coactivator - protein
Crtc$^{-/-}$	*Crtc*-deficient
CSQ	Calsequestrin
Ct	Threshold cycle
C-terminal	Carboxyl-terminal

Ctgf	Connective tissue growth factor - murine gene
Cu	Copper
d	Diastole
DAG	Diacylglycerol
dH_2O	Deionized water
DMEM	Dulbecco's Modified Eagle Medium
DMSO	Dimethyl sulfoxide
DNA	Deoxyribonucleic acid
dNTP	Deoxy nucleoside triphosphate
DPBS	Dulbecco's Phosphate-Buffered Saline
DTT	Dithiothreitol
E / ET	Endothelin-1
EC_{50}	Half maximal effective concentration
ECL	Enhanced chemiluminescence
E. coli	Escherichia coli
EDTA	Ethylenediaminetetraacetic acid
EF	Ejection fraction
EGTA	Ethylene glycol-bis(β-aminoethyl ether)-N,N,N',N'-tetraacetic acid
ERK	Extracellular signal-regulated kinase
ESI	Electrospray ionization
Et al.	Et alii (and others)
F	Forskolin
FBS	Fetal bovine serum
Forw	Forward
FS	Fractional shortening
g	Gram

$G_{\alpha\ q/11}$	G-protein α q/11 subunit
GαS	G-protein α s subunit
GDP	Guanosine diphosphate
GFP	Green fluorescent protein
G-protein	Guanine nucleotide binding protein
GSK3β	Glycogen synthase kinase 3β
GTP	Guanosine triphosphate
h	Hours
HBSS	Hank's Balanced Salt Solution
HCl	Hydrogen chloride
HEK	Human embryonic kidney
HEPES	4-(2-hydroxyethyl)-1-piperazineethanesulfonic acid
HR	Heart rate
HRP	Horseradish peroxidase
HW	Heart weight
I / Iso	Isoprenaline
IgG	Immunoglobulin G
IP_3	Inositol-1,4,5-triphosphate
ITS	Insulin-Transferrin-Selenium
kb	Kilobase
kDa	Kilodalton
KEGG	Kyoto Encyclopedia of Genes and Genomes
KID	Kinase inducible domain
KO	*Crtc1*-deficient mice
L	Liter
LB	Lysogen broth
Log	Logarithm

L-type Ca^{2+} channel	Long lasting-type calcium channel
Luc	Luciferase reporter gene
LV	Left ventricle
LVAW	Left ventricular anterior wall
LVH	Left ventricular hypertrophy
LVID	Left ventricular inner diameter
LVM	Left ventricular mass
LVPW	Left ventricular posterior wall
mA	Milliampere
MEM	Minimum essential medium
µg	Microgram
mg	Milligram
MHz	Megahertz
min	Minutes
µL	Microliter
mL	Milliliter
µm	Micrometer
mm	Millimeter
µmol	Micromol
mmol	Millimol
mRNA	Messenger ribonucleic acid
MS	Mass spectrometry
Mut	Mutant
Myh7	Myosin heavy chain 7, cardiac muscle - murine gene
NC	Nitrocellulose
NES	Nuclear export signal
NFAT	Nuclear factor of activated T-cells

NLS	Nuclear localization signal
NMCM	Neonatal mouse cardiomyocytes
NMDA	N-methyl-D-aspartate
nm	Nanometer
nmol	Nanomol
Nppa	Natriuretic peptide A - murine gene
Nppb	Natriuretic peptide B - murine gene
NR4A2	Nuclear receptor subfamily 4, group A, member 2 - human gene
N-terminal	Amino-terminal
P / PE	Phenylephrine
PA diam	Diameter of pulmonary artery
PBS	Phosphate-buffered saline
PCR	Polymerase chain reaction
PDE	Phosphodiesterase
PDK	Phosphoinositide-dependent kinase
pH	$-\log_{10}$ hydrogen ion activity
PI3K	Phosphatidylinositol-4,5-bisphosphate 3-kinase
PIP3	Phosphatidylinositol-3,4,5-triphosphate
PIPES	1,4-Piperazinediethanesulfonic acid
PKA	Protein kinase A
PKC	Protein kinase C
PLC-β	Phospholipase C-β
PKD	Protein kinase D
PLN	Phospholamban
PVDF	Polyvinylidene fluoride
PWTh	Posterior wall thickness
qPCR	Quantitative real-time PCR

R^2	Correlation coefficient
Rev	Reverse
Rgs	Regulator of G protein signaling - murine gene
RGS	Regulator of G protein signaling - protein
RIN	RNA integrity number
rRNA	Ribosomal RNA
RT	Reverse transcription
s	Systole
SDS	Sodium dodecyl sulfate
sec	Seconds
SEM	Standard error of the mean
Seq	Sequencing
SERCA	Sarcoplasmic/endoplasmic reticulum Ca^{2+}-ATPase
Sig1R	Sigma-1 receptor
SIK	Salt inducible kinase
SOB	Super optimal broth
SOC	SOB with catabolite repression
SR	Sarcoplasmic reticulum
TAD	Transactivation domain
TBS	Tris-buffered saline
TBS-T	TBS with Tween 20
TE	Tris-EDTA
TEMED	Tetramethylethane-1,2-diamine
TFA	Trifluoroacetic acid
Timp	Tissue inhibitor of metalloproteinases - murine gene
TIMP	Tissue inhibitor of metalloproteinases - protein
TL	Tibia length

TnI	Troponin I
TORC	Transducer of regulated CREB
Tris	2-Amino-2-(hydroxymethyl)propane-1,3-diol
U	Unit
V	Volt
Vol	Volume
vs.	versus
VTI	Velocity time integral
v/v	Volume/volume
WT	Wild-type mice
w/v	Weight/volume
x	times
x *g*	x gravity
°C	Degree Celsius

1 Zusammenfassung

Maladaptive Herzhypertrophie führt zu Herzinsuffizienz, eine der häufigsten Ursachen für einen stationären Krankenhausaufenthalt in der westlichen Welt. Chronische Aktivierung β-adrenerger, PKA-abhängiger Signalwege trägt zur Entwicklung einer maladaptiven kardialen Hypertrophie bei. Dies wird durch die therapeutische Wirksamkeit von β-Adrenozeptor-Antagonisten verdeutlicht. CRTC1 ist ein cAMP-regulierter transkriptioneller Koaktivator der Gentranskription. CRTC1 wird durch β-adrenerg-induzierte Erhöhung der intrazellulären cAMP-Konzentration und folgender PKA und Calcineurin Aktivität dephosphoryliert und damit aktiviert. Dephosphoryliertes CRTC1 transloziert in den Zellkern, wo es die CREB-abhängige Gentranskription aktiviert.

Um die Funktion von CRTC1 im Herzen zu erläutern, wurden für diese Arbeit Mäuse, in denen das *Crtc1* Gen global ausgeschaltet ist, untersucht. Die Funktion der Herzen wurde mittels Echokardiografie ermittelt; die mRNA- und Protein-Expressionen wurden per quantitativer Reverse-Transkriptase PCR und Immunoblot-Analyse ermittelt. In isolierten Kardiomyozyten von adulten Mäusen wurden Veränderungen der Signaltransduktion hinsichtlich veränderter Proteinphosphorylierung unter Verwendung von Immunoblot-Analysen untersucht.

Die *Crtc1*$^{-/-}$ Mäuse wiesen Zeichen einer kardialen Hypertrophie und einer verminderten Herzfunktion auf. Ventrikuläre Kardiomyozyten der *Crtc1*$^{-/-}$ Mäuse zeigten eine verminderte Phosphorylierung der Sarkomer-Proteine Troponin I und cMybpC in Reaktion auf eine akute β-adrenerge Behandlung. Die Phospholamban-Phosphorylierung war vergleichbar mit den Wildtyp-Geschwistertieren.

Die mRNA- und Protein-Expression des antihypertrophen *regulator of G-protein signaling 2* (RGS2) war in Herzen von *Crtc1*$^{-/-}$ Mäusen vermindert. Zusätzlich wurde CRTC1 an den *Rgs2*-Promoter in murinem Herzgewebe sowie in isolierten neonatalen Mauskardiomyozyten rekrutiert. Es ist bekannt, dass RGS2 $G_{\alpha\, q/11}$-gekoppelte Rezeptoren inhibiert und damit die Übermittlung hypertropher Signalwege hemmt. Die nachgeschalteten Signalkinasen Akt und PKD wurden, verglichen mit Wildtyp-Kardiomyozyten, in *Crtc1*$^{-/-}$ ventrikulären Kardiomyozyten vermindert phosphoryliert, während ERK vermehrt phosphoryliert wurde.

Als Modell einer β-adrenerg-vermittelten Hypertrophie wurde *Crtc1*$^{-/-}$ Mäusen und ihren Wildtyp-Geschwistertieren über eine Woche Isoprenalin verabreicht. Dadurch verbesserte sich die Herzfunktion der *Crtc1*$^{-/-}$ Mäuse auf das Niveau der Wildtyp-Geschwistertiere.

Zusammengefasst zeigt diese Arbeit, dass CRTC1 eine protektive Funktion bei der Entwicklung einer maladaptiven Hypertrophie einnimmt und vermutlich den Krankheitsverlauf hinauszögert. Durch den geläufigen Gebrauch von β-Adrenozeptor-Antagonisten zur Behandlung der Herzhypertrophie könnte dieser schützende Mechanismus übergangen werden.

2 Abstract

Maladaptive cardiac hypertrophy leads to heart failure, one of the common causes for hospitalization in the western world. Chronic β-adrenergic, PKA-dependent signaling contributes to the development of cardiac hypertrophy, elucidated by the therapeutic success of β-adrenoceptor antagonists. CRTC1 is a cAMP-regulated transcriptional coactivator activated by β-adrenergic signaling-induced increases in cAMP and subsequent PKA and calcineurin activation. Active CRTC1 translocates to the nucleus where it contributes to the CREB dependent gene transcription.

To elucidate the role of CRTC1 in the heart, mice globally deficient in *Crtc1* were investigated in this thesis. The heart function was studied by echocardiography; mRNA and protein expression were investigated by quantitative reverse transcription PCR and immunoblot analysis. In isolated adult ventricular myocytes changes in signaling transduction concerning protein phosphorylation were studied by immunoblot analysis.

Crtc1$^{-/-}$ mice exhibited cardiac hypertrophy and reduced cardiac function. *Crtc1*$^{-/-}$ ventricular cardiomyocytes showed a reduced phosphorylation of the sarcomeric proteins troponin I and cMybpC in response to acute β-adrenergic signaling; phospholamban phosphorylation was comparable to wild-type ventricular myocytes.

The antihypertrophic regulator of G-protein signaling 2 (RGS2) was reduced in mRNA and protein expression in hearts of *Crtc1*$^{-/-}$ mice. Additionally, CRTC1 was recruited to the *Rgs2* promoter in murine heart tissue and in neonatal cardiomyocytes. RGS2 is known to inhibit $G_{\alpha\ q/11}$-coupled receptor-mediated signaling. The downstream signaling kinases Akt and PKD were found to be less phosphorylated in *Crtc1*$^{-/-}$ ventricular myocytes than in wild-type cardiomyocytes while ERK phosphorylation was increased.

To induce β-adrenergic-induced cardiac hypertrophy, *Crtc1*$^{-/-}$ mice and their wild-type littermates received isoprenaline for 7 days. This treatment ameliorated cardiac function in *Crtc1*$^{-/-}$ mice to wild-type functional level.

Taken together, this thesis provides evidence that CRTC1 plays a protective role in the development of cardiac hypertrophy presumably prolonging disease progression. By the common use of β-adrenoceptor antagonists in the treatment of cardiac hypertrophy this protective mechanism might be reduced.

3 Introduction

3.1 Heart structure and function

The heart is a muscular organ pumping blood through the vessels to provide the body with oxygen and nutrients. It is usually situated in the middle of the thorax and consists of four chambers, two upper atria and two lower ventricles, separated by a muscular structure called the septum. Four heart valves are responsible for one-way directed flow by preventing backflow. The heart pumps blood by rhythmic, repeated contractions determined by pacemaking cells in the sinoatrial node. They generate a depolarizing action potential, which stimulates the atria to contract and travels through the atrioventricular node to the His bundle and the Purkinje fibers to the ventricular myocytes, which leads to contraction of the ventricles.

Venous blood low in oxygen enters the heart from the *venae cavae superior* and *inferior* into the right atria. It passes through the tricuspid valve into the right ventricle from where it is pumped through the pulmonary artery into the lungs, where carbon dioxide is exchanged for oxygen. Blood high in oxygen enters the heart through the pulmonary veins into the left atria and then the left ventricle. From the left ventricle the blood is pumped into the aorta and into the body (Figure 3.1). Cardiac physiological properties are characterized by inotropy (the force of contraction), chronotropy (the heart rate), dromotropy (the rate of electrical impulses), bathmotropy (the ability to respond to mechanical stimulation), and lusitropy (the rate of myocardial relaxation).

The heart consists to 30% of cardiomyocytes, accounting for 70-80% of cardiac mass. Other cardiac cells include fibroblasts, vascular smooth muscle cells, endothelial cells, and immune cells (Bernardo et al. 2010). Cardiomyocytes mostly lose the ability to proliferate after birth and mainly grow in size.

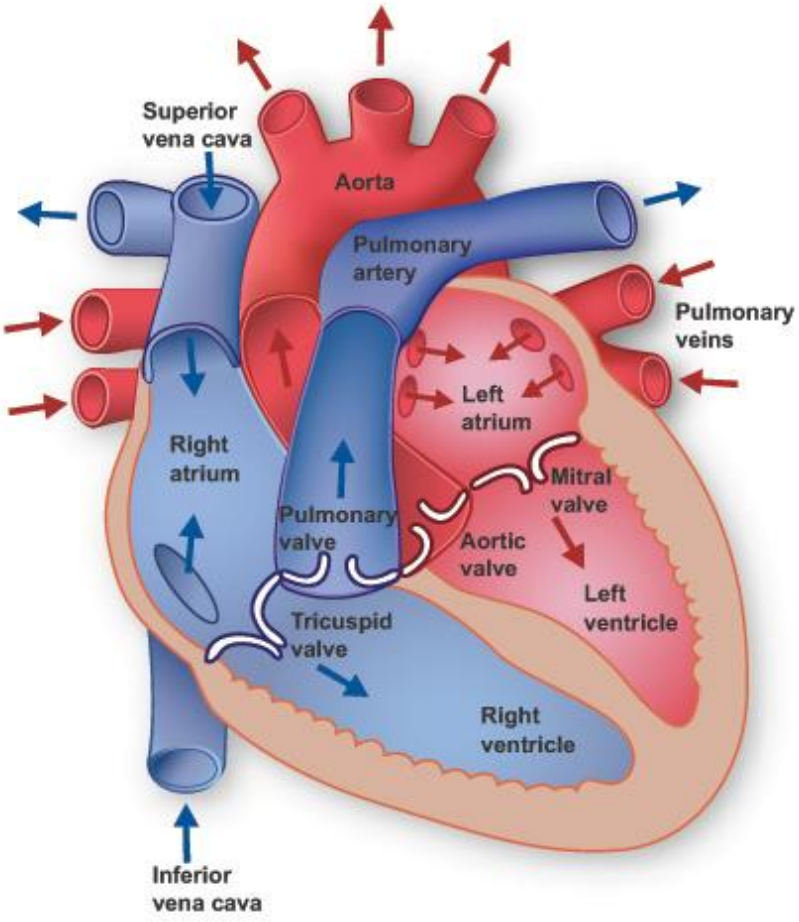

Figure 3.1: Cardiac anatomy. Cross section of a heart showing its anatomical structures. Blue arrows indicate the flow of oxygen-low blood from the *venae cavae* into the right atrium, the right ventricle, and through the pulmonary artery into the lungs. Red arrows indicate the flow of oxygen-rich blood from the lungs through the left atrium and the left ventricle to the aorta and the rest of the body. Illustration taken from the website of the Texas Heart Institute.

3.2 Cardiac hypertrophy

Cardiovascular diseases rank among the number one causes of mortality in the western world. Heart failure is the greatest growing subclass of cardiovascular diseases with a five year survival rate of 50% (Heineke and Molkentin 2006). In response to increased workload due to, among others, arterial hypertension, aortic stenosis, genetic mutations, or diabetic cardiomyopathies, myocytes grow to increase cardiac pump function and decrease wall tension. This adaptive remodeling of the heart leads to left ventricular hypertrophy (LVH) and can result in the loss of cardiomyocytes, ventricular dilation, decrease in contractile function and ultimately heart failure, if chronic stress or underlying disease persist. LVH is associated with an increase in fibrosis and beginning cardiac dysfunction while cardiac dilation and subsequent heart failure are associated with extensive fibrosis, advanced cardiac dysfunction, and myocyte death (Heineke and Molkentin 2006; Hill and Olson 2008; Heinzel et al. 2015) (Figure 3.2). The Framingham Heart Study identified LVH as an independent cardiovascular risk factor (Levy 1991).

A widely accepted model differentiates three types of morphological left ventricular growth: concentric remodeling, concentric hypertrophy, and eccentric hypertrophy. In concentric remodeling, relative wall thickness increases while cardiac mass remains normal. In concentric hypertrophy, often caused by pressure overload, relative wall thickness, and cardiac mass increase with an increase in myocyte thickness by addition of sarcomeres in parallel. In eccentric hypertrophy, caused by volume overload or infarction, cardiac mass and chamber volume increase while relative wall thickness may remain normal, de- or increase. Sarcomere series are added longitudinally leading to myocyte elongation (Ganau et al. 1992; Barry and Townsend 2010). In maladaptive cardiac hypertrophy genes normally expressed during embryogenesis are induced. This induction of genes includes the natriuretic proteins atrial natriuretic peptide (ANP, encoded by *Nppa*) and brain natriuretic peptide (BNP, encoded by *Nppb*), β-myosin heavy chain (β-MHC, encoded by *Myh7*), and α-skeletal actin (encoded by *Acta1*) and is referred to as the reactivation of the fetal cardiac gene program (Kuwahara et al. 2003; Harvey and Leinwand 2011).

LVH is also often observed in well-trained athletes and during pregnancy. This physiological hypertrophy serves to enhance performance and satisfy the higher oxygen demand of the body. It is not associated with fibrosis, apoptosis or cardiac dysfunction. Physiological hypertrophy is fully reversible. It seems as if the type of trigger, not the duration, is responsible for the development of either physiological or pathological cardiac hypertrophy (Maillet et al. 2013).

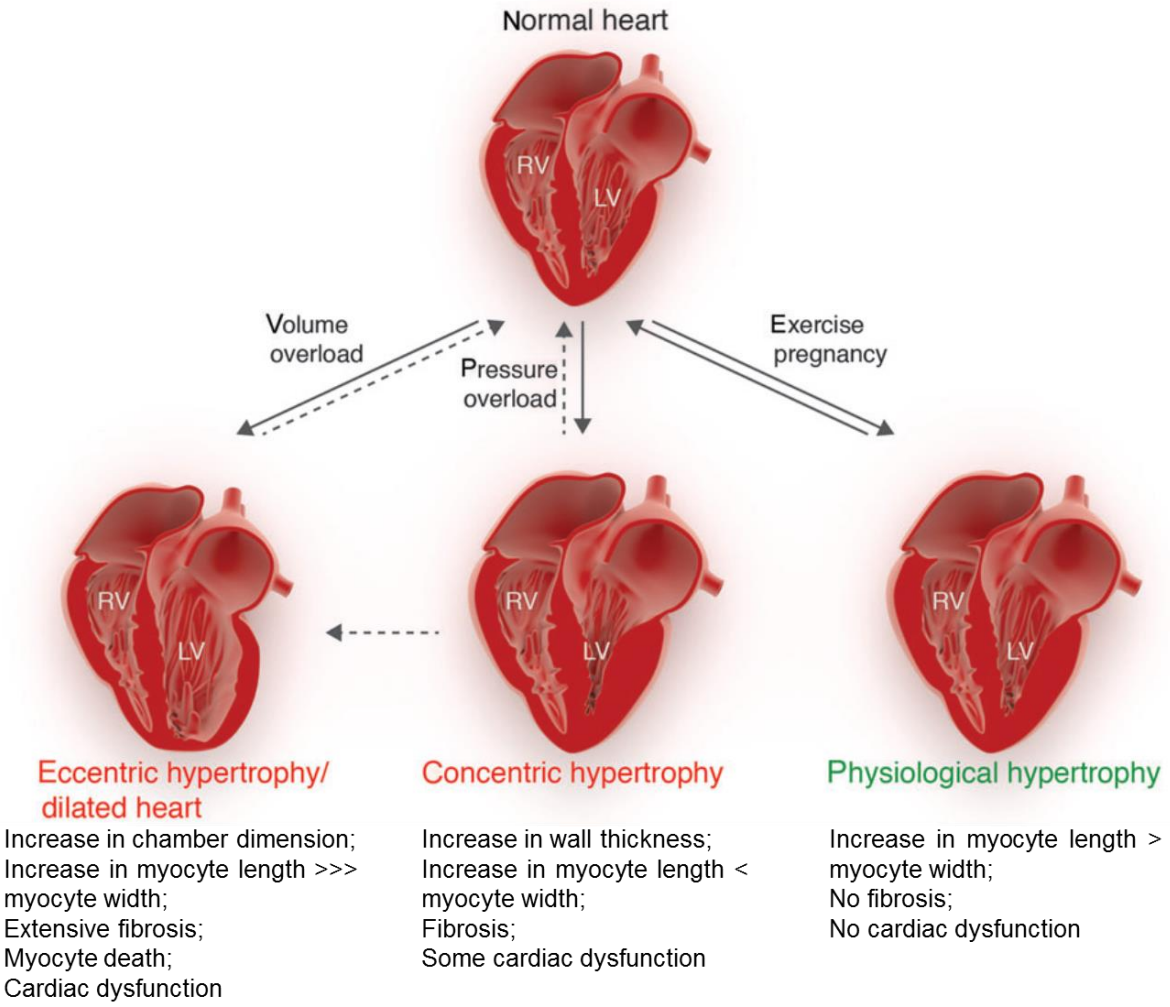

Figure 3.2: Morphometric alterations in cardiac hypertrophy. Physiological hypertrophy is associated with an increase in myocyte size without development of fibrosis or cardiac dysfunction. Concentric hypertrophy is associated with an increase in mainly left ventricular wall thickness, fibrosis, and beginning cardiac dysfunction. It is only partly reversible and can develop into eccentric hypertrophy. Eccentric hypertrophy is associated with an increase in chamber dimension, extensive fibrosis, myocyte death, and cardiac dysfunction. LV, left ventricle; RV, right ventricle. Adapted from Chung and Leinwand, 2014.

3.3 β-adrenergic signaling

As cardiac output decreases, due to an infarct or hypertension, the sympathetic nervous system is activated and signals via catecholamines. Activation of β-adrenoceptors in the heart leads to an initial increase in inotropy, chronotropy, and lusitropy to preserve blood pressure and cardiac output under increased energy consumption and cardiomyocyte growth. Chronic activation leads to a decrease in β-adrenoceptor density and a desensitization of the β-adrenergic signaling pathway, decreasing force, frequency, and cardiac output (El-Armouche and Eschenhagen 2009).

The healthy heart contains mainly β_1-adrenoceptors (75-80%), about 15% β_2-adrenoceptors, and about 5% β_3-adrenoceptors. In the failing heart, β_1-adrenoceptor density decreases and β_2-adrenoceptors become nonfunctional. β_1-adrenoceptors are associated with apoptotic signaling while β_2-adrenoceptors are associated with anti-apoptotic signaling (Siryk-Bathgate et al. 2013).

β-adrenoceptors are seven transmembrane heterotrimeric guanine nucleotide-binding (G) protein coupled receptors. The G proteins consist of the three intracellular subunits α, β, and γ. Upon activation of the receptor, guanosine diphosphate (GDP) bound to the G_α-subunit is exchanged for guanosine triphosphate (GTP). This exchange triggers the dissociation of the G_α-subunit from the receptor until GTP is again hydrolyzed to GDP and the G_α-subunit re-associates with the β/γ-subunit complex. Depending on the class of G_α-subunit, for example $G_{\alpha\,s}$ (stimulatory), $G_{\alpha\,i}$ (inhibitory), or $G_{\alpha\,q/11}$, different effector enzymes are activated or inhibited (Aktories et al. 2013).

β-adrenoceptors in the healthy heart are coupled to the $G_{\alpha\,s}$-subunit. The dissociated G_α-subunit activates the enzyme adenylyl cyclase (AC), which catalyzes the formation of cyclic adenosine monophosphate (cAMP) from adenosine triphosphate (ATP). Two cAMP molecules each bind to a regulatory subunit of the serine/threonine protein kinase A (PKA), releasing its two catalytic subunits (Whelan et al. 2013). The catalytic subunits phosphorylate long-lasting (L)-type calcium (Ca^{2+}) -channels, resulting in an increase in intracellular Ca^{2+}-concentration, a larger systolic Ca^{2+}-transient, and therefore increased inotropy. This effect is supported by PKA-induced phosphorylation of the ryanodine receptor, which leads to increased Ca^{2+}-flow out of the sarcoplasmic reticulum (SR) and phospholamban (PLN) phosphorylation, leading to increased Ca^{2+}-reuptake into the SR. Phosphorylation of the myofilament proteins troponin I (TnI) and cardiac myosin binding protein C (cMybpC) leads to decreased myofilament Ca^{2+}-sensitivity resulting in an accelerated relaxation.

In the failing heart, β-adrenoceptors uncouple from the $G_{\alpha\,s}$-subunit and increase binding to the $G_{\alpha\,i}$-subunit, inhibiting AC activity (El-Armouche and Eschenhagen 2009).

3.4 Therapeutic options for maladaptive cardiac hypertrophy

Current therapeutic options for cardiac hypertrophy include ACE-inhibitors, angiotensin II-receptor antagonists, aldosterone-receptor antagonists, β-adrenoceptor antagonists, diuretics, and Ca^{2+}-channel antagonists. Activation of the sympathetic nervous system leads to subsequent activation of the renin-angiotensin-aldosterone system resulting in increased blood pressure. Induced by β_1-adrenergic activation, decreases in blood pressure, or decreases in blood sodium concentration, renin is secreted from juxtaglomerular cells in the kidney. Renin is an enzyme that converts the peptide angiotensinogen to angiotensin I, which is then converted to angiotensin II by the angiotensin-converting enzyme (ACE). Angiotensin II acts as a potent vasoconstrictor and stimulates the secretion of aldosterone from the adrenal cortex, which increases reabsorption of sodium in the kidneys. ACE-inhibitors such as ramipril, angiotensin II-receptor antagonists such as candesartan, aldosterone-receptor antagonists such as spironolactone, as well as β-adrenoceptor antagonists such as metoprolol decrease blood pressure by reducing the activity of the renin-angiotensin-aldosterone system, resulting in a decreased afterload and conserving the heart's energy. Through inhibition of β-adrenoceptors in the heart, β-adrenoceptor antagonists diminish inotropy, chronotropy, and lusitropy resulting in reduced energy consumption of the heart. Activation of $G_{\alpha\, q/11}$-coupled receptors in the heart by angiotensin II, endothelin-1, or α-adrenergic signals such as phenylephrine leads to activation of phospholipase C-β (PLC-β) which induces generation of the second messengers diacylglycerol (DAG) and inositol-1,4,5-triphosphate (IP_3). DAG activates protein kinase C (PKC), which phosphorylates L-type Ca^{2+}-channels and myofilament proteins. IP_3 leads to increased Ca^{2+}-release from the sarcoplasmic reticulum by enhancing the open probability of the ryanodine receptor. Angiotensin II-receptor type 1 in cardiomyocytes can also be activated by mechanical stretch, without involvement of angiotensin II (Hill and Olson 2008). Chronic activation of $G_{\alpha\, q/11}$-coupled receptors can cause cardiac hypertrophy (Wettschureck et al. 2001). Angiotensin II-receptor antagonists are a valuable part of the treatment of cardiac hypertrophy and heart failure while endothelin-receptor antagonists are currently used for the treatment of pulmonary arterial hypertension.

3.5 The transcriptional coactivator CRTC

β-adrenergic signaling has been researched intensively, but mechanisms leading to cardiac hypertrophy after intracellular cAMP increases have not been completely understood. The cAMP regulated transcriptional coactivator (CRTC), formerly known as transducer of regulated CREB (TORC), has been found to increase the expression of cAMP responsive genes. CRTC is a coactivator of the ubiquitously expressed transcription factor cAMP response element (CRE) binding protein (CREB), first identified by Conkright et al. and Iourgenko et al. (Conkright et al. 2003; Iourgenko et al. 2003). The CRTC family consists of three members, CRTC1, CRTC2, and CRTC3. They are evolutionarily conserved proteins. Functional homologues have been identified in *Takifugu rubripes*, *Drosophila melanogaster,* and *Caenorhabditis elegans* (Conkright et al. 2003; Iourgenko et al. 2003). Human CRTC2 and CRTC3 share 30-40% homology with CRTC1. All three members of the CRTC family are expressed in most tissues while the amount of expression differs between isoforms. CRTC1 is most highly expressed in the brain, mainly in the prefrontal cortex and the cerebellum. CRTC1 is associated with long-term memory, energy balance, neuronal function, and mood disorders (Kovacs et al. 2007; Altarejos and Montminy 2011; Breuillaud et al. 2012). CRTC2 is predominantly expressed in the liver where it promotes glucose homeostasis (Koo et al. 2005). Mice deficient in *Crtc2* show reduced glucose production without leading to hypoglycemia (Wang et al. 2010). Under diet-induced obesity *Crtc2*$^{-/-}$ mice show improved insulin sensitivity (Le Lay et al. 2009). CRTC3 is highly expressed in white and brown adipose tissue and is involved in energy balance (Conkright et al. 2003; Altarejos and Montminy 2011). *Crtc3*$^{-/-}$ mice appear to be more insulin sensitive than wild-type mice on a normal chow diet and have 50% lower adipose tissue mass, despite normal food intake. On a high fat diet, *Crtc3*$^{-/-}$ mice gain less weight than wild-type littermates and have elevated energy expenditure (Song et al. 2010).

3.5.1 Structure of CRTC

Human *CRTC2* and *CRTC3* genes share 32% identity with CRTC1. The CRTC proteins display a highly conserved predicted N-terminal coiled-coil domain which mediates the association with the dimerized leucine zipper domain of the transcription factor CREB. Conkright et al. showed in a glutaraldehyde crosslinking assay that CRTCs oligomerize and bind to CREB as tetramers (Conkright et al. 2003). Analysis of CRTC2 revealed a nuclear localization signal (NLS) within the amino acid region 56-144 and two nuclear export signals (NES) within the amino acid region 145-320 (Figure 3.3). These NLS and NES

are conserved among the CTRC isoforms. Only CRTC3 presents an alteration of amino acid 282 within the NES 1, which leads to a disrupted nuclear export activity and greater transcriptional activity compared to CRTC2. Phosphorylation of serine 171 in CRTC2 and the conserved serine in the isoforms is responsible for complex formation with 14-3-3 proteins, inhibiting nuclear translocation of CRTC. All three CRTC isoforms contain a conserved 200 amino acid C-terminal transactivation domain (Screaton et al. 2004).

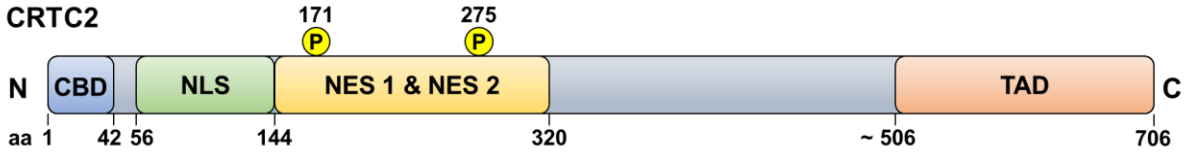

Figure 3.3: Structure of the CRTC2 protein. N-terminally, CRTC2 contains a highly conserved predicted coiled-coil domain with which it binds to the dimerized leucine zipper of CREB (CBD=CREB binding domain). Further C-terminally, CRTC2 contains a nuclear localization signal (NLS) and two nuclear export signals (NES 1 and NES 2). At the C-terminus, CRTC2 contains an about 200 amino acid long transactivation domain (TAD). “P” indicates phosphorylation sites at amino acids 171 and 275 leading to 14-3-3 protein interaction. aa, amino acid; N, N-terminus; C, C-terminus.

3.5.2 Regulation of CRTC

CRE sites are found in about one third of the mammalian genome (Conkright et al. 2003). The transcription factor CREB recognizes palindromic CRE sites (5’-TGACGTCA-3’) or CRE half-sites (5’-TGACG-3’ or 5’-CGTCA-3’) of promoter regions, initiating gene transcription. Upon serine 133 phosphorylation by PKA the coactivator CREB binding protein (CBP) is recruited to CREB. CRTC is another coactivator of CREB dependent gene transcription, binding to CREB in a serine 133 phosphorylation-independent way. (Screaton et al. 2004; Altarejos and Montminy 2011). Under basal conditions of the cell CRTC is phosphorylated and therefore retained in the cytoplasm. It has been shown that the salt inducible kinase (SIK) directly phosphorylates CRTC2 at serine 171 and thereby induces the association with 14-3-3 phosphoprotein binding-proteins leading to a cytosolic sequestration (Screaton et al. 2004). Upon activation of the β-adrenoceptor and concomitant increases in intracellular cAMP and PKA activity, SIK is phosphorylated at serine 577 and thereby inactivated (Katoh et al. 2004; Kanyo et al. 2009). Increased intracellular Ca^{2+}-concentrations lead to the binding of the Ca^{2+}-binding adaptor protein calmodulin to the serine/threonine protein-phosphatase calcineurin, which leads to its subsequent activation and thereby CRTC dephosphorylation. Dephosphorylated CRTC is liberated from 14-3-3 proteins and translocates into the nucleus (Bittinger et al. 2004; Kang et al. 2007). In the nucleus, CRTC interacts with the dimerized leucine zipper of the transcription factor CREB. Conkright et al. showed that the CRTC N-terminal coiled-coil domain interacts with the

dimerized leucine zipper domain of CREB forming a homotetramer (Conkright et al. 2003). It has been shown that CRTC-binding to CREB is sufficient to initiate transcriptional activity. Furthermore, CRTC is able to interact with CBP, stabilizing the transcriptional activation complex (Figure 3.4) (Ravnskjaer et al. 2007; Xu et al. 2007; Heinrich et al. 2013). Phosphorylation of CRTC2 by SIK in the nucleus terminates coactivation of gene transcription and leads to CRTC2 translocation to the cytoplasm (Dentin et al. 2007).

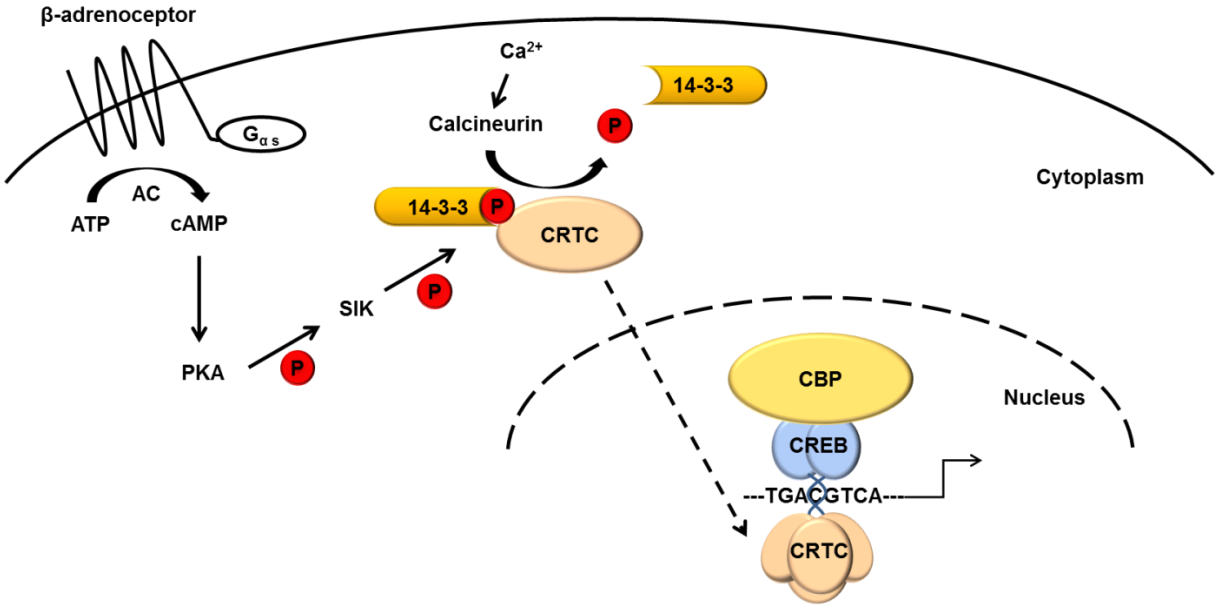

Figure 3.4: Regulation of CRTC. Under basal conditions, CRTC is sequestered in the cytoplasm through phosphorylation by the salt inducible kinase (SIK) and subsequent association with 14-3-3 proteins (14-3-3). Upon β-adrenergic stimulation, adenylyl cyclase (AC) catalyzes the formation of cyclic adenosine monophosphate (cAMP) from adenosine triphosphate (ATP). cAMP activates protein kinase A (PKA) which in turn inhibits SIK through phosphorylation. Increased intracellular Ca^{2+}-concentrations lead to an activation of the phosphatase calcineurin which dephosphorylates CRTC. Dephosphorylated CRTC translocates into the nucleus where it binds to the dimerized leucine zipper of the DNA-bound cAMP response element binding protein (CREB) and coactivates gene transcription. Phosphorylation of CREB at serine 133 leads to interaction with CREB binding protein (CBP). CRTC is able to interact with CBP and stabilize the transcriptional activation complex (not shown). “P” indicates inhibitory phosphorylation.

3.6 Aim of the thesis

The role of CRTC has been evaluated in various tissues while its role in the heart remains unknown. Previous results from the group of Prof. Elke Oetjen showed increased CRTC1 protein content in human heart tissue with acquired (aortic valve stenosis) and inherited (hypertrophic cardiomyopathy) hypertrophy. They showed the same increase in CRTC1 protein in two distinct mouse models of cardiac hypertrophy, either induced by afterload enhancement by transverse aortic constriction or by genetic mutation of the *cMybpc* gene. In neonatal rat cardiomyocytes β-adrenergic treatment resulted in CRTC1 dephosphorylation and therefore activation.

The goal of this study was to determine the role of CRTC1 in the heart and its influence on the pathogenesis of cardiac hypertrophy.

For that purpose mice globally deficient in *Crtc1* were investigated regarding their cardiac phenotype. Hypertrophic development in the heart was assessed on morphological, functional, mRNA, and protein levels. Hypertrophic signaling and phosphorylation of contractile proteins were researched in isolated ventricular myocytes from neonatal and adult mice. As a model for β-adrenergic-induced hypertrophy, mice were treated with the β-adrenoceptor agonist isoprenaline for one week. The effect of CRTC1 on cardiac function and mRNA expression was assessed in these mice.

4 Results

4.1 *Crtc1*-deficient mice

In order to investigate the role of CRTC1 in the heart, mice globally deficient in *Crtc1* (*Crtc1*$^{-/-}$) were investigated. These mice were previously generated and described regarding neuronal function and behavior by the laboratory of Dr. Jean-René Cardinaux (University of Lausanne, Switzerland). The mice were mostly investigated at an age of 10 to 13 weeks, if not otherwise stated, and compared to their wild-type littermates (WT).
mRNA and immunoblot analysis confirmed the lack of *Crtc1* on transcriptional and protein levels in the hearts of *Crtc1*$^{-/-}$ mice (Figure 4.1 A and B). Furthermore, mRNA of the two isoforms *Crtc2* and *Crtc3* was not differentially expressed in *Crtc1*$^{-/-}$ mice compared to their wild-type littermates (Figure 4.1 C and D).

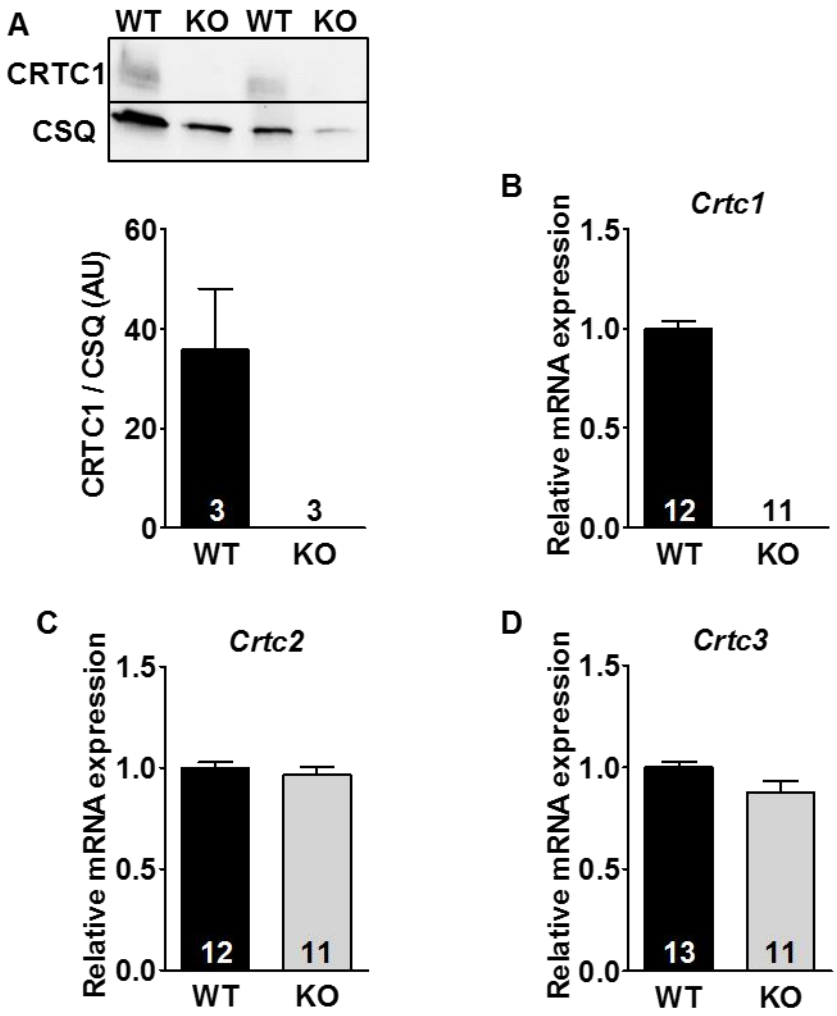

Figure 4.1: No expression of *Crtc1* and unchanged *Crtc2* and *Crtc3* mRNA expression in *Crtc1*$^{-/-}$ mice. A. Protein lysates from hearts of *Crtc1*$^{-/-}$ mice (KO) and their wild-type littermates (WT) were analyzed by immunoblot using an antibody against CRTC1 and normalized to calsequestrin (CSQ). Typical immunoblot (top); quantitative evaluation (bottom). **B-D.** Quantitative evaluation of mRNA expression of *Crtc1, Crtc2,* and *Crtc3,* respectively, normalized to *GαS* using ΔΔCt-method. Data are expressed as mean±SEM; number of samples is given within the bars.

4.1.1 Cardiac hypertrophy

To investigate the effect of *Crtc1* absence on cardiac size, the ratio of heart weight to body weight was determined as a marker for hypertrophy. Since it has previously been described that *Crtc1*$^{-/-}$ mice express a hyperphagic phenotype at the age of 16 weeks (Breuillaud et al. 2009), the ratio of heart weight to tibia length was measured as well. *Crtc1*$^{-/-}$ mice show an increase in the ratio of heart weight to body weight as well as to tibia length by 20±6% and 27±9%, respectively (Figure 4.2).

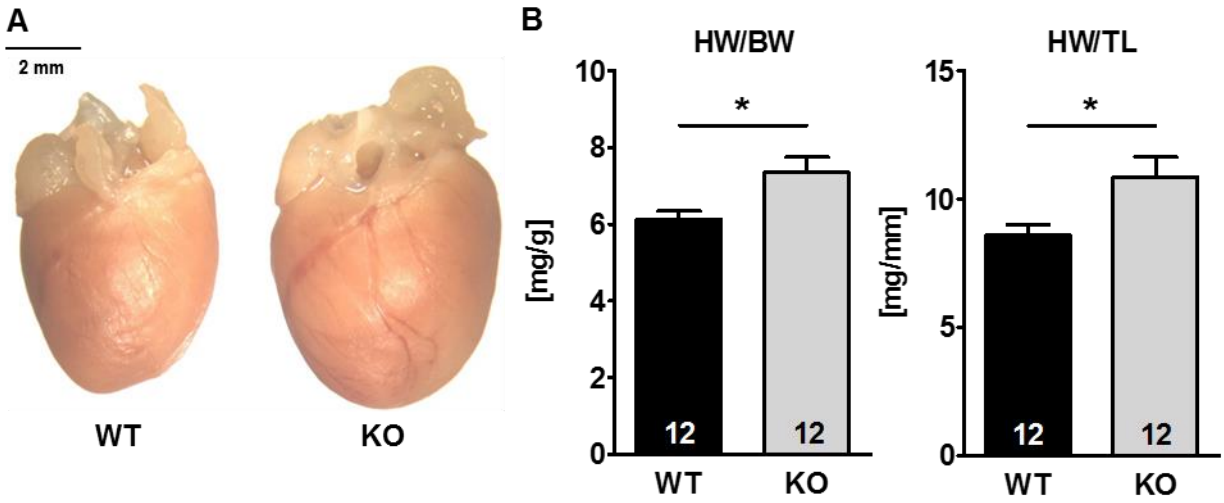

Figure 4.2: Cardiac hypertrophy in *Crtc1*$^{-/-}$ mice. In *Crtc1*$^{-/-}$ mice (KO) and their wild-type littermates (WT), the ratio of heart weight (HW) to body weight (BW) or to tibia length (TL) was determined as a marker for cardiac hypertrophy. **A.** Representative formalin fixed hearts. **B.** Quantitative evaluation of HW/BW and HW/TL. Data are expressed as mean±SEM. *p<0.05; unpaired Student's t-test; number of mice is given within the bars.

For the analysis of cardiomyocyte size, cross sections from hearts of mice aged 25 to 27 weeks were stained with an antibody against dystrophin. Dystrophin is a protein of the sarcolemma expressed in muscle fibers. Using ImageJ®, the outlines of single cells were surrounded and the cardiomyocyte area was calculated by the program. In *Crtc1*$^{-/-}$ mice, cardiomyocyte size was increased by 17±2% in the septum and 12±2% in the left ventricle but remained unchanged in the right ventricle (Figure 4.3 A and B).

To support these findings, isolated adult mouse ventricular myocytes (AMVM) were stained for α-actinin, a protein of the sarcomere, and measured by the *Opera® High Content Screening System* in cooperation with Maksymilian Prondzynski (University Medical Center, Hamburg, Germany). This analysis revealed an increase in cardiomyocyte size by 17±4% in total; 11±4% in width and 6±1% in length indicating a concentric hypertrophy (Figure 4.3 C and D).

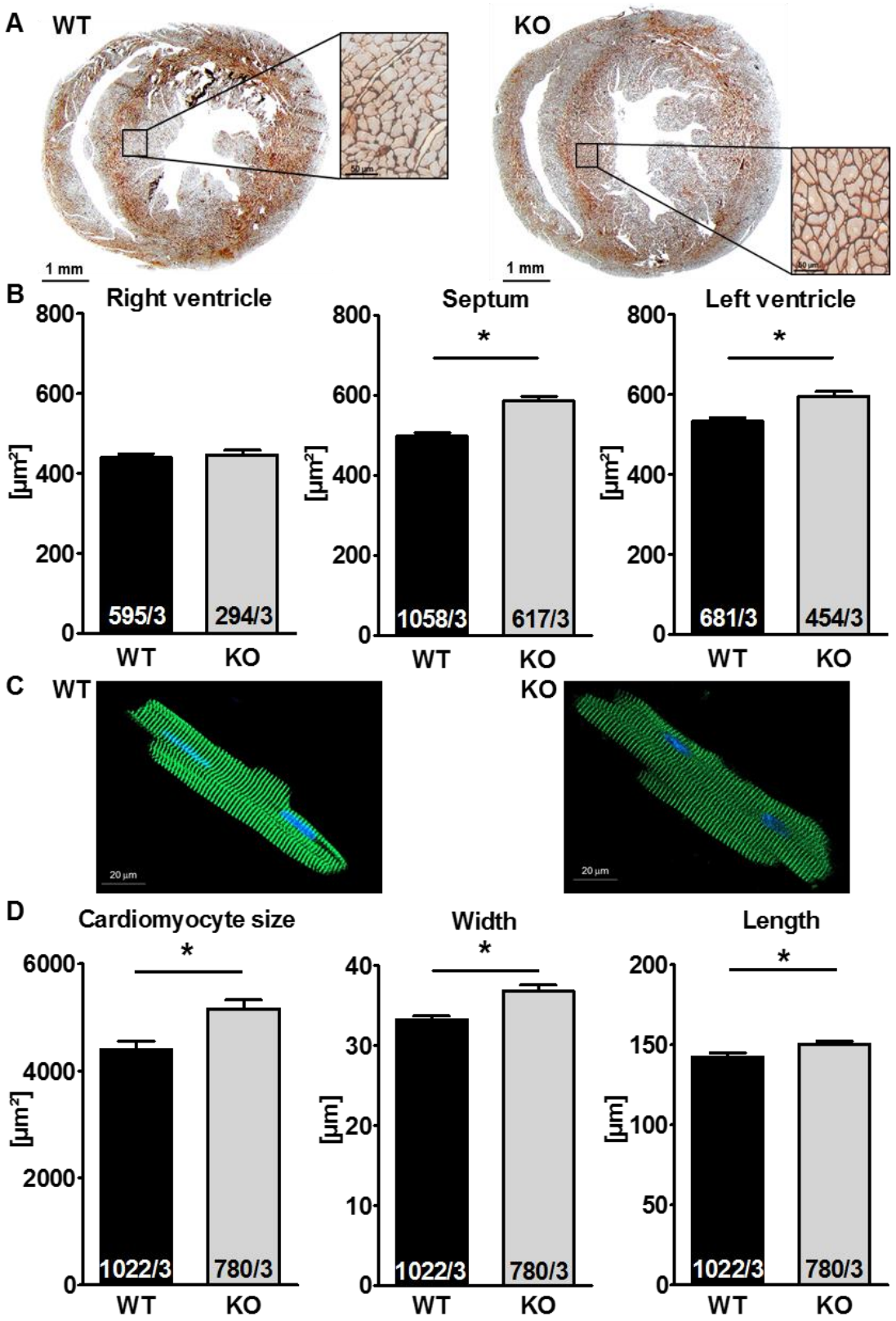

Figure 4.3: Increased cardiomyocyte size in *Crtc1*$^{-/-}$ mice. Cross sections of hearts from *Crtc1*$^{-/-}$ mice (KO) and their wild-type (WT) littermates (25-29 weeks old) were stained with an antibody against dystrophin. **A.** Representative cross sections. **B.** Quantitative evaluation of cardiomyocyte area. Isolated adult mouse ventricular myocytes (AMVM) were stained for α-actinin and analyzed by the *Opera*® *High Content Screening System.* **C**. Representative AMVM. **D.** Quantitative evaluation of cardiomyocyte total size, width, and length. Data are expressed as mean±SEM. *p<0.05; unpaired Student's t-test; number of cells and hearts is given within the bars.

4.1.2 Fibrosis

In many cases, cardiac hypertrophy goes along with an increase in fibrosis (Hill and Olson 2008). To assess the amount of collagenous tissue in cross sections of *Crtc1*$^{-/-}$ and WT hearts, a Masson's-Trichrome staining was performed. This standard staining method stains muscle tissue red, collagenous tissue blue, and cell nuclei brown. Microscopic evaluation of these cross sections showed no difference between WT and *Crtc1*$^{-/-}$ hearts (Figure 4.4 A). A second collagen staining was conducted. Sirius Red/Fast Green staining Kit stains collagenous tissue red and non-collagenous tissue green. Microscopic evaluation of this staining supported the findings from the Masson's-Trichrome staining (Figure 4.4 B).

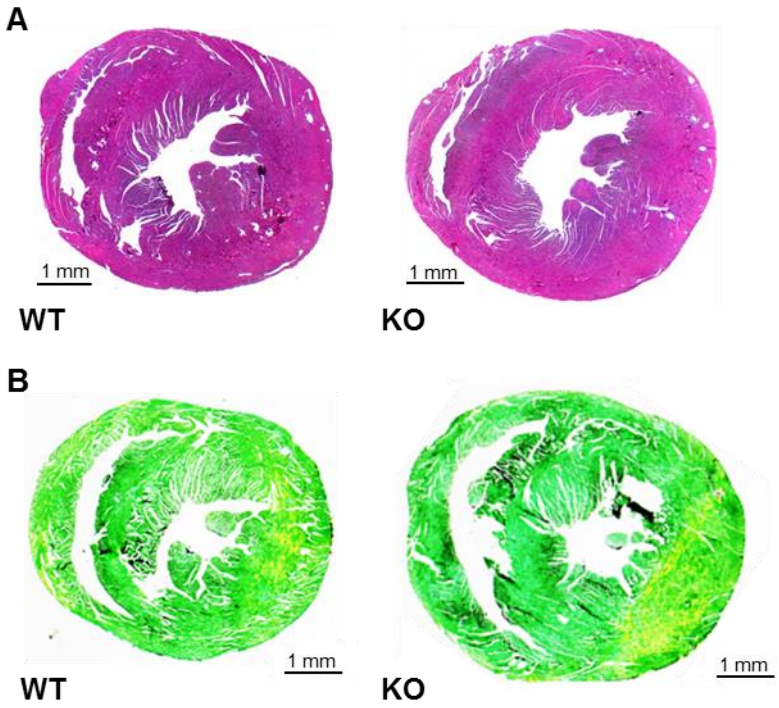

Figure 4.4: No fibrosis in *Crtc1*$^{-/-}$ mice. A. Cross sections of hearts from *Crtc1*$^{-/-}$ mice (KO) and their wild-type littermates (WT; 25 weeks old) were subjected to Masson's-Trichrome staining; representative cross sections after staining. **B.** Cross sections of hearts from *Crtc1*$^{-/-}$ mice (KO) and their wild-type littermates (WT; 31 weeks old) were subjected to Sirius Red/Fast Green staining; representative cross sections after staining.

To further evaluate the presence of fibrosis, mRNA expression of the connective tissue growth factor (*Ctgf*), a factor associated with tissue remodeling (Koshman et al. 2015), of collagen 1α1 (*Col1a1*), and collagen 3α1 (*Col3a1*) was assessed. This evaluation showed no differences between WT and *Crtc1*$^{-/-}$ heart tissue (Figure 4.5).

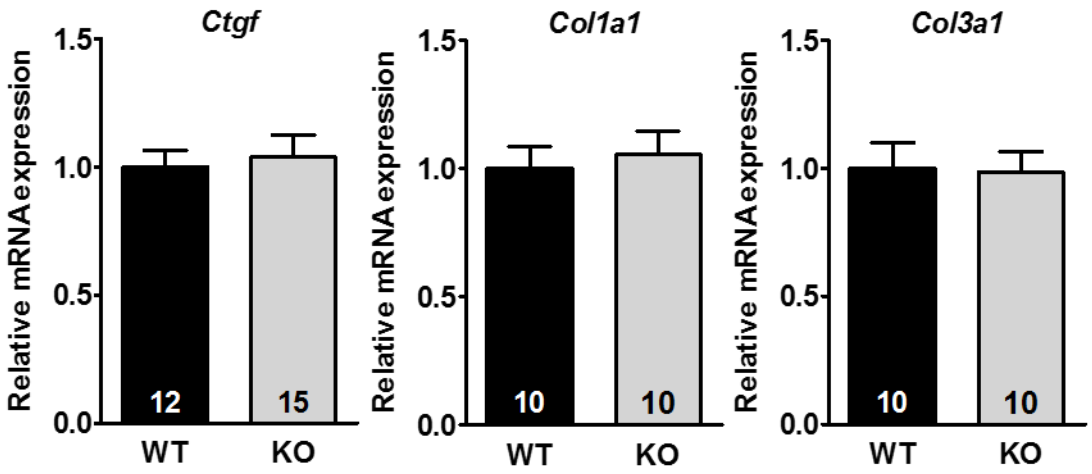

Figure 4.5: Unchanged *Ctgf*, *Col1a1*, and *Col3a1* mRNA expression in *Crtc1*$^{-/-}$ mice. Quantitative mRNA expression of the connective tissue growth factor (*Ctgf*), collagen 1α1 (*Col1a1*), and collagen 3α1 (*Col3a1*) normalized to *GαS* in heart tissue from *Crtc1*$^{-/-}$ mice (KO) and their wild-type littermates (WT) analyzed by quantitative real time PCR. Data are expressed as mean±SEM relative to WT using ΔΔCt-method. Number of samples is given within the bars.

4.1.3 mRNA marker for hypertrophic development

Under maladaptive hypertrophic conditions, the activation of the so called "fetal gene program" can be observed (Kang et al. 2007). To identify if the fetal gene program was activated in *Crtc1*$^{-/-}$ mice, genes encoding for atrial natriuretic peptide (ANP, encoded by *Nppa*), brain natriuretic peptide (BNP, encoded by *Nppb*), α-skeletal actin 1 (encoded by *Acta1*), and β-myosin heavy chain (β-MHC, encoded by *Myh7*) were analyzed by RT-qPCR. ANP and BNP are natriuretic peptides released by the atria and ventricles upon cardiac wall stress. ANP and BNP induce local vasodilation and reduce blood volume systemically. Under conditions of maladaptive hypertrophy, α-skeletal actin 1 and the β-MHC are upregulated. MHC initiates contraction by directly interacting with actin molecules in the thin filament. It carries the ATPase activity, which is required for physical translocation. In mice, the α-MHC isoform is predominant in postnatal life. It has a higher ATPase activity with increased shortening velocity and higher energy consumption. In cardiac hypertrophy, it is replaced by the slower but more efficient β-MHC isoform (Nadal-Ginard and Mahdavi 1989; Kang et al. 2007; Harvey and Leinwand 2011).

In *Crtc1*$^{-/-}$ mice, none of these fetal genes were upregulated. Moreover, *Acta1* mRNA expression was downregulated (Figure 4.6). According to the CREB target gene database designed by the group of Prof. Marc Montminy (Salk Institute, La Jolla, USA), the *Nppb, Acta1,* and *Myh7* promoters contain a CRE half-site and might therefore be regulated by CRTC1.

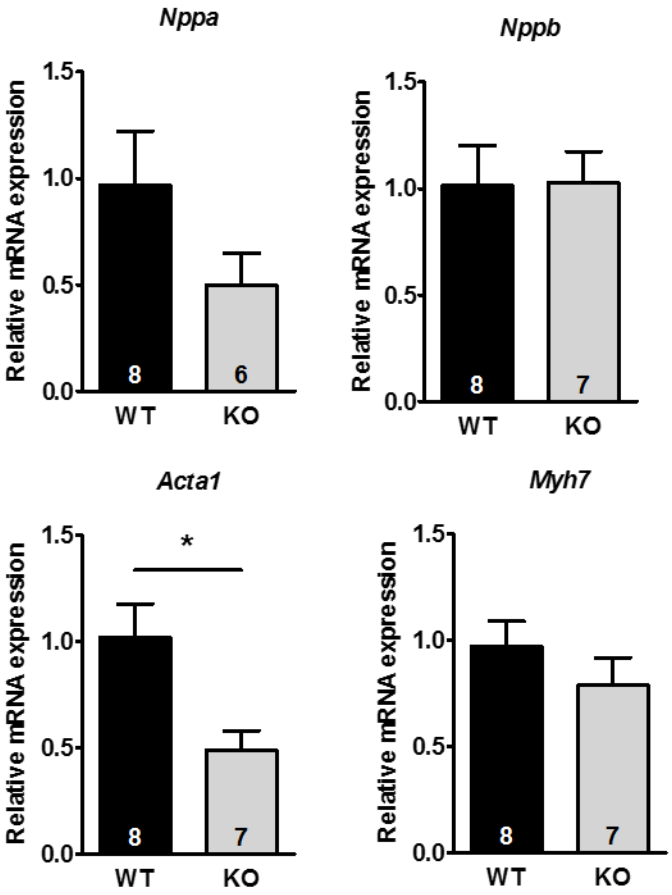

Figure 4.6: mRNA expression of fetal genes in *Crtc1*$^{-/-}$ mice. Quantitative evaluation of mRNA expression of *Nppa, Nppb, Acta1, and Myh7,* respectively, normalized to *GaS* in heart tissue from *Crtc1*$^{-/-}$ mice (KO) and their wild-type littermates (WT) using ΔΔCt-method. Data are expressed as mean±SEM relative to WT; *p<0.05; unpaired Student's t-test; number of samples is given within the bars.

4.1.4 Micro-array based expression analysis of mRNA

To identify a broader field of genes differentially regulated in *Crtc1*$^{-/-}$ mice, a micro-array based expression analysis for mRNA sequencing (mRNA-Seq) was conducted.

Heart powder from 3 WT and 3 *Crtc1*$^{-/-}$ mice was used for mRNA extraction. The obtained mRNA was analyzed by the group of Prof. Norbert Hübner (MDC, Berlin, Germany). Differentially expressed mRNA is depicted in figure 4.7. The analysis did not reveal differentially expressed mRNAs involved in cardiac disease. This might be due to the small sample number of three mice per genotype.

mRNA expression upregulated in *Crtc1*$^{-/-}$ mice is mainly involved in morphogenesis, metabolic, and signaling processes according to the Kyoto Encyclopedia of Genes and Genomes (KEGG) database. mRNA expression downregulated in *Crtc1*$^{-/-}$ mice is mainly involved in the regulation of the immune system.

The upregulated chondroadherin (*Chad)* mRNA expression in *Crtc1*$^{-/-}$ mice might have an influence on cardiac growth. According to the KEGG database, it can be involved in the PI3K-Akt-signaling pathway.

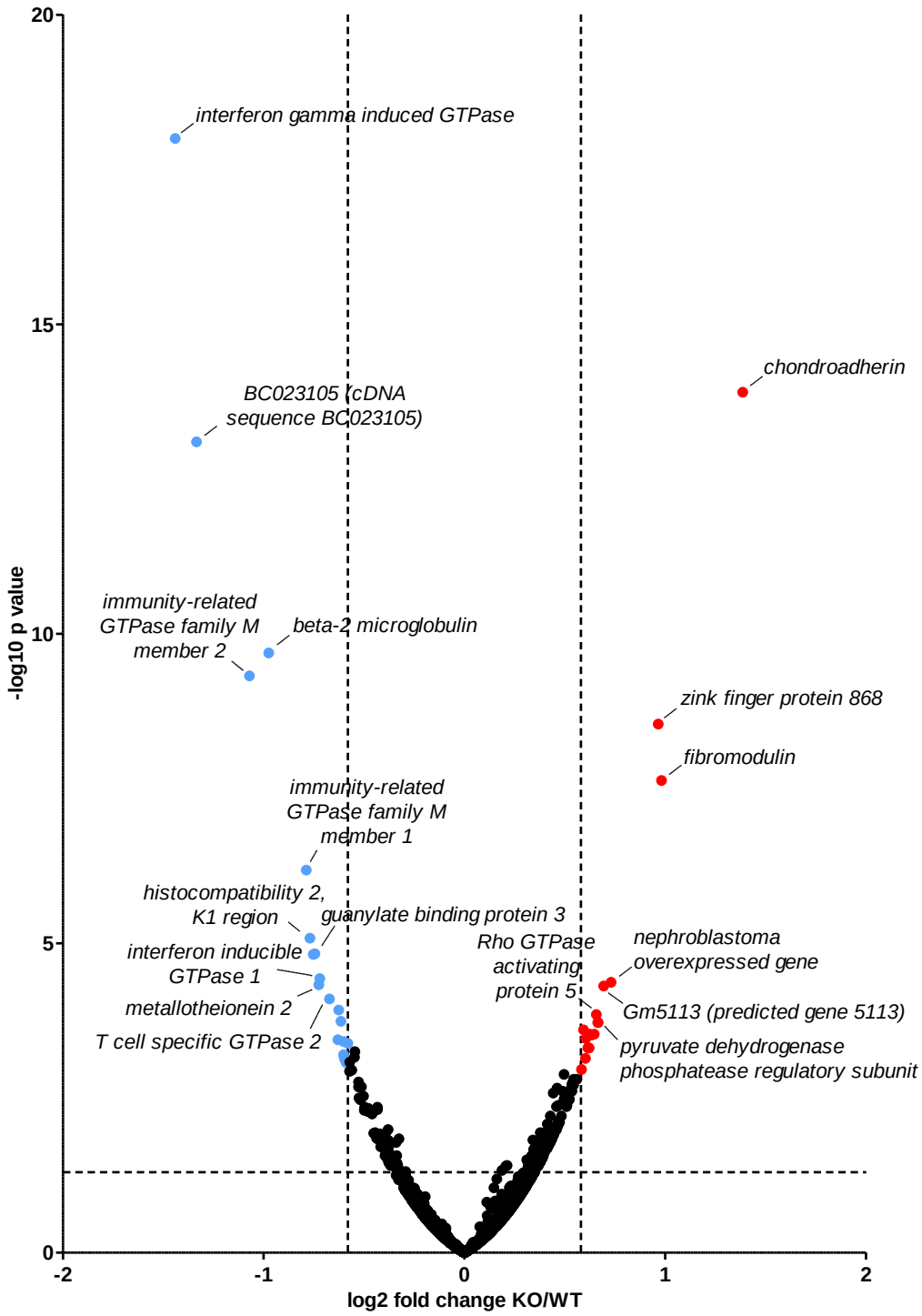

Figure 4.7: Differentially expressed mRNA in *Crtc1*$^{-/-}$ mice. mRNA from *Crtc1*$^{-/-}$ mice (KO) or WT was subjected to mRNA sequencing. Volcano plot showing - log10 p-values plotted against log2 KO/WT. Horizontal line at y=1.3 represents a p-value of 0.05, vertical lines at x=- 0.58 and x=0.58 represent a fold change of 1.5. Blue indicates downregulation > 1.5 fold change and red indicates upregulation > 1.5 fold change with p<0.05. Unpaired Student's t-test; n=3 per genotype.

4.1.5 Proteomics

To evaluate differentially expressed proteins in *Crtc1*$^{-/-}$ mice, a proteomics analysis was performed in cooperation with the laboratory of Prof. Marcus Krüger (CECAD, Cologne, Germany). Proteins were separated by molecular mass using gel electrophoresis, digested in-gel and analyzed by mass spectrometry. Proteins differentially expressed in *Crtc1*$^{-/-}$ mice are shown in figure 4.8. Three differentially expressed proteins involved in morphogenesis linked to cardiac function, α-actinin-3 (downregulated in *Crtc1*$^{-/-}$), myosin heavy chain 2 (downregulated in *Crtc1*$^{-/-}$), and Ankyrin repeat domain-containing protein 1 (upregulated in *Crtc1*$^{-/-}$), were identified. Other differentially expressed proteins are involved in cellular component organization (both up- and downregulated in *Crtc1*$^{-/-}$) and metabolic processes (mostly downregulated in *Crtc1*$^{-/-}$).

A discrepancy between the mRNA-Seq and proteomics analysis was detected. Proteomics revealed more differentially expressed proteins involved in cardiac function than mRNA-Seq. Differentially expressed proteins were found to be involved in cellular component organization and metabolic processes, as were differentially expressed mRNAs. No up- or downregulated protein matched a differentially expressed mRNA. Down-regulation of mRNAs involved in the regulation of the immune system was not confirmed on protein level.
For subsequent mRNA and protein quantifications, RT-qPCR and immunoblot methods were used to allow the increase of sample number and the analysis of specific mRNAs and proteins.

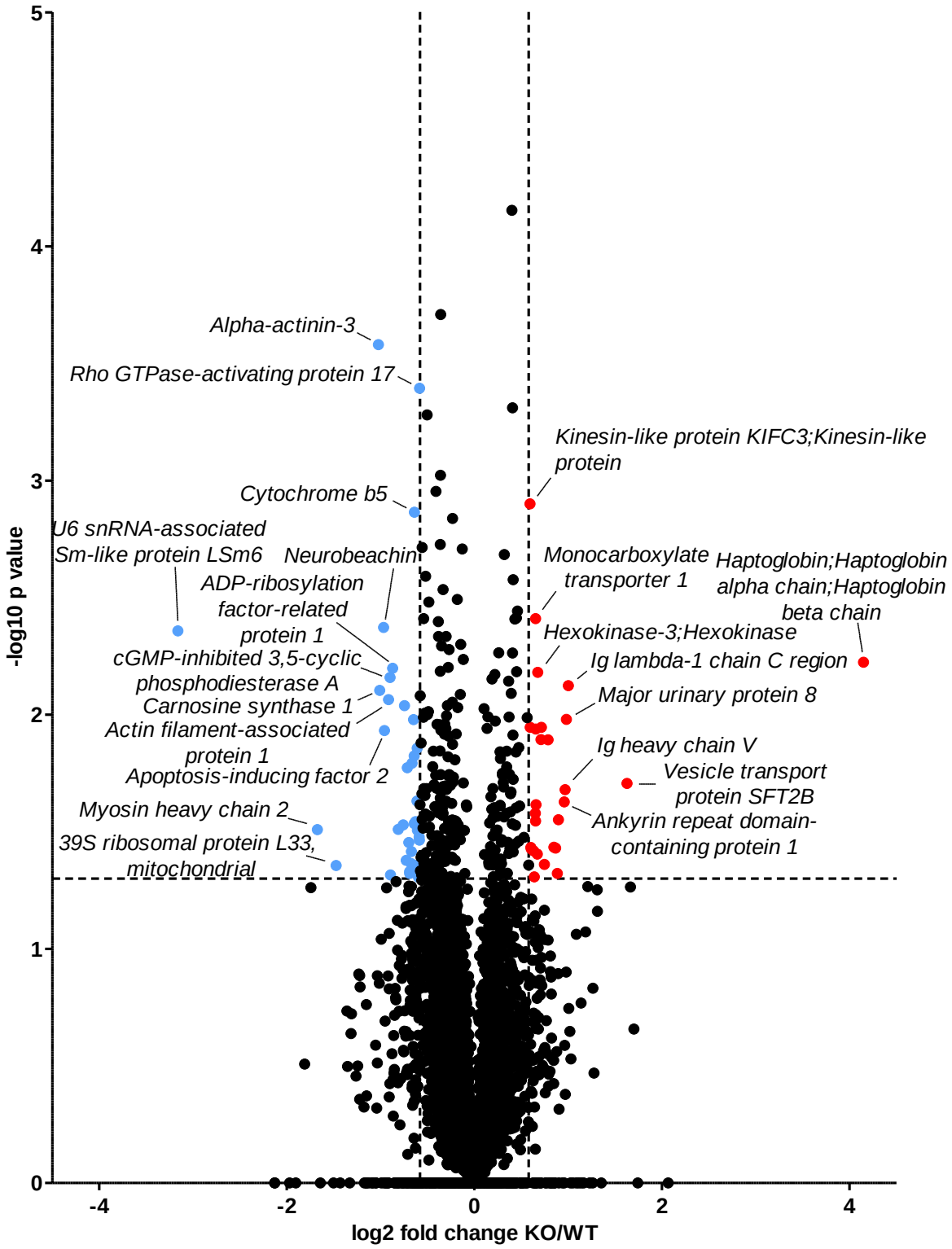

Figure 4.8: Differentially expressed proteins in *Crtc1*$^{-/-}$ mice. Total protein from hearts of *Crtc1*$^{-/-}$ mice (KO) or WT was subjected to proteomics analysis. Volcano plot showing - log10 p-values plotted against log2 KO/WT. Horizontal line at y=1.3 represents a p-value of 0.05, vertical lines at x=- 0.58 and x=0.58 represent a fold change of 1.5. Blue indicates downregulation > 1.5 fold change and red indicates upregulation > 1.5 fold change with p<0.05. Unpaired Student's t-test; n=3 per genotype.

4.1.6 Summary

Crtc1$^{-/-}$ mice exhibited cardiac hypertrophy with an increase in cardiomyocyte size.
They showed no signs of fibrosis and the fetal gene program was not activated. Furthermore, mRNA expression of α-skeletal actin was decreased. Proteomics and mRNA-Seq analysis did not reveal many differentially expressed proteins or mRNAs with known involvement in cardiac hypertrophy or heart failure.
To reveal the underlying mechanism for cardiac hypertrophy in *Crtc1*$^{-/-}$ mice CRE-dependent pathways were investigated.

4.2 Hypertrophic signaling in *Crtc1*$^{-/-}$ mice

4.2.1 Regulator of G-protein signaling (*Rgs*)

The results of chapter 4.1 indicate a hypertrophic development caused by the lack of *Crtc1* and therefore presumably the downregulation of antihypertrophic genes regulated by *Crtc1*. The regulator of G-protein signaling proteins are known to interact with GTP-bound G_{α} subunits and accelerate GTPase activity. The over 20 identified isoforms are known to differ in selectivity among $G_{\alpha\, i}$, $G_{\alpha\, q/11}$, and $G_{\alpha\, 12/13}$ subunits in distinct tissues (Mittmann et al. 2002; Kach et al. 2012).

4.2.1.1 Regulator of G-protein signaling 2 (Rgs2)

The regulator of G-protein signaling 2 (*Rgs2)* is a gene with a well-known involvement in cardiovascular disease. RGS2 is a selective inhibitor of $G_{\alpha\, q}$-coupled receptor dependent signaling (Gu et al. 2009; Tsang et al. 2010). In AMVM, it has been shown that short term treatment with the β-adrenoceptor agonist isoprenaline leads to an increase in RGS2 protein content (Chakir et al. 2011). Mice globally lacking *Rgs2* show no basal cardiac phenotype but develop cardiac hypertrophy and failure in response to afterload enhancement (Takimoto et al. 2009). Xie et al. identified a conserved cAMP-response element (CRE) in the murine *Rgs2* promoter that is critical for cAMP-response element-binding protein (CREB) binding and *Rgs2* promoter activation (Xie et al. 2011).

RT-qPCR and immunoblot analysis revealed a reduction in mRNA and protein expression of *Rgs2* in heart tissue of *Crtc1*$^{-/-}$ mice (Figure 4.9).

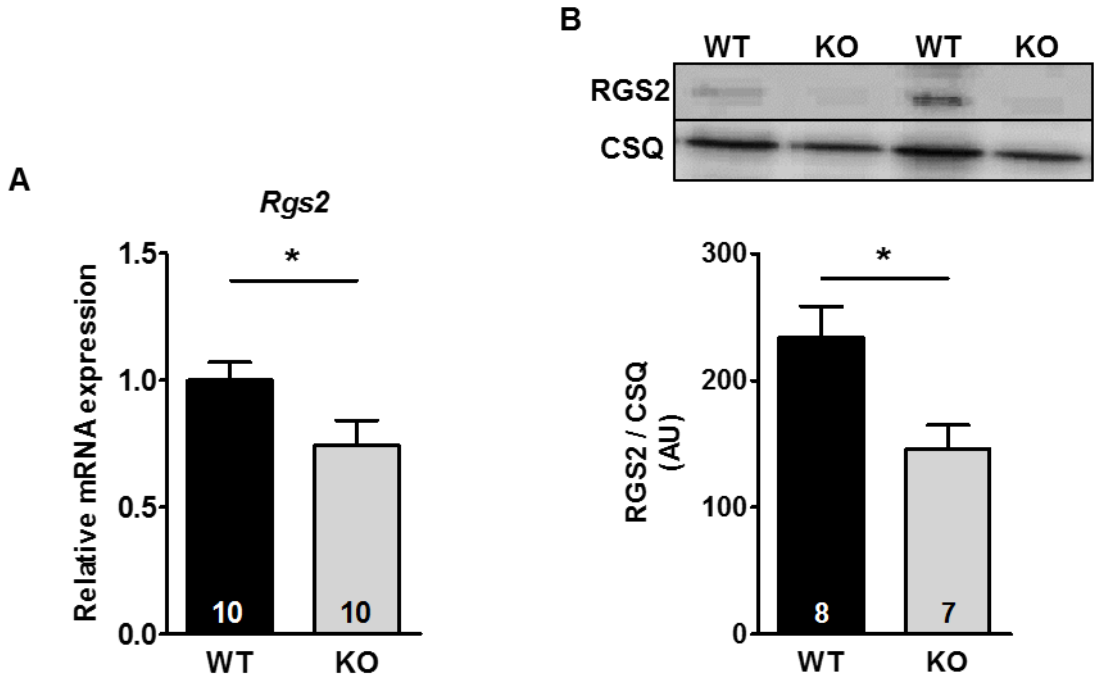

Figure 4.9: Reduced *Rgs2* mRNA and protein expression in *Crtc1*$^{-/-}$ mice. A. Quantitative evaluation of mRNA expression of *Rgs2* normalized to *GaS* in heart tissue of *Crtc1*$^{-/-}$ mice (KO) and their wild-type littermates (WT) relative to WT using ΔΔCt-method. **B**. Protein lysates from hearts of *Crtc1*$^{-/-}$ mice (KO) and their wild-type littermates (WT) were subjected to immunoblot analysis using an antibody against the regulator of G-protein signaling 2 (RGS2) normalized to calsequestrin (CSQ). Typical immunoblot (top)**;** quantitative evaluation (bottom). Data are expressed as mean±SEM; *p<0.05; unpaired Student's t-test; number of samples is given within the bars.

To investigate whether *Rgs2* promoter activity is regulated by CRTC1 or its isoform CRTC2, a luciferase reporter gene assay was conducted. HEK293T cells were transiently transfected with a luciferase reporter gene under control of the *Rgs2* promoter with either an intact or a mutated CRE, preventing CREB binding (Xie et al. 2011). These cells were cotransfected with either an expression vector for CRTC1, CRTC2 or an empty vector to even out the transfected amount of DNA. A GFP reporter gene under control of the CMV promoter was additionally cotransfected as control for transfection efficiency. To estimate the effect of CRTC1 and CRTC2 overexpression on the transcriptional activity of the *Rgs2* promoter, a titration with increasing amounts of the CRTC1 and CRTC2 expression vector (0.1 µg, 0.3 µg, or 1 µg) was performed (Figure 4.10). Transfection of 0.1 µg CRTC expression vector increased CRE-dependent transcriptional activity of the wild-type promoter construct. The transcriptional activity was further enhanced by increasing amounts of

CRTC expression vector. Transcriptional activity of the mutant *Rgs2* promoter was only observed after transfection of 1 µg CRTC2 expression vector.

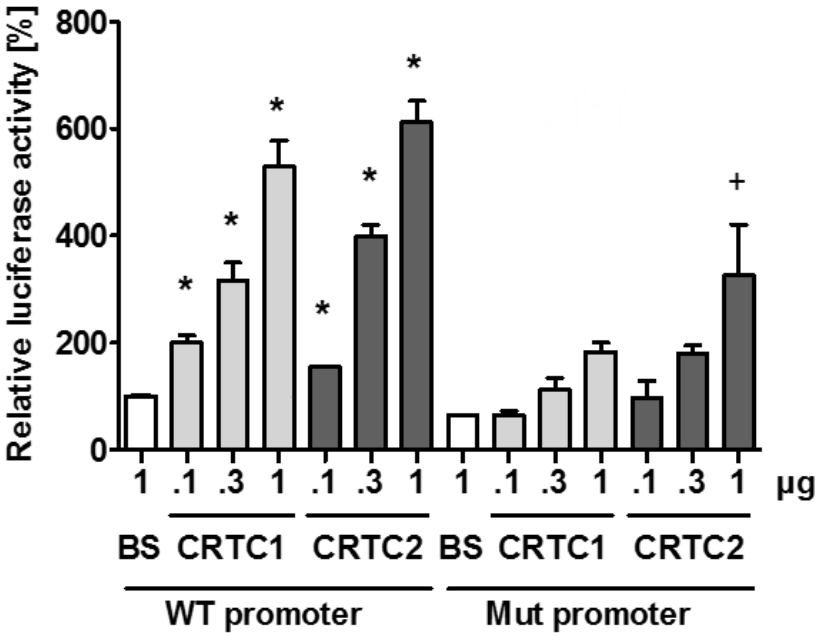

Figure 4.10: Concentration-response analysis of CRTC1 and CRTC2 on *Rgs2* promoter activity. A luciferase reporter gene under the control of the murine *Rgs2* promoter (-867 bp to +1 bp) (WT) or its mutant CREB binding-site (Mut) were transiently cotransfected into HEK293T cells together with the expression plasmids for Bluescript (BS), CRTC1 or CRTC2 (0.1 µg, 0.3 µg, 1 µg). Data are expressed as mean±SEM of three independent experiments performed in duplicates. *p<0.05 vs. WT *Rgs2* promoter transfected with BS; $^{+}$p<0.05 vs. Mut *Rgs2* promoter transfected with BS; one-way ANOVA followed by post hoc Bonferroni test.

For the following luciferase reporter gene assays, 0.1 µg CRTC1 or CRTC2 expression vector were used for transfection to diminish the effect of a CRTC1 or CRTC2 overload. Two days after transfection, cells were either left untreated or treated with the adenylyl cyclase activator forskolin (10 µmol/L) or isoprenaline (1 µmol/L) to increase intracellular cAMP concentration and thereby activate CRTC1 and CRTC2. This experiment showed an increase in basal activity of the wild-type *Rgs2* promoter by cAMP elevation through forskolin and isoprenaline as well as overexpression of CRTC1 and CRTC2. Forskolin treatment further increased the effect of the overexpressed CRTCs on transcriptional activity. The mutated *Rgs2* promoter exhibited less unstimulated transcriptional activity, which was not enhanced by forskolin or isoprenaline. Overexpression of CRTC1 or CRTC2 had no effect on *Rgs2* transcriptional activity of the mutated *Rgs2* promoter (Figure 4.11).

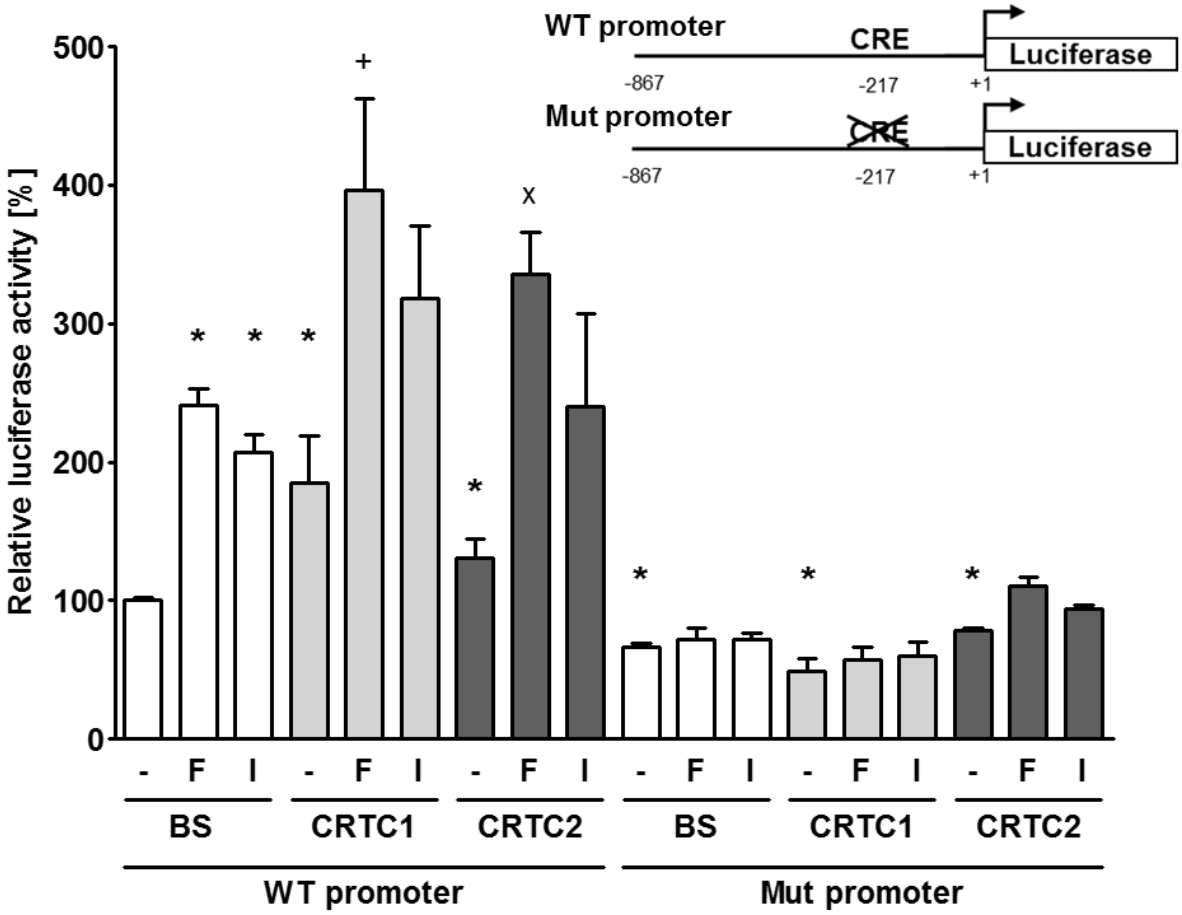

Figure 4.11: *Rgs2* promoter transcriptional activity was regulated by CRTC1 and CRTC2. A luciferase reporter gene under the control of the murine *Rgs2* promoter (-867 bp to +1 bp) (WT) or its mutant CREB binding-site (Mut) were transiently cotransfected into HEK293T cells together with the expression plasmids for Bluescript (BS), CRTC1 or CRTC2 (0.1 µg). Cells were treated with forskolin (F; 10 µmol/L) or isoprenaline (I; 1 µmol/L) 6 h prior to harvest. Data are expressed as mean±SEM of three independent experiments performed in duplicates. *p<0.05 vs. WT *Rgs2* promoter transfected with BS; $^{+}$p<0.05 vs. WT *Rgs2* promoter transfected with CRTC1; ^{x}p<0.05 vs. WT *Rgs2* promoter transfected with CRTC2; one-way ANOVA followed by post hoc Bonferroni test.

To investigate whether CRTC1 is recruited to the endogenous *Rgs2* promoter in murine heart tissue, a chromatin immunoprecipitation was performed. Recruitment of endogenous CRTC2 was not analyzed because no CRTC2 antibody applicable for chromatin immunoprecipitation was available.

In freshly removed adult murine heart tissue, CRTC1 cross-linked to DNA-bound CREB, was immunoprecipitated with an antibody directed against CRTC1. Immunoprecipitated DNA was subjected to PCR with specific primers for the *Rgs2* promoter. This revealed binding of CRTC1 to the *Rgs2* promoter *ex vivo*. Since IgG is not recruited to the *Rgs2* promoter, a chromatin immunoprecipitation using an antibody against IgG served as negative control (Figure 4.12 A). In neonatal mouse cardiomyocytes (NMCM) a chromatin immunoprecipitation revealed that CRTC1 recruitment to the *Rgs2* promoter relative to input

control could be increased by isoprenaline treatment (1 µmol/L; 30 min) by 38±18% (Figure 4.12 B).

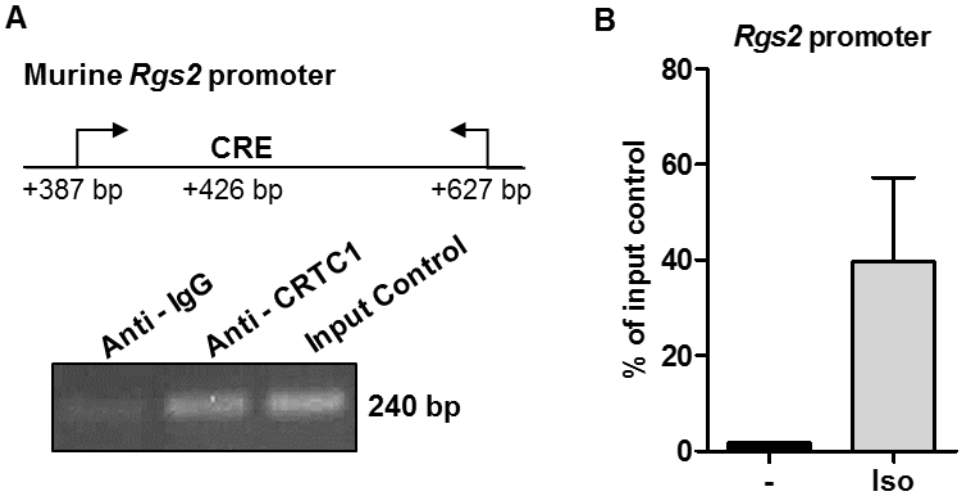

Figure 4.12: *Rgs2* promoter activity was regulated by CRTC1. A. Heart tissue from 9-week-old wild-type mice was subjected to chromatin immunoprecipitation using an antibody against CRTC1 and against IgG as negative control. The obtained DNA was amplified by PCR using specific primers for the *Rgs2* promoter. **B.** Neonatal mouse cardiomyocytes were incubated with isoprenaline (Iso; 1 µmol/L) 30 min before harvest. Cells were subjected to chromatin immunoprecipitation using an antibody against CRTC1. The obtained DNA was analyzed by RT-qPCR using specific primers for the *Rgs2* promoter and normalized to the input control. Data are expressed as mean±SEM.

4.2.1.2 Regulator of G-protein signaling 4 (Rgs4)

The regulator of G-protein signaling 4 (*Rgs4*) is another *Rgs* isoform capable of regulating G-protein-mediated hypertrophic signaling in the heart by inhibiting $G_{\alpha q}$- and $G_{\alpha i}$-coupled signaling (Gu et al. 2009). Davies et al. identified an activator protein (AP)-1R and AP-1F site including a CRE half-site, which is predicted to be a functional CRE and able to bind CREB, in the rat *Rgs4* promoter, making it a putative interaction target for CRTC1 (Davies et al. 2011).

Luciferase reporter gene constructs of the rat *Rgs4* promoter from the laboratory of Prof. David Carter (Cardiff University, UK) were used to determine CRTC1 influence on *Rgs4* promoter activity. Four different *Rgs4* promoter constructs were used for the luciferase reporter gene assay in HEK293T cells. To evaluate the effect of CRTC1 on the *Rgs4* promoter, decreasing amounts of the expression vector for CRTC1 (0.1 µg, 0.3 µg, 1 µg) were transfected in HEK293T cells together with either one of the four *Rgs4* promoter constructs (Figure 4.13). An empty vector to even out the amount of transfected DNA and a GFP

reporter gene to control for transfection efficiency were cotransfected. 1 µg CRTC1 expression vector led to an AP-1-dependent increase in transcriptional activity in both wild-type *Rgs4* promoter construct. Transcriptional activity was not induced by CRTC1 in the mutated *Rgs4* promoters.

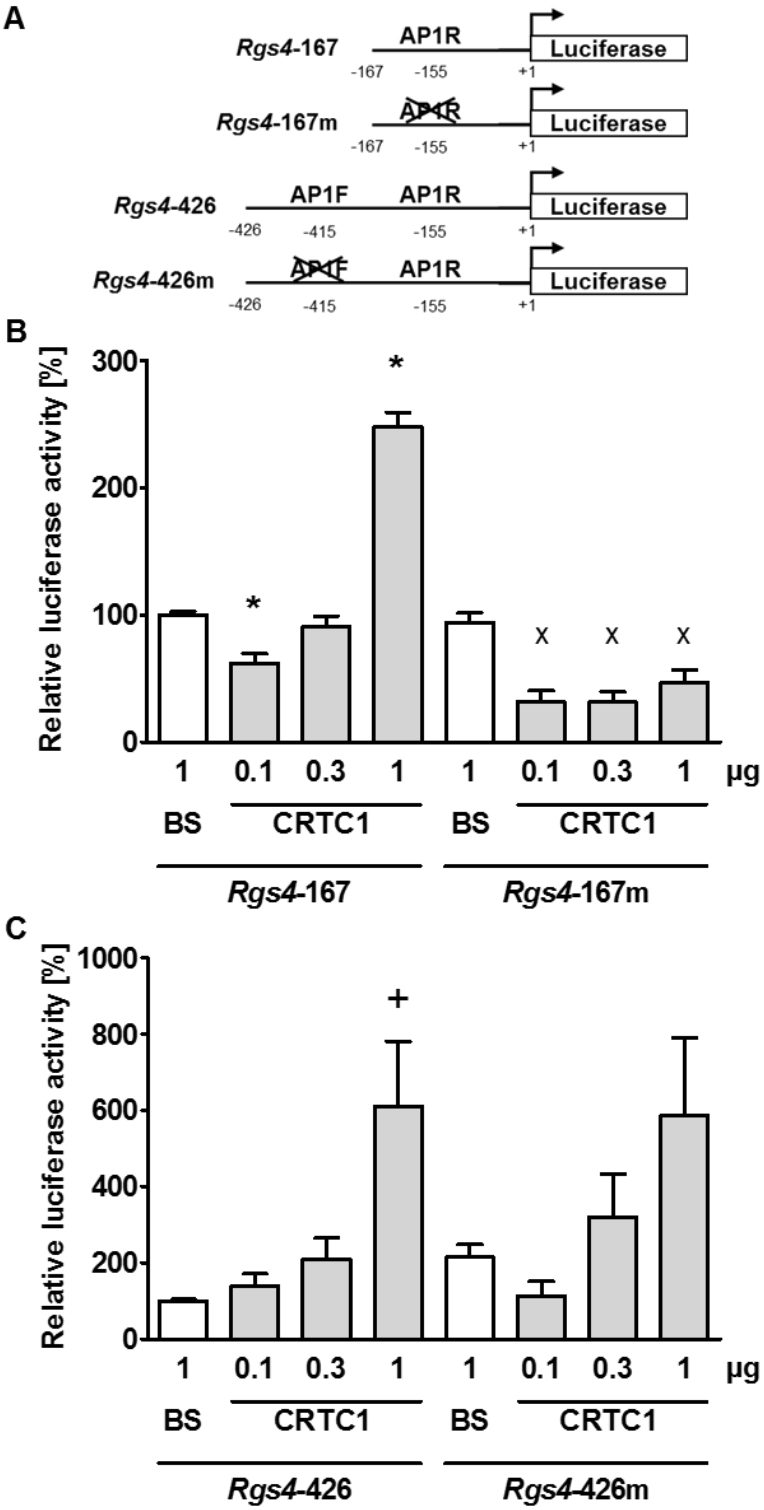

Figure 4.13: Concentration-response analysis of CRTC1 on *Rgs4* promoter activity. A. *Rgs4* luciferase reporter gene constructs. The positions of the -415 AP1F and -155 AP1R elements are indicated and are cancelled when mutated (*Rgs4*-167m and *Rgs4*-426m constructs). Adapted from Davies et al.

(2011). **B.** and **C.** Luciferase reporter genes under the control of different rat *Rgs4* promoter constructs were transiently cotransfected into HEK293T cells together with the expression plasmids for Bluescript (BS; 1 µg) and CRTC1 (0.1 µg, 0.3 µg, 1 µg). Data are expressed as mean±SEM of three independent experiments performed in duplicates. *p<0.05 vs. *Rgs4*-167 transfected with BS; ^{x}p<0.05 vs. *Rgs4*-167m transfected with BS; $^{+}$p<0.05 vs. *Rgs4*-426 transfected with BS; one-way ANOVA followed by post hoc Bonferroni test.

For the succeeding *Rgs4* luciferase reporter gene assays, 1 µg CRTC1 expression vector was used for transfection. Two days after transfection, HEK293T cells were either left untreated or treated with forskolin (10 µmol/L) or isoprenaline (1 µmol/L) to increase intracellular cAMP concentration and thereby activate endogenous CRTC1. This experiment showed an increase in *Rgs4*-167 promoter activity only when CRTC1 was overexpressed. Forskolin or isoprenaline treatment did not increase *Rgs4*-167 promoter activity. Transcriptional activity of the *Rgs4* promoter was decreased by additional treatment with forskolin or isoprenaline after CRTC1 overexpression. CRTC1 did not increase the transcriptional activity of the AP-1 site mutated promoter segments but transcriptional activity was increased after isoprenaline treatment additive to the effect of CRTC1 overexpression. The activity of the longer *Rgs4*-426 promoter was not increased by forskolin or isoprenaline. Overexpression of CRTC1 increased *Rgs4*-426 promoter activity. Additional treatment with forskolin or isoprenaline showed no differences in transcriptional activity. The activity of the mutated AP-1F site led to a loss of this activity increase induced by CRTC1 overexpression (Figure 4.14).

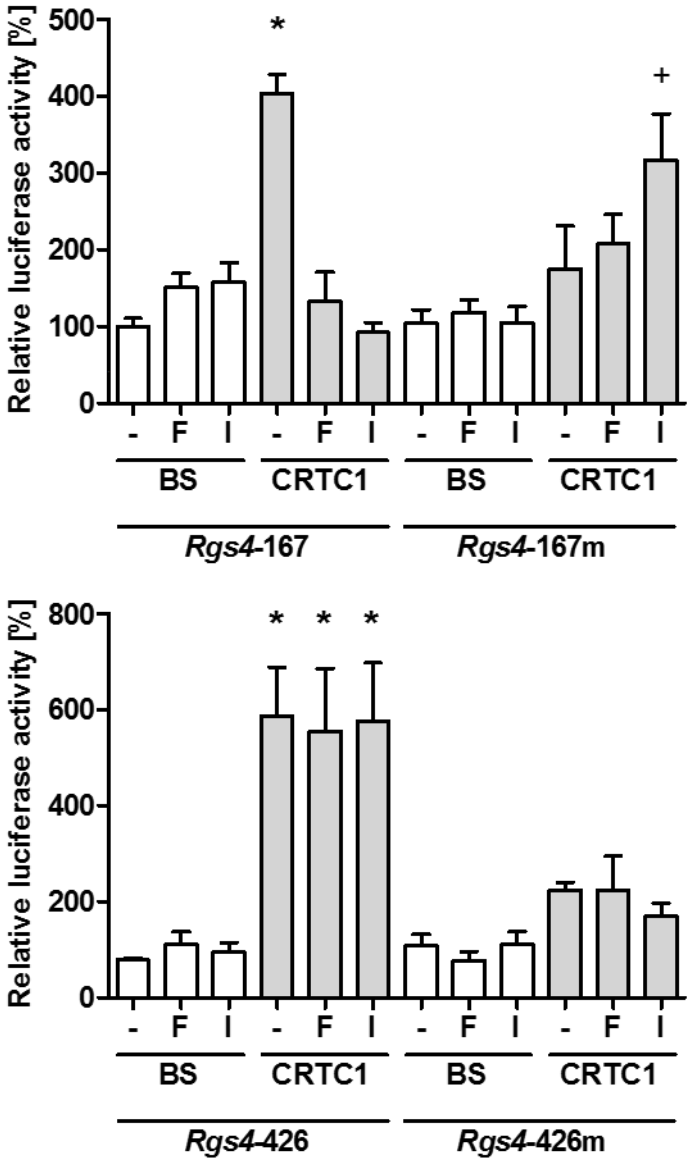

Figure 4.14: *Rgs4* promoter transcriptional activity was regulated by CRTC1. A luciferase reporter gene under the control of different rat *Rgs4* promoter constructs (see figure 4.13) were transiently co-transfected into HEK293T cells together with the expression plasmids for Bluescript (BS) or CRTC1 (1 µg). Cells were treated with forskolin (F; 10 µmol/L) or isoprenaline (I; 1 µmol/L) 6 h prior to harvest. Data are expressed as mean±SEM of three independent experiments performed in duplicates. *p<0.05 vs. *Rgs4*-167 or *Rgs4*-426 transfected with BS; one-way ANOVA followed by post hoc Bonferroni test.

To investigate whether CRTC1 is recruited to the *Rgs4* promoter in murine heart tissue, chromatin immunoprecipitation samples from NMCM treated with isoprenaline were amplified with PCR primers directed against the murine *Rgs4* promoter including its CRE half-site. This revealed binding of CRTC1 to the *Rgs4* promoter in NMCM with the possibility of an increase in binding after isoprenaline treatment (Figure 4.15).

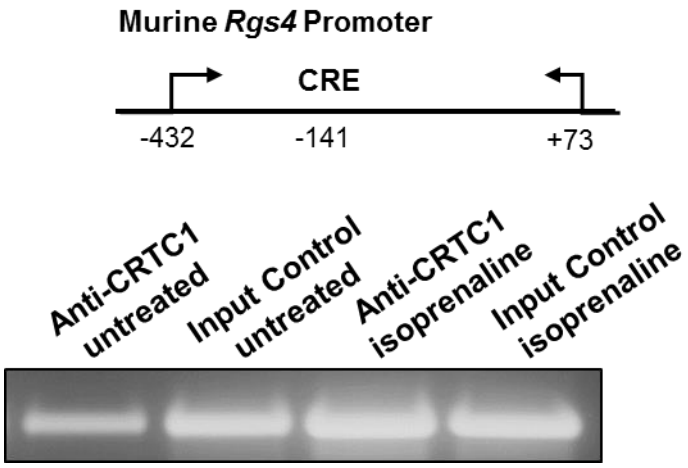

Figure 4.15: *Rgs4* promoter activity was regulated by CRTC1 in NMCM. Neonatal mouse cardiomyocytes were incubated with isoprenaline (1 µmol/L) 30 min before harvest. Cells were subjected to chromatin immunoprecipitation using an antibody against CRTC1. The obtained DNA and the input control were amplified by PCR using specific primers for the *Rgs4* promoter region including the CRE half-site.

Chromatin immunoprecipitation samples from adult heart tissue were amplified using the same PCR primers directed against the murine *Rgs4* promoter. Since IgG is not recruited to the *Rgs4* promoter, a chromatin immunoprecipitation using an antibody against IgG served as negative control. This immunoprecipitation showed that CRTC1 did not bind to this 505 bp region of the murine *Rgs4* promoter (Figure 4.16).

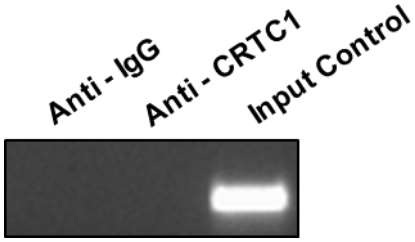

Figure 4.16: *Rgs4* promoter activity was not regulated by CRTC1 in heart tissue of adult mice. Heart tissue from 9-week-old wild-type mice was subjected to chromatin immunoprecipitation using an antibody against CRTC1 and against IgG as negative control. The obtained DNA was amplified by PCR using specific primers for the *Rgs4* promoter region including the CRE half-site site.

Furthermore, an immunoblot revealed no differences in RGS4 protein content in *Crtc1*$^{-/-}$ mice compared to WT (Figure 4.17).

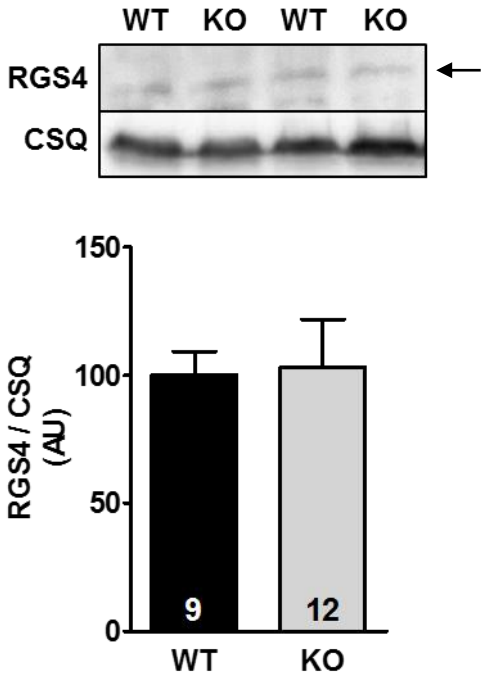

Figure 4.17: Unchanged RGS4 protein content. Protein lysates from hearts of 10- to 13-week-old *Crtc1*$^{-/-}$ mice (KO) and their wild-type littermates (WT) were subjected to immunoblot analysis using an antibody against the regulator of G-protein signaling 4 (RGS4) normalized to calsequestrin (CSQ). Typical immunoblot (top); quantitative evaluation (bottom). Data are expressed as mean±SEM; number of samples is given within the bars.

In concordance with the unchanged RGS4 protein content, *Rgs4* mRNA expression analysis revealed no difference between *Crtc1*$^{-/-}$ mice and WT. Moreover, mRNA expression of *Rgs3*, *Rgs5*, and *Rgs6*, all known to play a role in cardiac hypertrophy (Hao et al. 2006; Gu et al. 2009), did not differ between the genotypes (Figure 4.18).

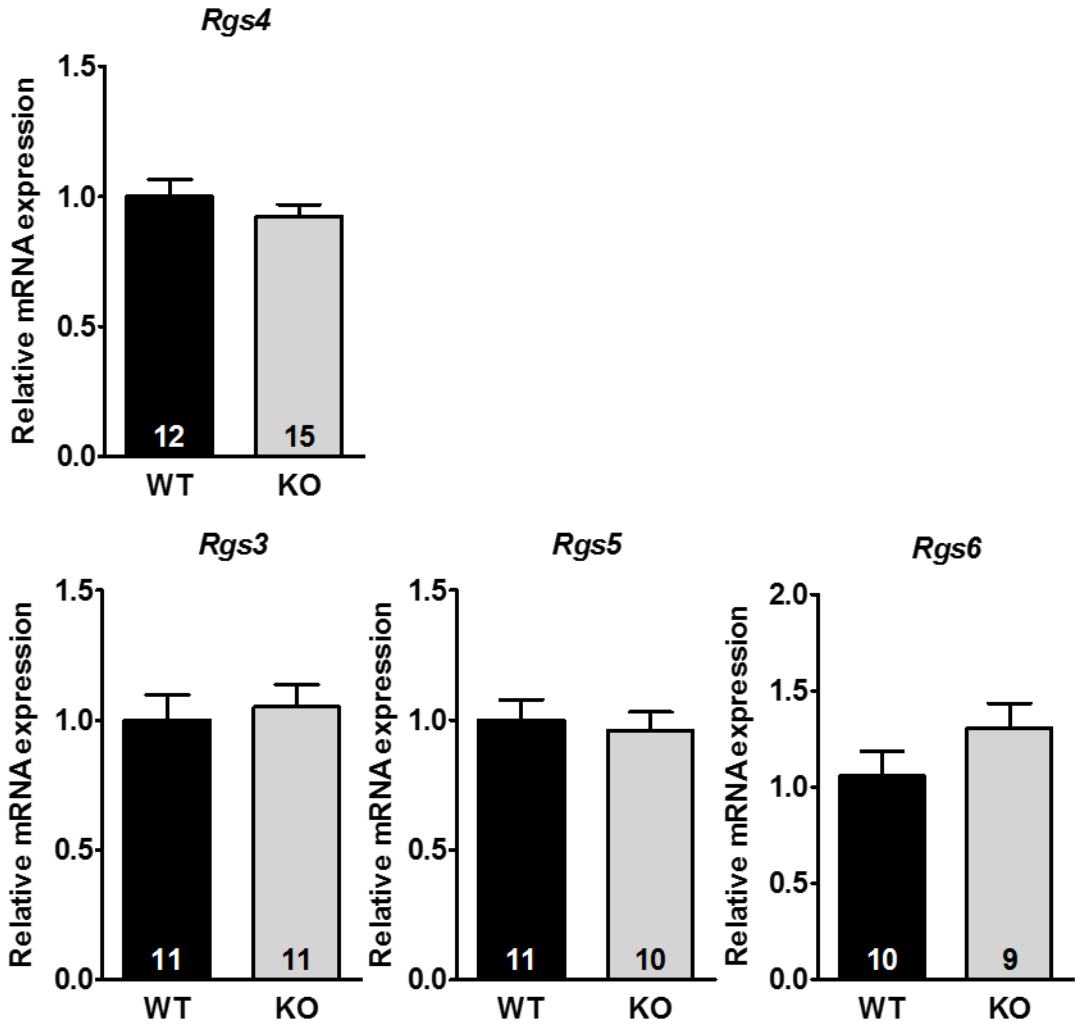

Figure 4.18: Unchanged *Rgs4*, *Rgs3*, *Rgs5*, and *Rgs6* mRNA expression in *Crtc1*$^{-/-}$ mice. Quantitative evaluation of mRNA expression of *Rgs4, Rgs3, Rgs5,* and *Rgs6* normalized to *GαS* using ΔΔCt-method. Data are expressed as mean±SEM relative to WT; number of samples is given within the bars.

These experiments revealed that the rat *Rgs4* promoter is regulated by CRTC1. In the murine heart however, *Rgs4* mRNA and protein expression were unchanged. The RGS4 antibody used seems to be untrustworthy due to a variety of detected proteins of different molecular weights. In NMCM a recruitment of CRTC1 to the *Rgs4* promoter was detectable while this recruitment was not seen in heart tissue of adult mice. A possible explanation might be the fact that CRTC1 content is more pronounced in neonatal than in adult mice (unpublished data from the group of Prof. Oetjen).

4.2.2 Phosphorylation of proteins following $G_{\alpha\ q/11}$ activation in *Crtc1*$^{-/-}$ mice

To investigate the effect of decreased RGS2 content in *Crtc1*$^{-/-}$ mice, signaling pathways downstream of the $G_{\alpha\ q/11}$-protein coupled receptor were investigated. Activation of the $G_{\alpha\ q/11}$-protein coupled receptor leads to phospholipase Cβ (PLCβ) -mediated generation of diacylglycerol (DAG), which leads to the activation of protein kinase C (PKC) and protein kinase D (PKD). PKC activation leads to an activating phosphorylation of the extracellular signal-regulated kinase 1 and 2 (ERK 1/2), which is known to contribute to concentric cardiomyocyte hypertrophy (Lorenz et al. 2009; Kehat et al. 2011). PKD has been shown to regulate contractile function through myofilament protein phosphorylation and contributes to pro-hypertrophic gene expression and therefore increases in cell size (Tilley 2011; Lorenz et al. 2014; Cotecchia et al. 2015). Akt is a protein kinase usually associated with physiological hypertrophy and activation by insulin and various growth factors. It has been reported that activated $G_{\alpha\ q}$-coupled receptor-mediated signaling inhibits phosphatidylinositol-4,5-bisphospate 3 kinase (PI3K). PI3K catalyzes the production of phosphatidylinositol-3,4,5-triphosphate (PIP3) which serves as second messenger to activate Akt (Sanchez-Fernandez et al. 2014). Phosphorylation of Akt by the phosphoinositide-dependent kinase-1 (PDK1) leads to an inhibition of the glycogen synthase kinase 3β (GSK3β) and subsequent inhibition of the nuclear factor of activated T-cells (NFAT) and thereby regulating cell size (Figure 4.19). While acute Akt activation is beneficial, chronic activation seems to increase cardiac hypertrophy (Heineke and Molkentin 2006; Harvey and Leinwand 2011; Maillet et al. 2013).

To investigate the crucial phosphorylation sites of these proteins in isolated cardiomyocytes, antibodies against the activating phosphorylation of Akt at serine 473, the autophosphorylation of PKD at serine 916 which correlates with catalytic activity, and activating phosphorylation of ERK 1/2 at threonine 202 and tyrosine 204 were used. All protein phosphorylation analysis was corrected for the unphosphorylated form of the proteins.

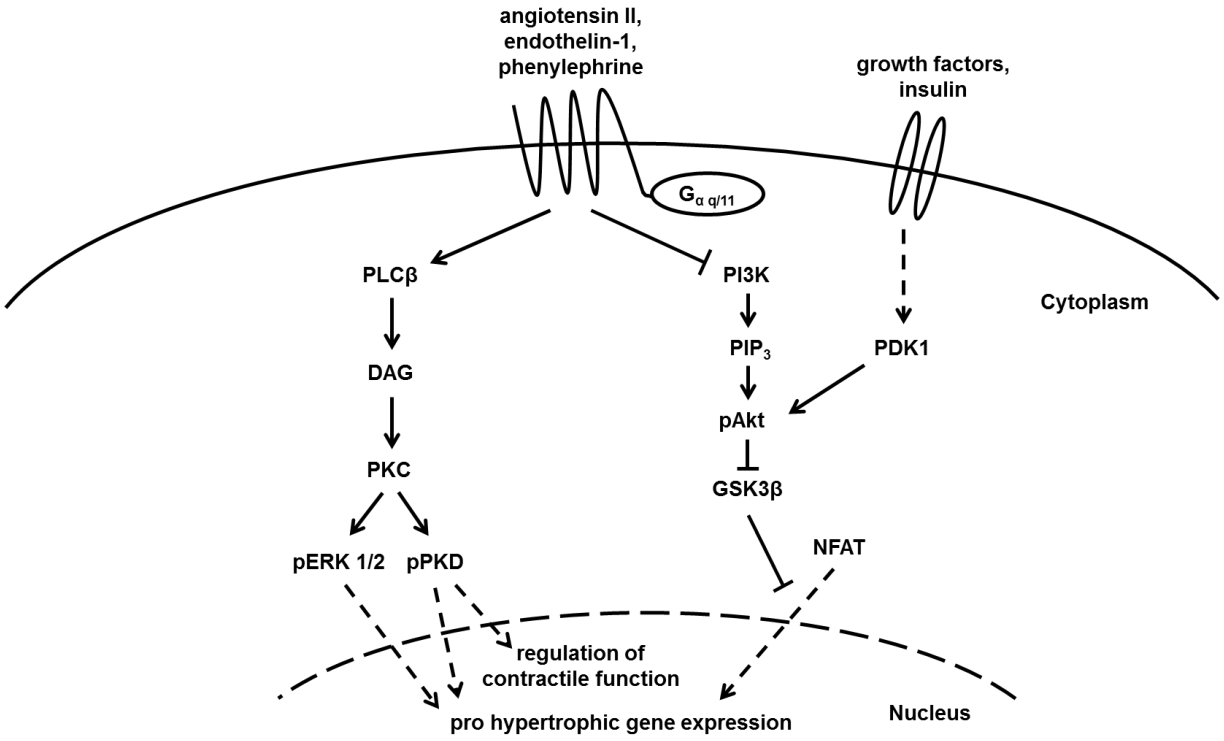

Figure 4.19: Akt, ERK 1/2, and PKD signaling pathway following $G_{\alpha\ q/11}$-coupled receptor activation. PLCβ, phospholipase Cβ; DAG, diacylglycerol; PKC, protein kinase C; PKD, protein kinase D; pERK 1/2, phosphorylated extracellular signal-regulated kinase 1/2; PI3K, phosphatidylinositol 3 kinase; PIP_3, phosphatidylinositol-3,4,5-triphosphate; pAkt, phosphorylated Akt; GSK3β, glycogen synthase kinase 3β; NFAT, nuclear factor for activated T-cells; PDK1, phosphoinositide-dependent kinase-1.

4.2.2.1 Phosphorylation of Akt, ERK 1/2, and PKD in AMVM

Isolated AMVM from 3 to 4 hearts were pooled and cultured overnight for recovery from digestion and sheer stress (Figure 4.20). After 20 h culture, the number of living, rod shaped cells was decreased but still sufficient for protein extraction. Cells were treated with isoprenaline (100 nmol/L), phenylephrine (100 µmol/L), an α_1-adrenoceptor agonist, a combination of both or angiotensin II (1 µmol/L), an agonist of $G_{\alpha q/11}$-coupled AT_1-receptors, endothelin-1 (100 nmol/L), an agonist of $G_{\alpha q}$-coupled endothelin receptors, or a combination of both for 10 min.

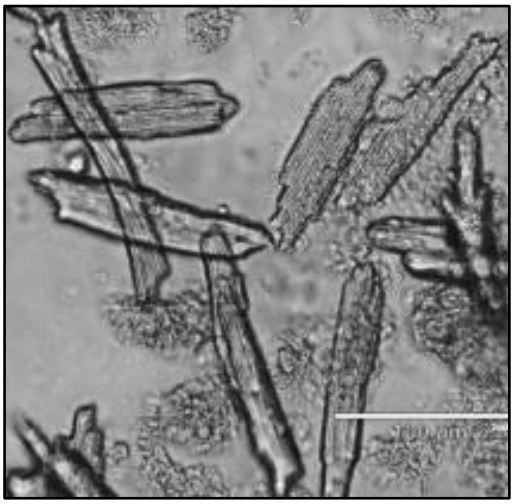

Figure 4.20: Isolated adult mouse ventricular myocytes. Representative microscopic image of cultured AMVM isolated from 10- to 13-week-old mice. Scale bar represents 100 µm.

Isoprenaline and phenylephrine treatment did not result in a phosphorylation of Akt nor ERK 1/2 neither in WT nor in *Crtc1*$^{-/-}$ AMVM. PKD phosphorylation was not detectable. Angiotensin II and endothelin-1 treatment led to no changes in Akt phosphorylation while an increase in ERK 1/2 phosphorylation in WT AMVM could be observed (Figure 4.21).

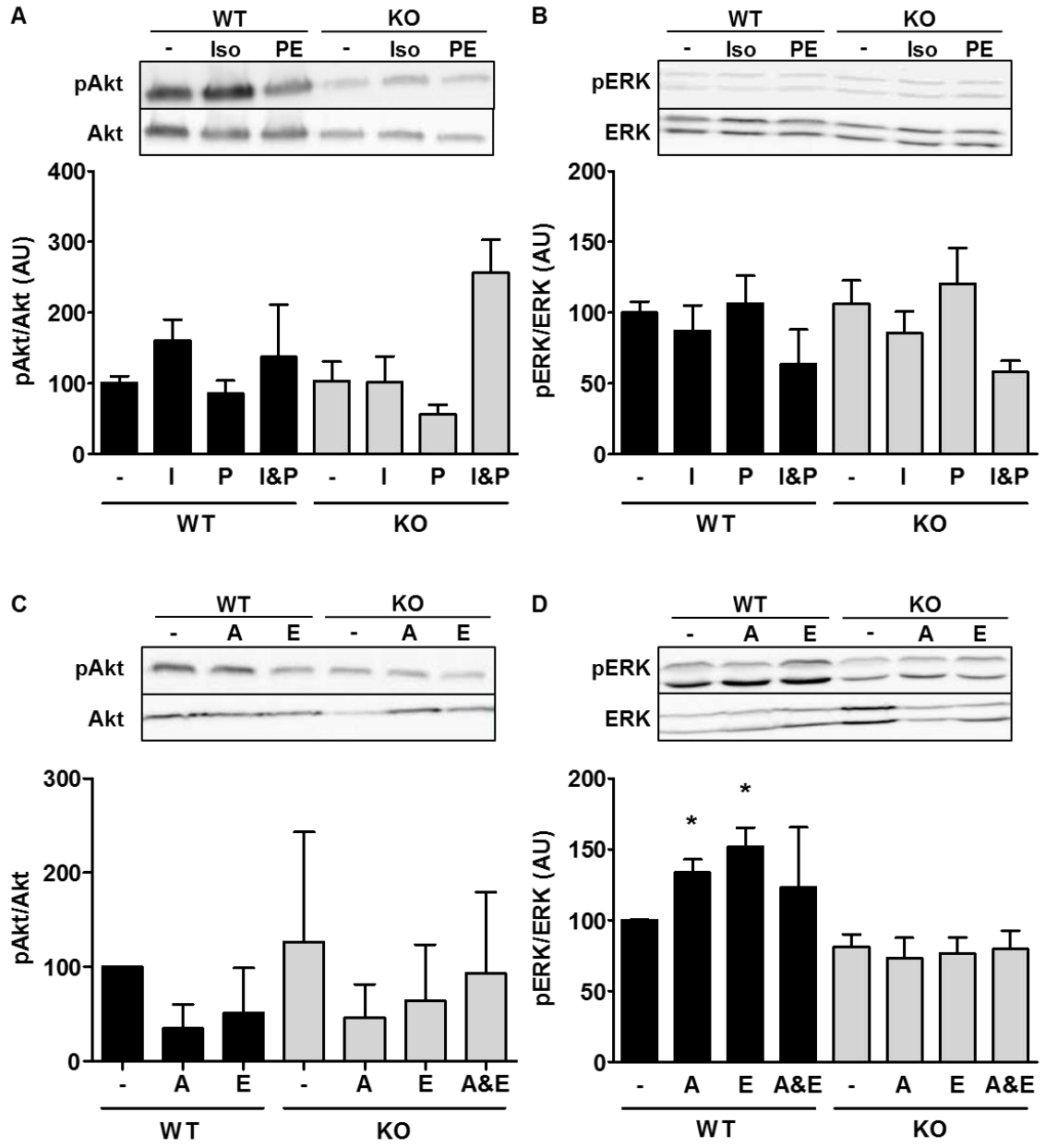

Figure 4.21: Akt and ERK 1/2 phosphorylation in cultured AMVM. Protein extracts from cultured adult mouse ventricular myocytes treated with isoprenaline (I; 100 nmol/L), phenylephrine (P, 100 µmol/L), angiotensin II (A; 1 µmol/L), and endothelin-1 (E; 100 nmol/L) 10 min prior to harvest were subjected to immunoblot analysis using antibodies for Ser473-phosphorylated Akt (pAkt; **A, C**) and Thr202/Tyr204-phosphorylated ERK 1/2 (pERK; **B, D**) normalized to total Akt and ERK 1/2, respectively. Typical immunoblot (top); quantitative evaluation of optical density relative to WT, untreated (bottom). Data are expressed as mean±SEM from AMVM preparations from 3 to 4 hearts; *p<0.05, one-way ANOVA followed by post hoc Bonferroni test.

The absence of response to $G_{\alpha\ s}$- and $G_{\alpha\ q/11}$-agonism and the observation that digestion of *Crtc1*$^{-/-}$ AMVM yielded a greater total number of isolated cardiomyocytes led to a change in the digestion protocol. Built upon the speculation, that *Crtc1*$^{-/-}$ AMVM may be overdigested, *Crtc1*$^{-/-}$ hearts were further on digested for 5.5 min instead of 7 min. With this change in protocol, about the same amount of cardiomyocytes was isolated from WT and

Crtc1$^{-/-}$ hearts. Additionally, AMVM were treated with endothelin-1 in this set of experiments.

Using this adapted protocol for AMVM isolation, phosphorylation of ERK 1/2 by the hypertrophic stimulus endothelin-1 was revealed. Endothelin-1 treatment did not result in a difference in Akt phosphorylation between genotypes. A decrease in basal phosphorylation could be observed in *Crtc1*$^{-/-}$ AMVM. PKD phosphorylation was increased in WT AMVM after endothelin-1 treatment. In *Crtc1*$^{-/-}$ AMVM, basal PKD phosphorylation was decreased and showed merely a tendency towards an increase by endothelin-1 treatment (Figure 4.22).

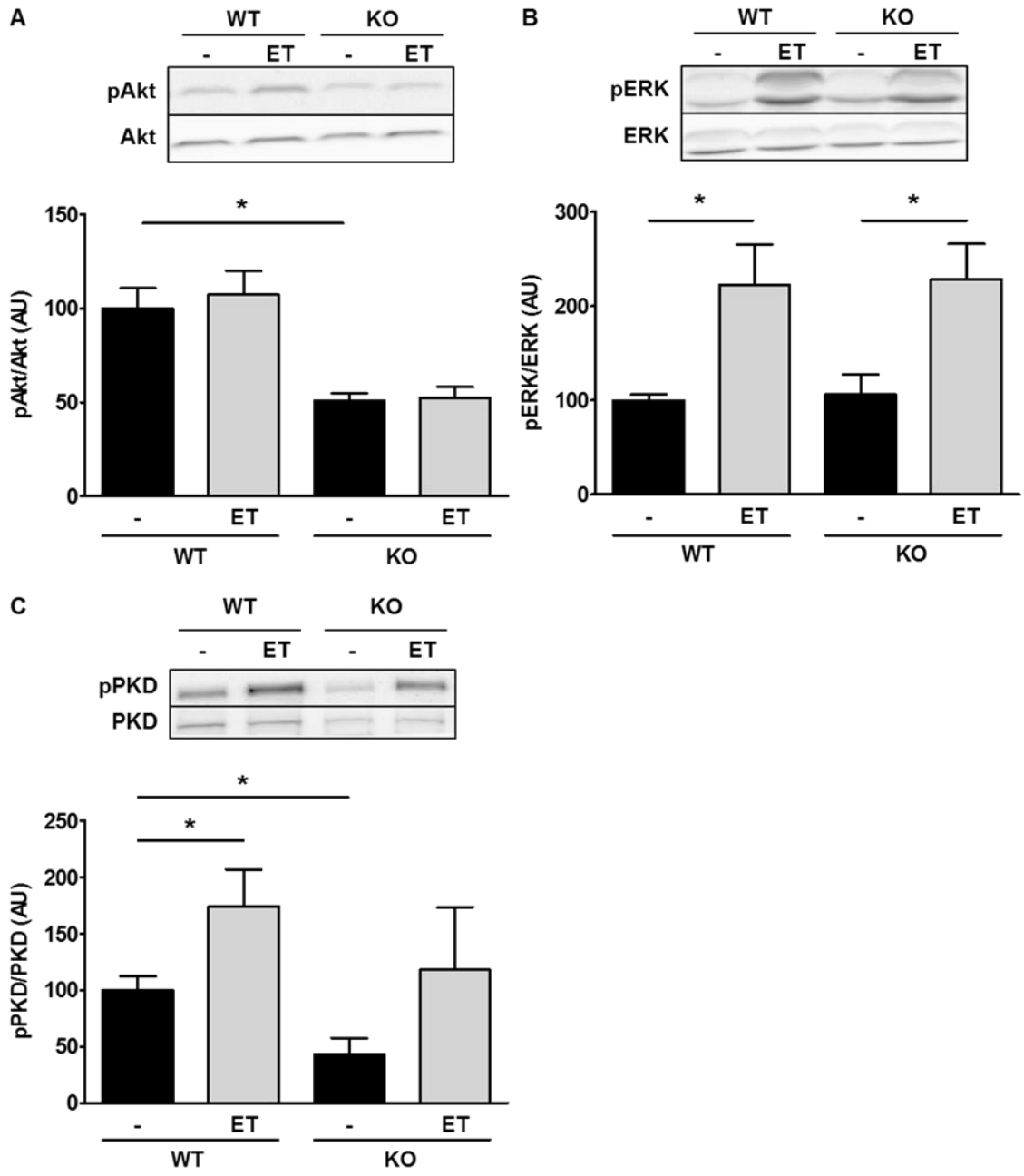

Figure 4.22: Protein phosphorylation in cultured AMVM. Protein extracts from cultured adult mouse ventricular myocytes treated with endothelin-1 (ET; 100 nmol/L) 10 min prior to harvest were subjected to immunoblot analysis using antibodies for (**A**) Ser473-phosphorylated Akt (pAkt), (**B**) Thr202/Tyr204-phosphorylated ERK 1/2 (pERK), and (**C**) Ser916-phosphorylated PKD (pPKD) normalized to total Akt, ERK 1/2, and PKD, respectively. Typical immunoblot (top); quantitative evaluation of optical density relative to WT, untreated (bottom). Data are expressed as mean±SEM from protein from 5-7 AMVM preparations; *p<0.05, one-way ANOVA followed by post hoc Bonferroni test.

In an additional set of experiments, AMVM were treated immediately after isolation to rule out a change of signaling transduction due to overnight culture conditions. Cells were treated with 10 nmol/L and 100 nmol/L isoprenaline for 10 min. This experiment revealed an increase in ERK 1/2 phosphorylation in *Crtc1*$^{-/-}$ AMVM while no effect of isoprenaline treatment could be detected (Figure 4.23).

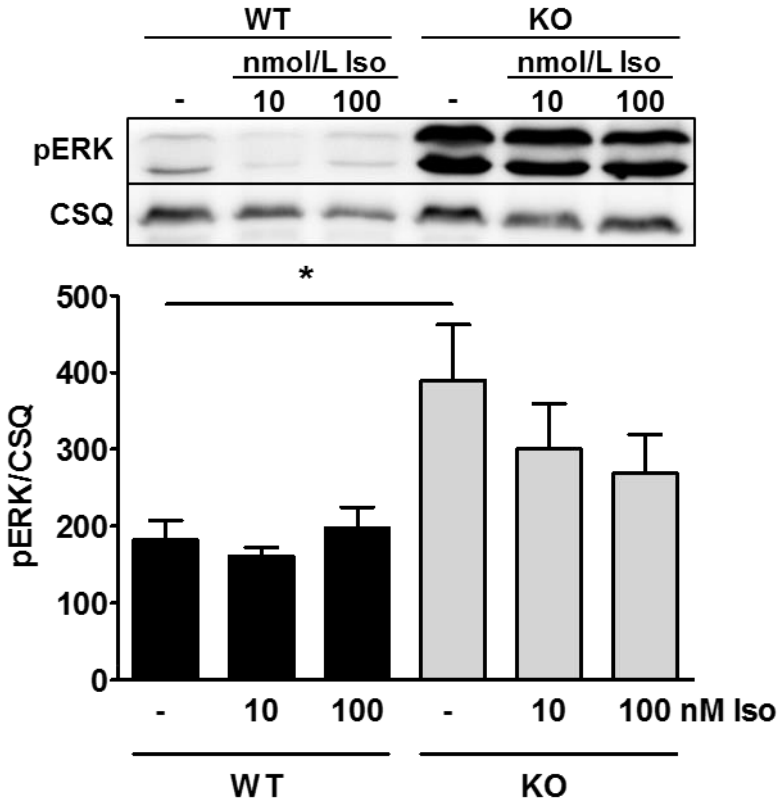

Figure 4.23: ERK 1/2 phosphorylation in AMVM. Protein extracts from AMVM stimulated with isoprenaline (Iso; 10 nmol/L or 100 nmol/L) 10 min prior to harvest were subjected to immunoblot analysis using an antibody for Thr202/Tyr204-phosphorylated ERK 1/2 (pERK) normalized to calsequestrin (CSQ). Typical immunoblot (top); quantitative evaluation of optical density relative to WT, untreated (bottom). Data are expressed as mean±SEM from 6 AMVM preparations; *p<0.05, one-way ANOVA followed by post hoc Bonferroni test.

4.2.3 Summary

mRNA and protein expression of the antihypertrophic *Rgs2* was decreased in *Crtc1*$^{-/-}$ mice. The murine *Rgs2* promoter activity was regulated by CRTC1 in HEK293T cells and murine heart tissue. Furthermore, rat *Rgs4* promoter activity was induced by CRTC1 in HEK293T cells. Murine *Rgs4* promoter activity was regulated by CRTC1 in NMCM but not in adult heart tissue. mRNA expression of *Rgs3, Rgs4, Rgs5,* and *Rgs6* was not differentially expressed in *Crtc1*$^{-/-}$ mice. In freshly isolated *Crtc1*$^{-/-}$ AMVM, ERK 1/2 phosphorylation was increased. In overnight cultured *Crtc1*$^{-/-}$ AMVM, Akt and PKD phosphorylation was decreased while ERK 1/2 phosphorylation remained unchanged.
This suggests increased $G_{\alpha\ q/11}$ -protein coupled receptor-mediated signaling due to decreased *Rgs2* expression in *Crtc1*$^{-/-}$ mice.
Since cardiac hypertrophy is often associated with changes in cardiac function, systolic and diastolic function were investigated in *Crtc1*$^{-/-}$ mice.

4.3 Cardiac function in *Crtc1*$^{-/-}$ mice

4.3.1 Echocardiographic analysis

To determine if the loss of *Crtc1* affects cardiac function, an echocardiographic analysis was performed under isoflurane anesthesia on mice aged 8 to 9 weeks (Figure 4.24). *Crtc1*$^{-/-}$ mice showed impaired systolic function indicated by a decrease in cardiac output, ejection fraction, and fractional shortening by 42±10%, 45±7%, and 50±14%, respectively. Furthermore, left ventricular volume was increased during systole (28±9%) and diastole (11±3%). The difference between systolic and diastolic left ventricular anterior wall thickness (AWTh) was measured to assess the contractile force. In *Crtc1*$^{-/-}$ mice this difference was reduced by 19% indicating decreased contractile abilities. Left ventricular posterior and anterior wall thicknesses themselves showed no difference in systole and diastole. Heart rate remained unchanged between genotypes (Table 4.1).

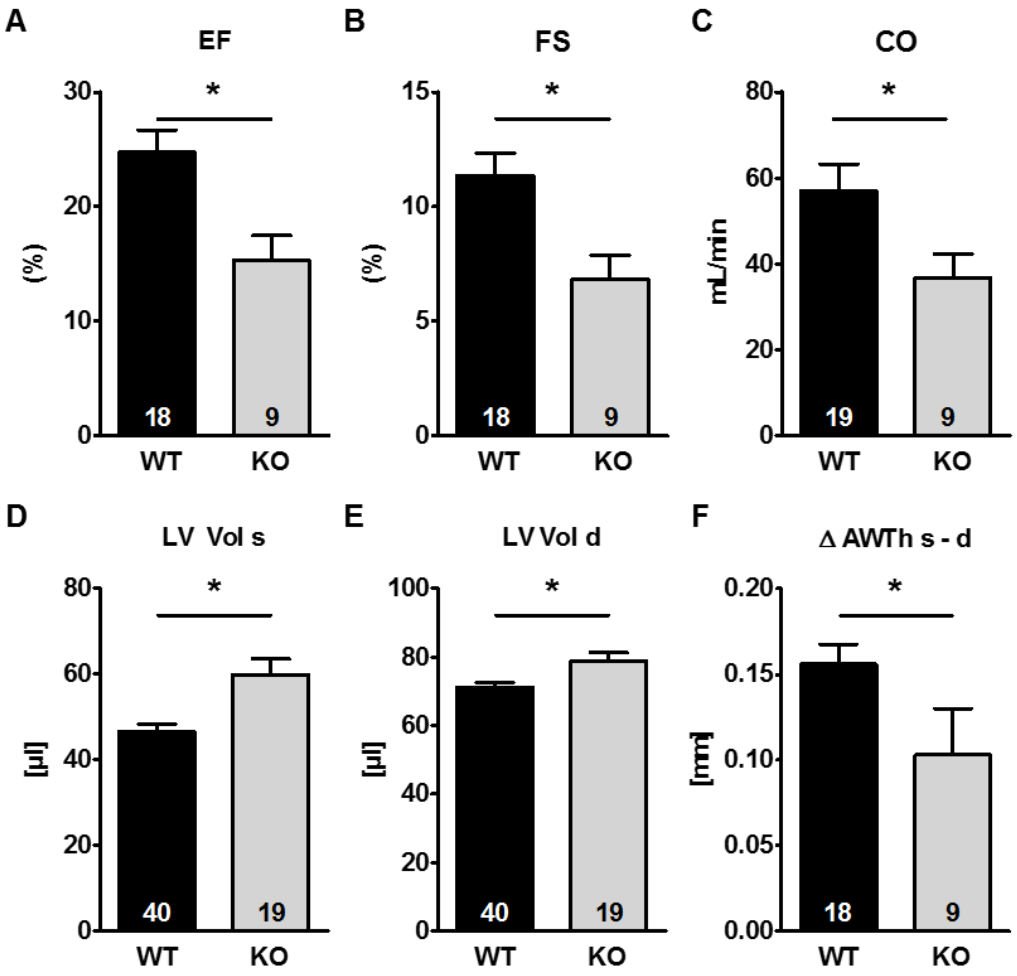

Figure 4.24: Decreased cardiac function in *Crtc1*$^{-/-}$ mice. Heart function of *Crtc1*$^{-/-}$ mice (KO) and their wild-type littermates (WT) was evaluated by echocardiography at the age of 8 to 9 weeks. Ejection fraction (EF), fractional shortening (FS), cardiac output (CO), endsystolic left ventricular volume (LV Vol s), enddiastolic left ventricular volume (LV Vol d), and fractional shortening of left ventricular anterior wall thickness (Δ AWTh s-d) was assessed. Data are expressed as mean±SEM; *p<0.05, Student's t-test; number of mice is given within the bars.

Table 4.1: Unchanged echocardiographic parameters in *Crtc1*$^{-/-}$ mice. Heart function of *Crtc1*$^{-/-}$ mice (KO) and their wild-type littermates (WT) was evaluated by echocardiography at the age of 8 to 9 weeks. Left ventricular endsystolic posterior wall thickness (PWTh s), enddiastolic posterior wall thickness (PWTh d), endsystolic anterior wall thickness (AWTh s), enddiastolic anterior wall thickness (AWTh d), and heart rate (HR) were measured. Data are expressed as mean±SEM.

	PWTh s (mm)	PWTh d (mm)	AWTh s (mm)	AWTh d (mm)	HR (bpm)
WT	0.47±0.02 (n=19)	0.35±0.02 (n=19)	0.45±0.02 (n=19)	0.28±0.02 (n=19)	400±10 (n=19)
KO	0.46±0.02 (n=9)	0.34±0.02 (n=9)	0.39±0.03 (n=9)	0.29±0.02 (n=9)	404±14 (n=9)

4.3.2 Phosphorylation of contractile proteins in *Crtc1*$^{-/-}$ mice

To further elucidate the cardiac function, the phosphorylation of phospholamban (PLN) and the sarcomeric proteins troponin I (TnI) and cardiac myosin binding protein C (cMybpC) in cardiomyocytes was investigated. Phospholamban is an inhibitor of cardiac muscle sarcoplasmic reticulum Ca^{2+}-ATPase (SERCA2a). Serine 16 phosphorylated phospholamban dissociates from the SERCA2a calcium pump, increasing its activity. This leads to a higher Ca^{2+}-reuptake into the sarcoplasmic reticulum. Troponin I is part of the troponin protein complex in the myofilament next to troponin C, troponin T, and tropomyosin. Phosphorylation of TnI at serine 23/24 by PKA leads to a reduced association between TnI and TnC followed by a decrease in Ca^{2+}-binding affinity of TnC and therefore decreased myofilament Ca^{2+}-sensitivity. cMybpC is a protein of the myofilament binding to myosin, actin, and titin playing a role in the sarcomere organization. Upon phosphorylation by PKA at serine 282, binding to actin is enhanced followed by accelerated cross bridge formation. All three proteins are responsible for enhancement in force development and accelerated relaxation when phosphorylated (Solaro and Rarick 1998; El-Armouche and Eschenhagen 2009; Lopes and Elliott 2014; Yin et al. 2015).

To study the phosphorylation status of these three proteins, adult cardiomyocytes were isolated, treated with 10 nmol/L or 100 nmol/L isoprenaline for 10 min, and protein lysates were subjected to immunoblot analysis. In AMVM from WT mice phosphorylation of all three contractile proteins was increased in response to both 10 nmol/L and 100 nmol/L isoprenaline. AMVM from *Crtc1*$^{-/-}$ mice showed a reduced response to isoprenaline: TnI phosphorylation was increased after treatment with 100 nmol/L isoprenaline (Figure 4.25 A), while cMybpC phosphorylation was not increased by either isoprenaline concentration (Figure 4.25 B). PLN phosphorylation was increased by 10 and 100 nmol/L isoprenaline in both genotypes (Figure 4.25 C). This suggests a decreased contractile function of the myofilaments in *Crtc1*$^{-/-}$ mice in response to isoprenaline while signaling from the β-adrenoceptor to PKA seems to be intact as indicated by functioning PLN phosphorylation.

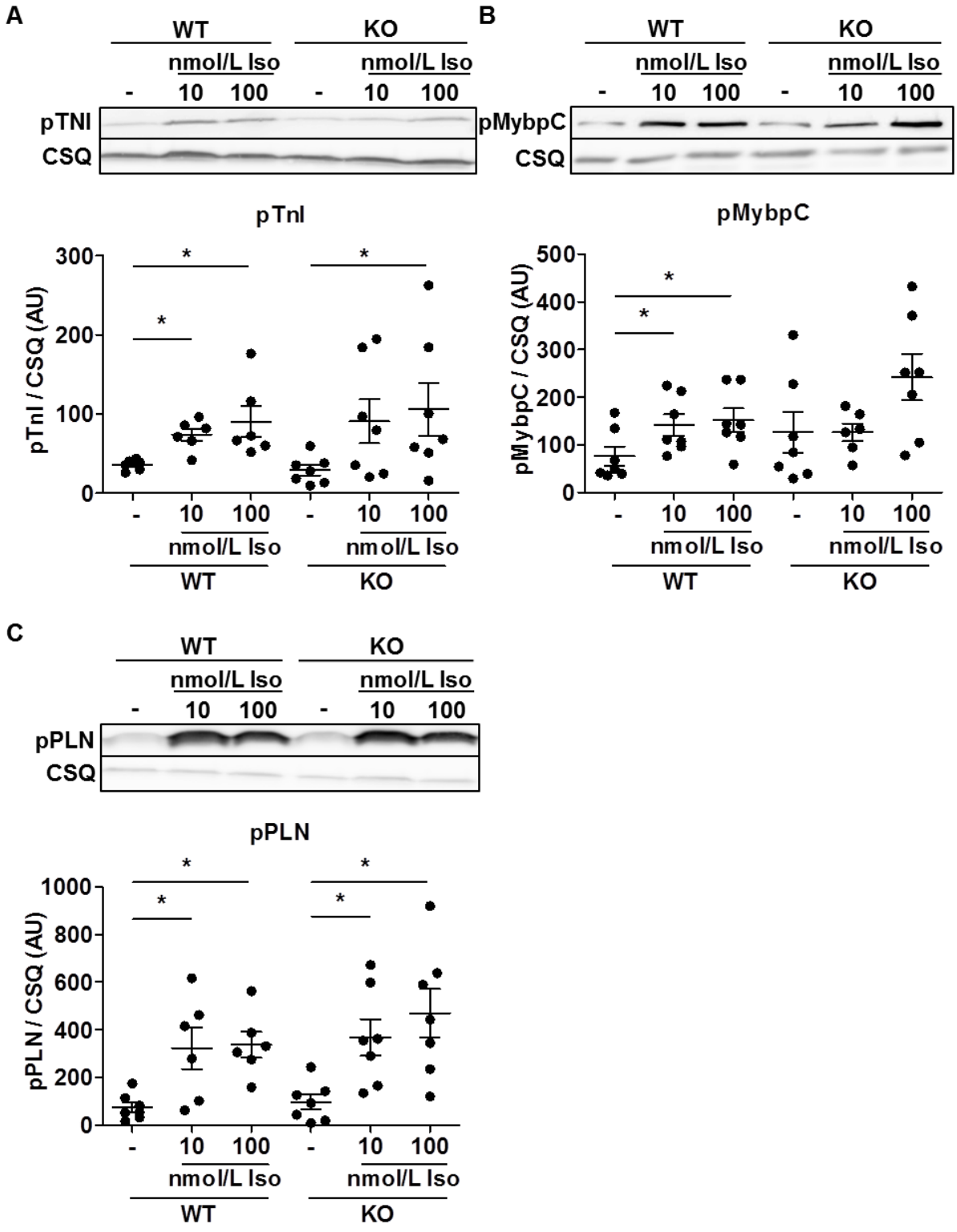

Figure 4.25: Phosphorylation of PKA-target proteins in *Crtc1*$^{-/-}$ mice and their wild-type littermates. Protein extracts from adult mouse ventricular cardiomyocytes treated with 10 nmol/L or 100 nmol/L isoprenaline (Iso) for 10 min were subjected to immunoblot analysis using antibodies for (**A**) Ser23/24-phosphorylated cardiac troponin I (pTnI), (**B**) Ser282-phosphorylated MybpC (pMybpC), or (**C**) Ser16-phosphorylated phospholamban (pPLN) normalized to calsequestrin (CSQ). Typical immunoblot (top); quantitative evaluation of optical density relative to reference (bottom). KO, *Crtc1*$^{-/-}$ mice; WT, wild-type littermates. Data are expressed as mean±SEM; *p<0.05, one-way ANOVA, followed by post hoc Bonferroni test.

4.3.3 Summary

Crtc1$^{-/-}$ mice showed impaired systolic function with decreased cardiac output, ejection fraction, and fractional shortening. Ventricular filling volume was increased in *Crtc1*$^{-/-}$ mice. The sarcomeric contractile proteins TnI and cMybpC exhibited a decreased phosphorylation response to isoprenaline treatment in isolated AMVM.
In the following experiments, the effect of chronic isoprenaline treatment on cardiac function was investigated in *Crtc1*$^{-/-}$ mice.

4.4 Isoprenaline-induced hypertrophy in *Crtc1*$^{-/-}$ mice

As a model for hypertrophy induced by increased β-adrenergic signaling, the effect of 7-day isoprenaline treatment in *Crtc1*$^{-/-}$ mice was assessed. For this matter, osmotic micro pumps, releasing isoprenaline at 30 µg/g body weight per day, were implanted into WT and *Crtc1*$^{-/-}$ mice at the age of 7 to 8 weeks. Control animals received 0.9% NaCl solution. To evaluate the effect of isoprenaline on heart function, hearts were analyzed by echocardiographic analysis before and 7 days after implantation.

4.4.1 Cardiac function

The isoprenaline treatment in *Crtc1*$^{-/-}$ mice led to an amelioration of cardiac output, ejection fraction, and fractional shortening to the functional level of treated WT. In *Crtc1*$^{-/-}$ mice the increase in cardiac output, ejection fraction, and fractional shortening between NaCl and isoprenaline treated mice was 1.28 fold, 1.25 fold, and 2 fold higher, respectively, compared to WT. Even though, no difference in left ventricular mass (LVM) to tibia length (TL) could be observed between the genotypes at this age (8 to 9 weeks), isoprenaline treatment increased the LVM/TL ratio in WT and *Crtc1*$^{-/-}$ mice indicating a hypertrophic effect of isoprenaline (Figure 4.26). Parameters increased by isoprenaline treatment that remained unchanged between genotypes are shown in table 4.2.

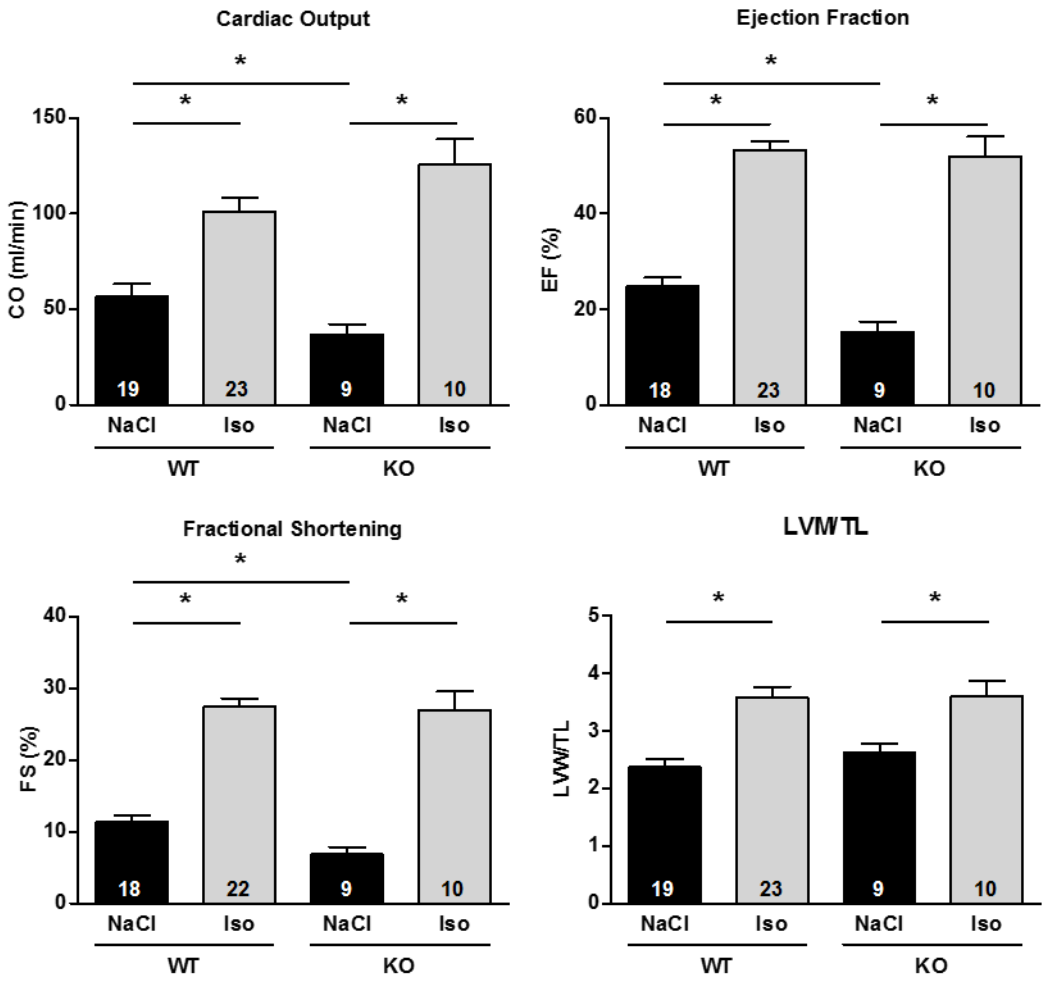

Figure 4.26: Ameliorated cardiac function in *Crtc1*$^{-/-}$ mice after isoprenaline treatment. Cardiac output (CO), ejection fraction (EF), fractional shortening (FS), and the ratio of left ventricular mass (LVM) to tibia length (TL) were investigated by echocardiography in mice at the age of 8 to 9 weeks. *Crtc1*$^{-/-}$ mice (KO) and their wild-type littermates (WT) were either treated with isoprenaline (Iso; 30 µg/g/day) or solvent (NaCl) for 7 days. Data are expressed as mean±SEM. *p<0.05; one-way ANOVA followed by post hoc Bonferroni test; number of mice is given within the bars.

Table 4.2: Echocardiographic parameters increased by isoprenaline treatment with no difference between genotypes. Left ventricular endsystolic posterior wall thickness (PWTh s), enddiastolic posterior wall thickness (PWTh d), endsystolic anterior wall thickness (AWTh s), enddiastolic anterior wall thickness (AWTh d), and heart rate (HR) were measured by echocardiography in 8- to 9-week-old mice treated with isoprenaline (Iso; 30 µg/g/day) or solvent (NaCl) for 7 days. Data are expressed as mean±SEM.

	PWTh s NaCl (mm)	PWTh s Iso (mm)	PWTh d NaCl (mm)	PWTh d Iso (mm)		
WT	0.47±0.02 (n=19)	0.9±0.03 (n=22)	0.35±0.02 (n=19)	0.48±0.02 (n=23)		
KO	0.46±0.02 (n=9)	0.76±0.04 (n=19)	0.34±0.02 (n=9)	0.41±0.02 (n=10)		
	AWTh s NaCl (mm)	AWTh s Iso (mm)	AWTh d NaCl (mm)	AWTh d Iso (mm)	HR NaCl (bpm)	HR Iso (bpm)
WT	0.45±0.02 (n=19)	0.95±0.04 (n=22)	0.28±0.02 (n=19)	0.41±0.02 (n=23)	400±10 (n=19)	530±16 (n=23)
KO	0.39±0.03 (n=9)	0.87±0.06 (n=10)	0.29±0.02 (n=9)	0.39±0.03 (n=10)	404±14 (n=9)	538±20 (n=10)

4.4.2 mRNA expression

Heart tissue from isoprenaline- or NaCl-treated mice was analyzed for *Crtc1*, *Col1α1*, and *Col3α1* mRNA expression by RT-qPCR. 7-day isoprenaline treatment did not change the mRNA expression (Figure 4.27). A longer treatment with isoprenaline or evaluation of more mice might reveal differences in mRNA expression.

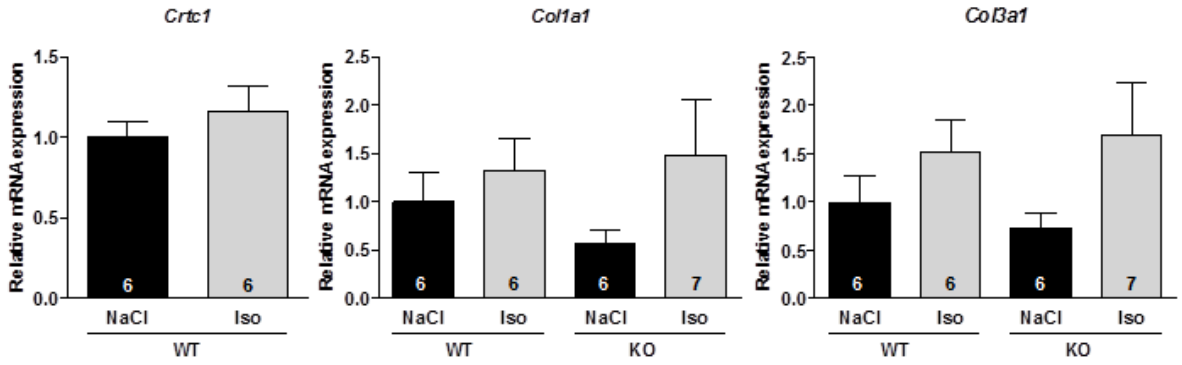

Figure 4.27: Isoprenaline treatment did not change *Crtc1*, *Col1α1,* and *Col3α1* mRNA expression. Quantitative evaluation of mRNA expression of *Crtc1*, *Col1α1,* and *Col3α1* normalized to *GαS* using ΔΔCt-method in *Crtc1*$^{-/-}$ mice (KO) and their wild-type littermates (WT) treated with isoprenaline (Iso; 30 µg/g/day) or solvent (NaCl) for 7 days. Data are expressed as mean±SEM relative to WT treated with NaCl; number of samples is given within the bars.

4.4.3 Micro-array based expression analysis of mRNA

To identify genes regulated by isoprenaline-induced hypertrophy, a micro-array based expression analysis was conducted. This deep-sequencing approach reveals differentially expressed mRNA after isoprenaline treatment.

Heart powder from WT mice treated with NaCl or isoprenaline were used for mRNA extraction. The obtained mRNA was analyzed by the group of Prof. Norbert Hübner (MDC, Berlin). Differentially expressed mRNA is depicted in figure 4.28. Upregulated mRNA was mostly involved in metabolic and biosynthetic processes as well as signal transduction. Downregulated mRNA expression was mostly involved in cell proliferation, cell death, organ development, and also metabolic processes.

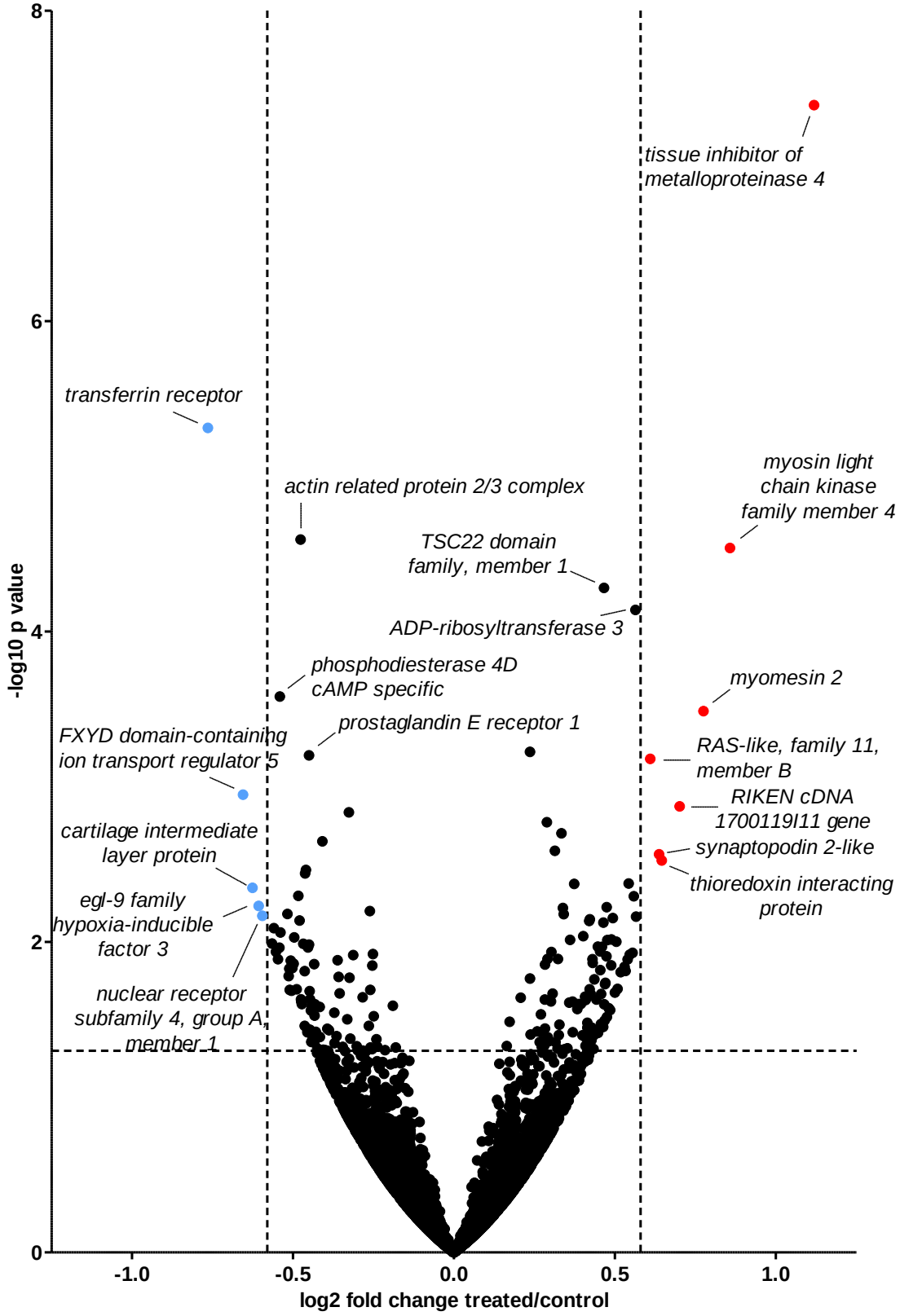

Figure 4.28: Differentially expressed mRNA by isoprenaline treatment. mRNA from mice treated with isoprenaline (treated) or solvent (control) for 7 days was subjected to mRNA sequencing. Volcano plot showing - log10 p-values plotted against log2 treated/control. Horizontal line at y=1.3 represents a p-value of 0.05, vertical lines at x=- 0.58 and x=0.58 represent a fold change of 1.5. Blue indicates downregulation > 1.5 fold change and red indicates upregulation > 1.5 fold change with p<0.05. Unpaired Student's t-test; n=5 per genotype.

4.4.3.1 Tissue inhibitor of metalloproteinases 4 (Timp4)

The mRNA-Seq analysis described in the previous chapter revealed an upregulation of *Timp4* mRNA expression in mice after isoprenaline treatment. *Timp4* is an inhibitor of matrix metalloproteinases, which degrade extracellular matrix proteins such as collagen.
Crtc1$^{-/-}$ mice showed a reduced mRNA expression of *Timp4* (Figure 4.29 A). A reduced inhibition of metalloproteinases due to a reduction in *Timp4* might explain the lack of fibrosis in *Crtc1*$^{-/-}$ hearts.
Immunoblot analysis revealed unchanged TIMP4 protein content in heart tissue of *Crtc1*$^{-/-}$ mice (Figure 4.29 B). To investigate if metalloproteinase activity was changed in *Crtc1*$^{-/-}$ mice, a zymography was conducted. Protein extracts were separated by size in an electric field on a gelatin-SDS gel. Gelatin serves as a substrate for metalloproteinases and clear bands on the coomassie-stained gel reveal metalloproteinase activity. No difference could be seen in heart tissue of 25- to 30-week-old *Crtc1*$^{-/-}$ mice and their wild-type littermates (Figure 4.29 C).

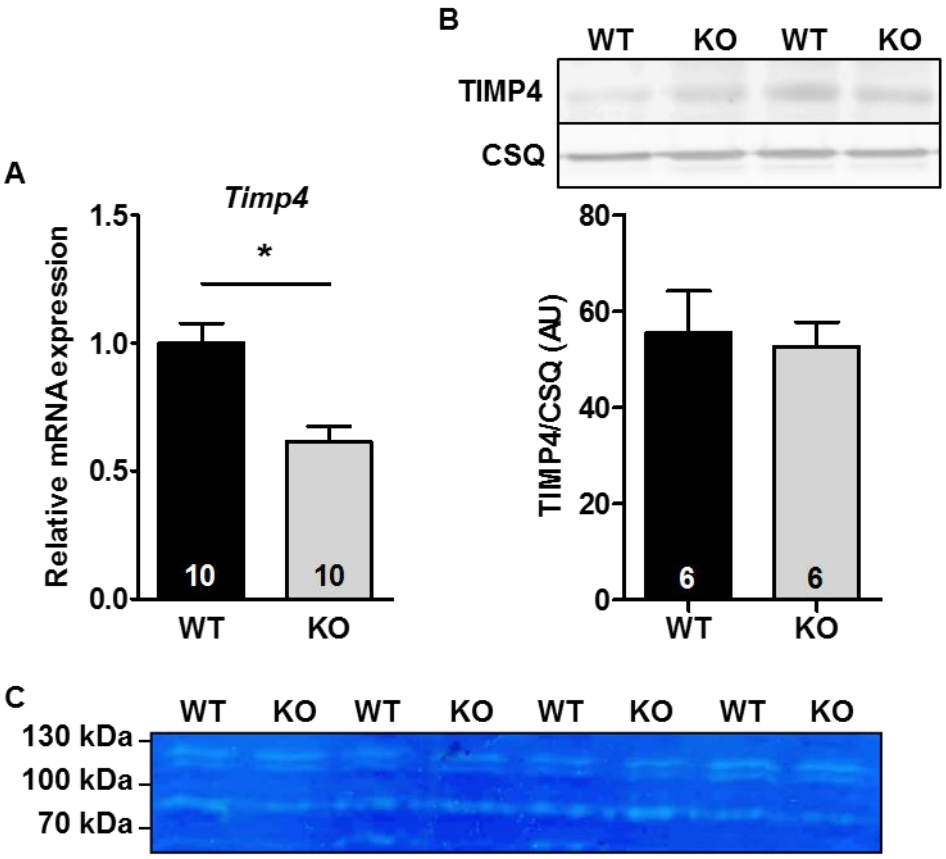

Figure 4.29: Reduced *Timp4* mRNA expression in *Crtc1*$^{-/-}$ mice with unchanged TIMP4 protein expression or metalloproteinase activity. A. Quantitative mRNA expression of the tissue inhibitor of metalloproteinases 4 (*Timp4*) normalized to *GαS* in heart tissue from *Crtc1*$^{-/-}$ mice (KO) and their wild-type littermates (WT) analyzed by quantitative real time PCR. Data are expressed as mean±SEM relative to WT using ΔΔCt-method. *p<0.05; number of samples is given within the bars. **B.** Protein lysates from hearts of *Crtc1*$^{-/-}$ mice (KO) and their wild-type littermates (WT) were analyzed by immunoblot using an antibody against TIMP4. Typical immunoblot (top); quantitative evaluation normalized to calsequestrin (CSQ) (bottom). Data are expressed as mean±SEM; number of samples is given within the bars. **C.** Protein lysates from hearts of 25- to 30-week-old *Crtc1*$^{-/-}$ mice (KO) and their wild-type littermates (WT) were analyzed by zymography on a gelatin-SDS gel; n=4 per genotype.

4.4.4 Summary

7-day isoprenaline treatment ameliorated cardiac function in *Crtc1*$^{-/-}$ mice. mRNA expression analysis by RT-qPCR revealed no difference between treated and untreated mice. mRNA-Seq analysis revealed an upregulation of *Timp4* mRNA expression after isoprenaline treatment. mRNA expression of *Timp4* was decreased in 10- to 13-week-old *Crtc1*$^{-/-}$ mice while protein expression remained unchanged. Metalloproteinase activity was not changed in *Crtc1*$^{-/-}$ mice at the age of 25 to 30 weeks.

4.5 Effects of CRTC1 on the human *NR4A2* promoter

CRTC1 is not only involved in signaling processes in the heart, but regulates gene transcription in various other tissues. CRTC1 has been shown to play a role in neuronal development and depressive disorders. In her doctoral thesis, Annette Heinrich (2009a) showed that lithium induces the recruitment of CRTC1 to the human nuclear receptor subfamily 4, group A, member 2 (*NR4A2*) promoter. To follow up on these findings, a chromatin immunoprecipitation was performed in peripheral blood monocyte cells of patients with bipolar disorder treated with or without lithium. Protein:DNA complexes were crosslinked and precipitated by an antibody against CRTC1. This experiment served as an exploratory study to investigate different variables on CRTC1 recruitment to the *NR4A2* promoter and was performed in cooperation with Dr. Annette Masuch (born Heinrich; University of Greifswald).

The relative amount of CRTC1 recruited to the *NR4A2* promoter was measured. The median of these values was calculated and values were divided into two groups with values higher or lower than the median (Table 4.3 and 4.4). A multivariate binary logistic regression for the recruitment of CRTC1 to the promoter categorized by median was calculated including the covariables age, sex, and treatment with lithium (Table 4.5). This showed a greater odds ratio of CRTC1 recruitment to the *NR4A2* promoter in patients with male sex and without lithium treatment.

Table 4.3: Cross tabulation of percentiles versus sex. Percent of input values were divided by greater or lower values than median and sex.

	Sex		Total
	male	female	
Lower values than median	6	4	10
Higher values than median	6	5	11
Total	12	9	21

Table 4.4: Cross tabulation of percentiles versus lithium treatment. Percent of input values were divided by greater or lower values than median and lithium treatment.

	Lithium treatment		Total
	No	Yes	
Lower values than median	4	6	10
Higher values than median	7	4	11
Total	11	10	21

Table 4.5: Adjusted odds ratio for percent of input values. Multivariate binary logistic regression for the percent of input values categorized by median.

Variable	Odds ratio (95% confidence interval)
Age	1.05 (0.95 - 1.17)
Male sex	1.62 (0.19 - 14)
Lithium	0.29 (0.04 - 2.13)

5 Discussion

In this thesis, the effect of CRTC1 in the murine heart was investigated. Mice globally deficient in *Crtc1* exhibited cardiac hypertrophy with cardiomyocyte growth in the left ventricle and the septum. No signs of fibrosis or induction of the fetal gene program were found. The regulator of G-protein signaling 2 is known to inhibit $G_{\alpha\ q/11}$-coupled receptor-mediated hypertrophic signaling. In *Crtc1*$^{-/-}$ mice, *Rgs2* mRNA and protein expression were reduced. CRTC1 was recruited to the murine *Rgs2* promoter in cardiac tissue and in isolated cardiomyocytes from neonatal mice. Decreased phosphorylation of Akt and increased phosphorylation of ERK 1/2 in isolated adult mouse ventricular myocytes of *Crtc1*$^{-/-}$ mice suggested increased $G_{\alpha\ q/11}$-coupled receptor-mediated hypertrophic signaling. *Crtc1*$^{-/-}$ mice developed a systolic dysfunction with reduced ejection fraction, fractional shortening, and cardiac output. Ventricular filling volume was increased. The sarcomeric contractile proteins TnI and cMybpC were less phosphorylated in response to isoprenaline treatment in ventricular myocytes of *Crtc1*$^{-/-}$ mice. Phospholamban phosphorylation was equal in cardiomyocytes of *Crtc1*$^{-/-}$ mice and wild-type littermates suggesting a signaling compartmentalization. 7-day β-adrenergic stimulation by isoprenaline ameliorated the reduced contractile function of *Crtc1*$^{-/-}$ mice.

5.1 *Crtc1*$^{-/-}$ mice as a model system

To elucidate the role of CRTC1, mice globally deficient in this gene have been generated. Breuillaud et al. created *Crtc1*$^{-/-}$ mice using a gene trap insertion between exon 4 and exon 5. These mice exhibited an obese phenotype (Breuillaud et al. 2009). Since the transcription factor CREB is involved in a wide range of processes in the nervous system and in depression (Lonze and Ginty 2002; Blendy 2006), Breuillaud et al. further investigated *Crtc1*$^{-/-}$ mice regarding mood disorders and behavior. The mice display enhanced aggressive behavior, avoidance of social contact, and depression-related behavior. Breuillaud et al. supposed that the increased feeding behavior with obesity were symptoms related to depression. They found decreased levels of dopamine and serotonin metabolites in the prefrontal cortex, a molecular endophenotype associated with aggressiveness and depressive-like behavior (Breuillaud et al. 2012). Supporting these findings, Meylan et al. showed an upregulation of agmatinase in the cortex of *Crtc1*$^{-/-}$ mice. Agmatinase is an enzyme degrading agmatine. Agmatine is a protein with antidepressant properties, which

binds to serotonergic 5HT-2A and 5HT-3 receptors and antagonizes glutamate NMDA receptors. Supposedly, the upregulation of agmatinase and ensuing decrease in agmatine contributes to the depressive phenotype in *Crtc1*$^{-/-}$ mice, which could be ameliorated by treatment with agmatine (Meylan et al. 2016). In neurons, a synergistic effect of Ca^{2+} and cAMP on CRE-dependent gene transcription has been shown to be mediated by CRTC1. CRTC1 seems to have an important effect on the molecular mechanisms of synaptic plasticity and long-term memory (Kovacs et al. 2007). Taken together, CREB and its coactivator CRTC play an important role in the development of depression. Incidentally, *CRTC1* polymorphisms have been associated with an increased body mass index and fat mass in human patients with major depressive disorder (Choong et al. 2013; Quteineh et al. 2016). In a greater cohort of over 100,000 individuals, Lu et al. (2016) found an association of *CRTC1* polymorphism with an increase in body fat percentage, especially in women (Lu et al. 2016). Altarejos et al. investigated the effect of *Crtc1* depletion on energy balance. *Crtc1*$^{-/-}$ mice are hyperphagic and obese (Altarejos et al. 2008; Breuillaud et al. 2009; Altarejos and Montminy 2011). It has been shown that obesity resulted from a higher food intake, lower energy expenditure, glucose intolerance, and higher circulating leptin concentrations in these mice. Hwijin Kim supposes a protective effect of CRTC1 against metabolic disorders (Kim 2016). He showed glucose intolerance, insulin resistance, and higher hepatic levels of DAG in *Crtc1*$^{-/-}$ mice with no apparent defects in liver insulin signaling. Hence, CRTC1 is involved in depression and metabolic processes.

Apparently, *Crtc1* is not exchangeable with its two isoforms *Crtc2* and *Crtc3*. Global deletion of *Crtc2* or *Crtc3* leads to different phenotypes in mice. While *Crtc1*$^{-/-}$ mice exhibit an increase in bodyweight and fat mass, *Crtc2*$^{-/-}$ mice appear to maintain a normal bodyweight, and *Crtc3*$^{-/-}$ mice exhibit 50% lower adipose tissue mass than wild-type littermates under a normal chow diet (Dentin et al. 2008; Song et al. 2010). Furthermore, *Crtc2*$^{-/-}$ mice, in which the CREB binding domain was deleted, exhibited improved insulin sensitivity while *Crtc1*$^{-/-}$ mice exhibit insulin resistance measured by an insulin tolerance test (Wang et al. 2010; Kim 2016).

Obesity has long been known as a risk factor for cardiovascular diseases. Left ventricular hypertrophy is often found in obese patients and is to some extent linked to hypertension. Obesity is also linked to depressive disorders: it has been shown that depression is predictive for the development of obesity and conversely, obesity increases the risk of developing a depression. Furthermore, depression is associated with increased cardiovascular morbidity (Eckel 1997; Rutledge et al. 2006; Lichtman et al. 2008; Luppino et al. 2010; Dhar and Barton 2016). The brain-derived neurotrophic factor (BDNF) enhances synaptic plasticity in the brain by activating ERK and Akt dependent signaling. It has been shown

that the sigma-1 receptor (Sig1R) upregulates BDNF expression in the hippocampus of mice via CRTC1 and CREB phosphorylation (Xu et al. 2015). Changes in Sig1R-BDNF signaling in the brain seem to play a role in diabetes-mellitus-induced depression. The Sig1R agonist and antidepressant agent fluoxetine increased BDNF in the prefrontal cortex of diabetic rats and ameliorated depressive-like behavior (Lenart et al. 2016).
Despite the great interest of many groups in the role of *Crtc1* in metabolic and neuronal processes, the role of this transcriptional coactivator in the heart remained unknown.

5.2 Cardiac dysfunction in *Crtc1*$^{-/-}$ mice

In the present study, cardiac function in *Crtc1*$^{-/-}$ mice was assessed. Deficits in systolic function, indicated by a reduced ejection fraction, cardiac output, and fractional shortening, were observed. A reduction in fractional shortening and ejection fraction is displayed in a mouse model for left ventricular hypertrophy by pressure overload after transverse aortic constriction (TAC) surgery (Liao et al. 2002; Gao et al. 2011). A mouse model associated with severe genetic hypertrophic cardiomyopathy, *Mybpc3*-targeted knock-in mice, exhibits decreased fractional shortening (Schlossarek et al. 2014). Therefore, *Crtc1*$^{-/-}$ mice displayed a cardiac function similar to that of models of acquired and inherited cardiac hypertrophy. The systolic dysfunction in *Crtc1*$^{-/-}$ mice was ameliorated to WT functional level after one week of isoprenaline treatment.
In *Mybpc3*-targeted knock-in mice phosphorylation of TnI is not increased in response to isoprenaline treatment while PLN phosphorylation is present in a normal level (Najafi et al. 2016). The authors suppose a change in cAMP-mediated PKA signaling leading to a reduced cardiac function. Two forms of the PKA holoenzyme have been described, differing in the structure of the regulatory subunit. The regulatory subunit I is found in the cytosol, while the regulatory subunit II is typically connected to subcellular organelles. *Mybpc3*-targeted knock-in mice express a higher amount of PKA regulatory subunit II with unchanged amounts of catalytic subunit (Najafi et al. 2016). By binding of cAMP to the regulatory subunits of PKA, the catalytic subunits are released. The local concentration and distribution of cAMP in the cytoplasm is regulated by phosphodiesterases (PDE). Inhibition of PDEs can lead to higher intracellular cAMP concentrations than maximal β-adrenoceptor stimulation in rat cardiomyocytes (Zaccolo and Pozzan 2002). Phosphorylation analysis of proteins in isolated cardiomyocytes of *Crtc1*$^{-/-}$ mice revealed a reduced response to short term isoprenaline treatment concerning TnI and cMybpC phosphorylation, while PLN phosphorylation remained unchanged. This suggests selective cAMP/PKA-mediated signaling depending on cell compartments in the AMVM. The specificity in cAMP/PKA-

mediated signaling is achieved by binding of PKA to A-kinase anchoring proteins (AKAPs). AKAPs are scaffold proteins with unique localization signals and the ability to form supramolecular complexes with PKA and different signaling molecules. Only PKA assembled with AKAPs are able to efficiently detect a localized change in cAMP induced by β-adrenoceptor activation (Zaccolo and Pozzan 2002; Ruehr et al. 2004; Wong and Scott 2004). Ruehr, Russell, and Bond (2004) showed that several AKAPs bind PKA substrates and regulate phosphorylation dependent signaling in cardiac tissue. This mechanism may be essential for regulation of cardiac muscle contraction. The myomegalin isoform 4 has been shown to play a role in cardiac function. It interacts with PDE4D, PKA, cMybpC, and TnI (Uys et al. 2011). The proteomics analysis in *Crtc1*$^{-/-}$ hearts performed for this thesis revealed no change of PDE4D compared to wild-type littermates. The decreased phosphorylation of TnI and cMybpC suggests an alteration in cAMP- and PKA-mediated signaling in *Crtc1*$^{-/-}$ mice even though PLN phosphorylation is comparable to wild-type. AKAP18δ has been shown to interact with PKA, SERCA, PLN, and PDE3A and is necessary for the recruitment of PKA to PLN (Lygren et al. 2007). PDE3A hydrolyzes cAMP and thereby attenuates PKA-mediated phosphorylation. Mice deficient in PDE3A exhibit increased contractility and relaxation with increased PLN phosphorylation and SERCA activity (Beca et al. 2013). The proteomics analysis in *Crtc1*$^{-/-}$ hearts revealed a downregulation in PDE3A. This suggests a decreased cAMP hydrolysis at the PDE3A/PKA/PLN/SERCA-complex leading to an increased PLN phosphorylation by PKA. Incidentally, in cardiomyocytes from a rat model of heart failure induced by myocardial infarction the β_2-adrenoceptor is redistributed to various cell surface areas, producing diffuse cAMP signals, while in healthy cardiomyocytes, the β_2-adrenoceptor is exclusively found in the transverse tubules, initiating spatially confined cAMP signaling (Nikolaev et al. 2010).

The results suggest a decreased cAMP signaling effect on TnI and cMybpC in cardiomyocytes of *Crtc1*$^{-/-}$ mice after short-term isoprenaline treatment. One-week chronic isoprenaline treatment might revoke this effect due to excessive β-adrenergic activation. This might explain the amelioration in cardiac function in *Crtc1*$^{-/-}$ mice after one-week isoprenaline treatment. Further experiments elucidating the phosphorylation of contractile proteins in AMVM isolated from *Crtc1*$^{-/-}$ mice after chronic isoprenaline treatment should be conducted. For example, a concentration response curve to possibly determine the half maximal effective concentration (EC_{50}) of TnI, cMybpC, and PLN phosphorylation could be studied.

5.3 Cardiac hypertrophy in *Crtc1*$^{-/-}$ mice

Similarities in cardiac function and contractile protein phosphorylation have been observed between *Crtc1*$^{-/-}$ mice and mice with acquired or inherited maladaptive cardiac hypertrophy. *Crtc1*$^{-/-}$ mice exhibit an increase in cardiac size with an increase in cardiomyocyte size in the left ventricle. The myocyte growth is more pronounced in width than it is in length. These are typical indicators for a maladaptive concentric cardiac hypertrophy (Ganau et al. 1992; Dorn et al. 2003). Nonetheless, the lack of fibrosis and the unchanged or reduced mRNA expression of fetal genes rather point to a physiological hypertrophy (Eghbali et al. 2005; Chung et al. 2012). Expression of *Nppa*, *Nppb,* and *Myh7*, genes normally induced by activation of the fetal gene program, is unchanged in *Crtc1*$^{-/-}$ mice. Expression of *Acta1* is reduced. According to a CREB target gene database designed by the group of Prof. Marc Montminy (Salk Institute, La Jolla, USA), *Nppb, Acta1,* and *Myh7*, contain CRE half sites. Possibly, the lack of *Crtc1* has an influence on the induction of fetal gene expression via CRE-induced transcriptional activity.

A possible explanation for the lack of fibrosis might be the decreased mRNA expression of *Timp4* in *Crtc1*$^{-/-}$ mice. Tissue inhibitors of metalloproteinases reduce metalloproteinase activity, resulting in a greater presence of collagenous tissue. The TIMP family consists of four members. Overexpression of all TIMP isoforms in cardiac fibroblasts leads to an increase in fibroblast proliferation, which is not inhibited by a broad-based metalloproteinase inhibitor. Supposedly, the effect of TIMP on proliferation is independent of metalloproteinase activity and a receptor-mediated effect. Different characteristics of the different isoforms have been identified. TIMP3 overexpression provoked greater fibroblast proliferation in AMVM and TIMP2 provoked fibroblast-induced collagen synthesis (Lovelock et al. 2005). TIMP4 is highly expressed in the heart. Mice deficient in *Timp4* show a normal development and exhibit the same response to pressure overload as wild-type due to a compensatory upregulation of *Timp2* (Koskivirta et al. 2010). Ketsawatsomkron et al. showed an increase in metalloproteinase activity after a decrease in TIMP4 protein in rat aortic smooth muscle cells (Ketsawatsomkron et al. 2016). In *Crtc1*$^{-/-}$ cardiac tissue, immunoblot analysis revealed no difference in TIMP4 protein content but it should be borne in mind that the antibody used did not provide a specific signal. Analysis of metalloproteinase activity in heart tissue by zymography revealed no difference between *Crtc1*$^{-/-}$ mice and WT littermates at the age of 25 to 30 weeks. mRNA and protein expression were investigated at an age of 10 weeks. Possibly, the age difference has an influence on metalloproteinase activity. To further investigate if the reduced mRNA expression of *Timp4* in 10-week-old *Crtc1*$^{-/-}$ mice has an effect on fibrotic growth in the hearts, metalloproteinase

activity should be investigated in younger mice and mRNA expression of *Timp1, Timp2,* and *Timp3* should be investigated.

The hypertrophic development in *Crtc1*$^{-/-}$ mice suggests the downregulation of antihypertrophic genes regulated by CRTC1. RGS are a family of GTPase-activating proteins for heterotrimeric G proteins. Increased GTPase activity leads to hydrolysis of GTP to GDP. GDP binds to the G_{α} subunit of G-protein coupled receptors, leading to a receptor inactivation. In high fat diet fed *Crtc3*$^{-/-}$ mice *Rgs2* gene expression remained low in white adipose tissue, while it increased in wild-type littermates (Song et al. 2010). Several RGS proteins, including RGS2, RGS3, RGS4, and RGS5, play an important role in cardiac hypertrophy (Tokudome et al. 2008; Takimoto et al. 2009; Li et al. 2010; Liu et al. 2014). In cultured cardiomyocytes, angiotensin II-, endothelin-1-, and phenylephrine-induced activation of $G_{\alpha\ i}$- and $G_{\alpha\ q/11}$-coupled receptors promotes a hypertrophic response (Simpson et al. 1982; Shubeita et al. 1990; Sadoshima and Izumo 1993). Angiotensin II and endothelin-1 induce $G_{\alpha\ q/11}$- and phenylephrine induces $G_{\alpha\ i}$- and $G_{\alpha\ q/11}$-coupled receptor signaling. RGS2 is a selective inhibitor of $G_{\alpha\ q/11}$-mediated signaling in the brain and the heart (Heximer et al. 1997; Hao et al. 2006). *Rgs2* deficient mice develop cardiac hypertrophy under afterload enhancement by transverse aortic constriction with fibrosis, increased heart mass, and reduced cardiac function. Inhibition of $G_{\alpha\ q/11}$-coupled receptor-mediated signaling by a PLCβ inhibitor prevented this decrease in cardiac function (Takimoto et al. 2009). Short term treatment of AMVM with the β-adrenoceptor agonist isoprenaline leads to an increase in RGS2 protein content (Chakir et al. 2011). Given that isoprenaline increases PKA activity and CREB-dependent gene transcription, it was investigated whether *Rgs2* gene transcription is regulated by CRTC1. Indeed, CRTC1 was recruited to the *Rgs2* promoter in murine heart tissue. *Rgs2* mRNA and protein expression was reduced in *Crtc1*$^{-/-}$ mice presumably leading to decreased inhibition of $G_{\alpha\ q/11}$-mediated hypertrophic signaling. Activation of the $G_{\alpha\ q/11}$-coupled receptor leads to decreased activation of Akt. Akt is a kinase often associated with physiological hypertrophy (Maillet et al. 2013). It is either activated by growth factor- or insulin-signaling via PDK1 or inhibited by $G_{\alpha\ q/11}$-coupled receptor signaling via PIP_3. Furthermore, $G_{\alpha\ q/11}$-mediated signaling leads to a phosphorylation and therefore activation of ERK 1/2 and PKD via PLCβ and DAG. ERK 1/2 and PKD phosphorylation induces pro-hypertrophic gene expression (chapter 4.2.2). ERK 1/2 belongs to the mitogen-activated protein kinases and has been found to be involved in growth signaling. The ERK pathway can be induced by α-adrenoceptor agonists, activation of the PKC pathway, and by β-adrenoceptor agonists (Xiao et al. 2001; Wang 2007). ERK 1/2 can be activated by the Ras-Raf-MEK pathway. Mice expressing a dominant negative Raf exhibit attenuated hypertrophy and gene induction after pressure overload (Harris et

al. 2004). Mice lacking cardiac ERK 1/2 protein exhibit eccentric growth of cardiomyocytes. Meanwhile, mice expressing an activated cardiac *Mek1* with subsequent ERK 1/2 activation exhibit concentric growth (Kehat et al. 2011). Incidentally, it has been supposed that a positive correlation between Ras expression and the severity of hypertrophy in patients with hypertrophic cardiomyopathy exists (Kai et al. 1998). Figure 5.1 depicts the hypothesis of CRTC1-mediated antihypertrophic signaling.

Overnight cultured *Crtc1*$^{-/-}$ AMVM exhibited a reduction in Akt phosphorylation, suggesting increased $G_{\alpha\ q/11}$-coupled receptor-mediated signaling. Endothelin-1 treatment could not increase Akt phosphorylation. Ineffectiveness of the substance can be excluded since phosphorylation of ERK and PKD by endothelin-1 was increased in the same batch of AMVM. While phosphorylation of ERK 1/2 was increased by endothelin-1 in overnight cultured AMVM, basal phosphorylation was unchanged. In freshly isolated AMVM however, ERK 1/2 phosphorylation was increased in *Crtc1*$^{-/-}$ AMVM. This also suggests an increase in $G_{\alpha\ q/11}$-coupled receptor-mediated signaling. Furthermore, it seems as if culture duration and conditions have an effect on ERK 1/2 phosphorylation in AMVM. ERK 1/2 phosphorylation could not be increased by isoprenaline-induced signaling. This may suggest a different compartmentalization in the isolated cells. PKD phosphorylation was decreased in overnight cultured AMVM and endothelin-1 treatment led to an increased phosphorylation of PKD only in WT AMVM. In adult rat ventricular myocytes activation of PKD by endothelin-1 has been shown before. PKD activity is attenuated by PKA. Supposedly, compartmentalization of cAMP, partially conducted by PDE isoforms directed by different AKAPs, results in localized regulation of PKA activity. Inhibition of PDE3 and PDE4 leads to upregulation of PKA activity that inhibits endothelin-1-induced PKD activation (Haworth et al. 2011; Nichols et al. 2014). PKA-mediated signaling seems to be functional *per se* in *Crtc1*$^{-/-}$ mice, as phospholamban phosphorylation is unchanged. The proteomics analysis performed for this thesis revealed a downregulation in PDE3A in *Crtc1*$^{-/-}$ mice suggesting subsequent PKD downregulation. Taken together, increased ERK 1/2 phosphorylation in uncultured *Crtc1*$^{-/-}$ AMVM, decreased Akt and decreased PKD phosphorylation in overnight cultured *Crtc1*$^{-/-}$ AMVM suggest increased $G_{\alpha\ q/11}$-coupled receptor-mediated signaling and compartmentalization of PKA leading to PKD inhibition.

Alterations in components of β-adrenoceptor-mediated signaling might be a reason for changed PKA signaling. In the failing heart, β-adrenoceptor density decreases and increased activity of the β-adrenoceptor kinase leads to uncoupling of the β-adrenoceptor from the $G_{\alpha\ s}$-subunit. It has been postulated that uncoupling of the β_2-adrenoceptor from

the $G_{\alpha s}$-subunit and coupling to the $G_{\alpha i}$-subunit is mediated by PKA dependent phosphorylation (Bristow et al. 1982; Ungerer et al. 1993; Daaka et al. 1997). β_1- and β_2-receptor density in heart tissue of *Crtc1*$^{-/-}$ mice poses an interesting subject for further research. Taken together, despite the lack of fibrosis these findings suggest the development of maladaptive hypertrophy resulting from deletion of *Crtc1.*

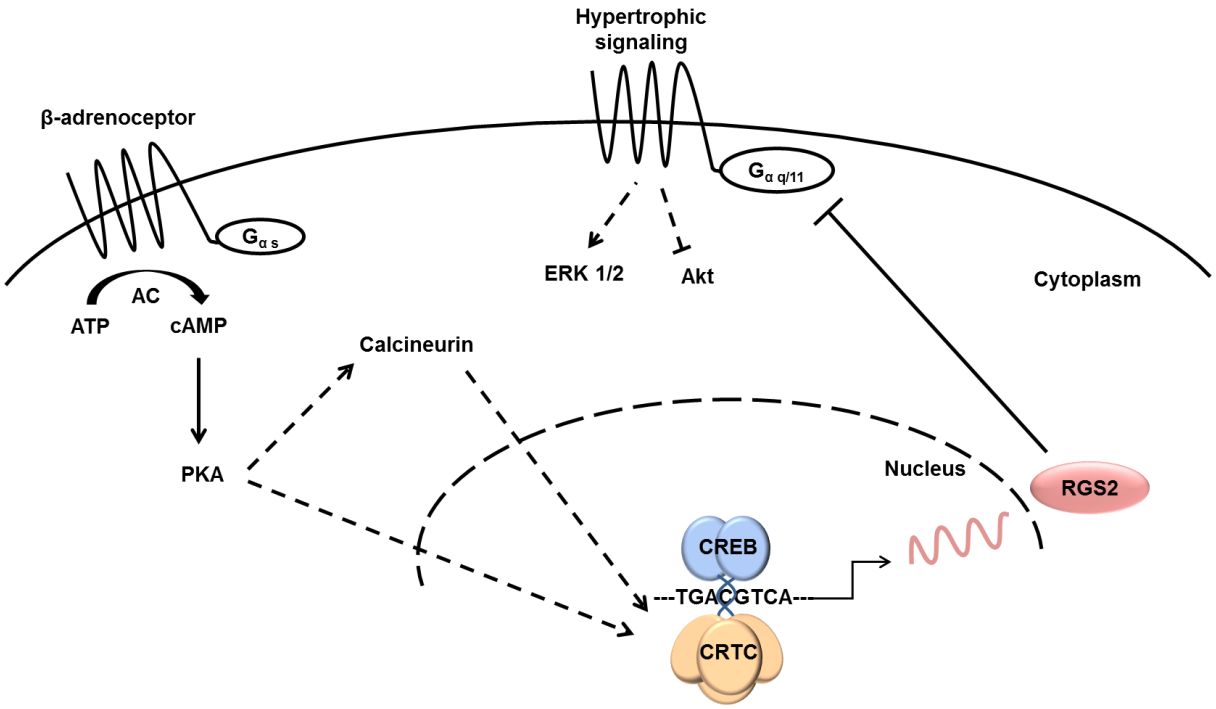

Figure 5.1: CRTC1-mediated antihypertrophic signaling. Upon β-adrenergic stimulation, adenylyl cyclase (AC) catalyzes the formation of cyclic adenosine monophosphate (cAMP) from adenosine triphosphate (ATP). cAMP activates protein kinase A (PKA), which in turn led to an activation of the phosphatase calcineurin, which dephosphorylates CRTC. Dephosphorylated CRTC translocates into the nucleus, where it binds to the dimerized leucine zipper of the DNA-bound cAMP response element binding protein (CREB) and coactivates gene transcription of the regulator of G-protein signaling 2 (RGS2). RGS2 inhibits $G_{\alpha q/11}$-coupled receptor-mediated hypertrophic signaling by inhibiting the reduction of Akt activation and the enhanced activity of the extracellular signal-regulated kinase 1/2 (ERK 1/2).

5.4 Involvement of CRTC1 in CREB-dependent gene transcription

The transcriptional coactivator CRTC1 is activated through dephosphorylation following increases in cAMP and PKA activity. Increased intracellular Ca^{2+}-concentration leads to the activation of the phosphatase calcineurin, which dephosphorylates CRTC1. Dephosphorylated CRTC1 translocates to the nucleus, where it coactivates CREB-dependent gene transcription. Calcineurin activity is generally considered to induce maladaptive hypertrophy by initiating nuclear translocation of transcription factors of the nuclear factor of activated T-cells (NFAT) family. In the nucleus, NFAT activates pro-hypertrophic

gene expression. NFAT activation by calcineurin is induced in pathological but not in physiological hypertrophy (Wilkins and Molkentin 2004). However, this thesis suggests that calcineurin activity does not always lead to the induction of maladaptive hypertrophy. By initiating the nuclear translocation of CRTC1 it might have a beneficial effect as well.

CREB belongs to the leucine zipper class of transcription factors mediating transcriptional regulation in response to β-adrenoceptor activation. Other CREB family members include the cAMP response element modulator (CREM) and the activating transcription factor (ATF1). All three CREB family members share the same primary structure consisting of a 60 aminoacid kinase inducible domain (KID), flanked by two hydrophobic glutamine rich domains, and a carboxy terminal leucine zipper dimerization domain (Mayr and Montminy 2001). After forming a homodimer through the leucine zipper domain, CREB family members bind to CRE-sites of DNA. *Crem*$^{-/-}$ mice exhibit a disruption of the circadian rhythm, lower anxiety levels, and male sterility (Nantel et al. 1996; Maldonado et al. 1999). Deletion of *Crem* protects mice overexpressing the β_1-adrenoceptor from cardiac hypertrophy, fibrosis, and left ventricular dysfunction. In response to β-adrenergic stimulation, CREM repressor isoforms are induced. Overexpression of these repressor isoforms in AMVM leads to arrhythmogenic alterations (Lewin et al. 2009; Schulte et al. 2016). CREB is ubiquitously expressed and involved in many physiological and developmental processes such as neuronal development, cell growth, and glucose homeostasis (Mayr and Montminy 2001; Mantamadiotis et al. 2002; Herzig et al. 2003). While *Creb*$^{-/-}$ mice die at birth, a cardiomyocyte specific expression of a dominant-negative CREB in mice leads to cardiac dilation, decreased left ventricular function, and attenuated contractile response to isoprenaline (Fentzke et al. 1998; Rudolph et al. 1998; Ichiki 2006). Upon phosphorylation of CREB by for example PKA, CREB binding protein (CBP) binds to CREB and initiates gene transcription. CRTC binds to CREB in a phosphorylation independent manner (Ichiki 2006). Binding of four CRTC-proteins to the dimerized leucine zipper is sufficient to initiate gene transcription (Conkright et al. 2003). It has been shown that CRTC1 is not only recruited to the transcription factor CREB, but also to the heterodimeric activating protein 1 (AP-1) transcription factor complex. AP-1 mainly consists of the proteins c-Jun and c-Fos and is involved in different cellular processes such as proliferation, differentiation, and apoptosis (Eferl and Wagner 2003). Just like CREB, CRTC1 interacts with the heterodimeric leucine zipper region of c-Jun and c-Fos. The recruitment of CRTC1 to either CREB or AP-1 seems to be an independent mechanism possibly resulting from posttranslational modifications of CRTC1 (Canettieri et al. 2009).

5.5 Involvement of CRTC1 in cardiac hypertrophy

When cardiac workload is increased due to chronic hypertension or arterial stenosis, the sympathetic nervous system is activated. β-adrenoceptor-mediated signaling leads to an increase in intracellular cAMP, resulting in increases in cardiac force and frequency to maintain cardiac function. Chronic β-adrenergic activation can lead to hypertrophy and apoptosis and subsequent reduced cardiac function. Overexpression of β-adrenoceptors or the $G_{\alpha s}$-subunit in mice leads to cardiomyopathy, arrhythmia, and premature death (Gaudin et al. 1995; Engelhardt et al. 1999; Liggett et al. 2000). Deletion of the adenylyl cyclase 5 in mice leads to protection from heart failure under pressure overload or chronic β-adrenergic stimulation with an enhanced lifespan (Okumura et al. 2007; Yan et al. 2007). Hence, chronic β-adrenergic signaling can lead to maladaptive cardiac hypertrophy and decreased survival rate. For this reason, β-adrenoceptor antagonists are widely used to treat cardiac hypertrophy and to prevent heart failure. They diminish inotropy, chronotropy, and lusitropy of the heart resulting in reduced energy consumption.

Hypertrophic signaling in pathological hypertrophy seems to be distinct from signaling in physiological hypertrophy. Physiological hypertrophy is initiated by growth factors, insulin, and thyroid hormones. The PI3K-Akt signaling pathway becomes activated. Acute Akt activation has been shown to be beneficial while chronic activation seems to induce pathological cardiac hypertrophy (Shiojima et al. 2005). In physiological hypertrophy, heart weight is increased while function is preserved, no fibrotic growth is initiated, and there is no induction of the fetal gene program or changes in genes encoding Ca^{2+}-handling proteins (Bernardo et al. 2010). In pathological hypertrophy, $G_{\alpha s}$- and $G_{\alpha q}$-coupled receptors become activated and PKA- and PKC-dependent signaling pathways lead to changes in Ca^{2+}-handling and protein phosphorylation. The fetal gene program is induced and an increase in fibrotic tissue can be observed.

The present study demonstrates that *Crtc1*-deficiency leads to cardiac hypertrophy and dysfunction. Unpublished results from the group of Prof. Elke Oetjen showed increased CRTC1 protein content in human hearts with acquired and inherited hypertrophy. Taken together, the development of cardiac hypertrophy after the deletion of *Crtc1* and the upregulation of CRTC1 in maladaptive hypertrophy suggests a compensatory mechanism of CRTC1, delaying the progression of maladaptive cardiac hypertrophy. This protective effect might be diminished when cardiac hypertrophy is treated with the commonly used β-adrenoceptor antagonists.

5.6 CRTC1 and the human *NR4A2* promoter

CRTC1 and CREB have been implicated to play a role in neuronal development (chapter 5.1). Heinrich et al. showed enhanced CREB-CRTC1 interaction and subsequent enhancement of cAMP-stimulated gene transcription by lithium. Additionally, lithium supports the formation of the CRTC1 tetramer complex (Heinrich et al. 2009b). Lithium salts are clinically used as a treatment for bipolar disorders and are up to date the only mood stabilizer for the prevention of manic episodes.

It has been shown that CRTC1 activates gene transcription of the human *NR4A2* promoter (Conkright et al. 2003). *NR4A2* encodes the orphan nuclear receptor Nurr1. Nurr1 is highly expressed in brain tissue and is involved in the differentiation and maintenance of dopaminergic neurons in the central nervous system (Perlmann and Wallen-Mackenzie 2004). Heinrich (2009a) showed increased cAMP-induced *NR4A2* gene transcription when CRTC1 was overexpressed. In prefrontal cortex tissue of patients with bipolar disorder reduced mRNA expression of *NR4A2* was found (Xing et al. 2006). Noteworthy, mRNA-Seq analysis in isoprenaline treated mice revealed a decrease in *Nr4a1* mRNA expression compared to solvent-treated littermates.

As the relation between CRTC1, *NR4A2*, and bipolar disorder pose an interesting research-matter, an explorative study in bipolar patients was conducted. CRTC1 recruitment to the *NR4A2* promoter was analyzed in peripheral blood monocyte cells from bipolar patients treated with or without lithium.

According to the results, patients not treated with lithium show a higher probability of CRTC1 recruitment to the *NR4A2* promoter. Furthermore, male sex posed a greater chance of CRTC1 recruitment. Age supposedly had no effect on promoter occupancy by CRTC1. Due to a high range of confidence intervals the analysis revealed only trends. To further investigate if lithium treatment or sex have an influence on CRTC1 recruitment to the *NR4A2* promoter, a randomized study should be conducted. To estimate the number of patients that should be included in such a study, the odds ratios from this exploratory study could be used. The trends from the exploratory study suggest a decreased CRTC1 recruitment to the *NR4A2* promoter under lithium therapy. This is contrary to results from Conkright et al. and Heinrich et al., but could suggest a difference in *NR4A2* promoter recruitment of CRTC1 in short-term and long-term lithium treatment (Conkright et al. 2003; Heinrich et al. 2009b).

Taken together, the present study demonstrates the involvement of CRTC1 in cardiovascular diseases. Cardiovascular diseases, obesity, and depression are all linked to each

other and *Crtc1* might be a gene involved in all three diseases. Hence, *Crtc1* polymorphisms or disturbed CRTC1-dependent signaling in humans may be responsible for the linked occurrence of these diseases.

6 Outlook

The results of the present study demonstrate that CRTC1 and its role in cardiovascular diseases represents an interesting research-subject worthy of future investigations.

β-adrenergic, cAMP-mediated signaling compartmentalization should be further researched. Since PDE3A has been found to be decreased in *Crtc1*$^{-/-}$ mice in the proteomics analysis, immunoblot analysis should be performed to confirm this result. mRNA expression of *Pde3a* should be investigated as well. In maladaptive cardiac hypertrophy constant β-adrenergic signaling leads to receptor desensitization. Possible differences in β_1- and β_2-adrenoceptor density should furthermore be identified in *Crtc1*$^{-/-}$ mice.

This thesis showed that phospholamban phosphorylation is intact in *Crtc1*$^{-/-}$ mice. Desensitization or redistribution of β-adrenoceptors or changes in the ryanodine receptor could still lead to changes in Ca^{2+}-signaling. Contractile force of isolated cardiomyocytes or cardiac tissue should be further studied.

Crtc1$^{-/-}$ mice exhibit more fat mass, insulin resistance, and hypertriglyceridemia. These three factors are symptoms of the metabolic syndrome. Hypertension is an additional factor for this syndrome. Therefore, investigation of blood pressure in *Crtc1*$^{-/-}$ mice is another interesting research-subject. Blood pressure can be measured in awake mice after implantation of telemetric devices. Furthermore, renin, angiotensin, and aldosterone blood levels should be investigated, if differences in blood pressure are found.

Changes in cardiac function and morphology lead to a change in cardiac metabolism. The RNA-Seq and proteomics analyses revealed differentially expressed mRNAs and proteins involved in metabolic processes in the *Crtc1*$^{-/-}$ mice. It would be interesting to further investigate how the lack of *Crtc1* influences cellular metabolic processes.

7 Material and methods

7.1 Material

7.1.1 Chemicals

Acetic acid 100%	H: 226, 290, 314 P: 210, 280, 303+361+353, 305+351+338, 310	Carl Roth, Karlsruhe, Germany
Acetonitrile anhydrous	H: 225, 302+312+332, 319 P: 210, 261, 280, 305+351+338, 370+378, 403+235	Sigma-Aldrich, St. Louis, MO, USA
Acid fuchsin	H: / P: /	Sigma-Aldrich, St. Louis, MO, USA
Acrylamide/Bis solution 37.5:1 30%	H: 302, 312, 315, 319, 317, 340, 350, 361, 372 P: 260, 280, 281, 305+351+338, 405, 501	Bio-Rad, München, Germany
Adenosine triphosphate (ATP) disodium salt	H: / P: /	Carl Roth, Karlsruhe, Germany
Agar-agar, bacteriological	H: / P: /	Carl Roth, Karlsruhe, Germany
Agarose, Standard	H: / P: /	Carl Roth, Karlsruhe, Germany
Albumin fraction V (BSA)	H: / P: /	Carl Roth, Karlsruhe, Germany
4-Aminophenylmercuric acetate (APMA)	H: 300+310+330, 373, 410 P: 260, 280, 301+310, 330, 302+352, 310, 304+340, 310, 403+233	Sigma-Aldrich, St. Louis, MO, USA

Ammonium bicarbonate (ABC)	H: 302 P: 301+312, 330	Sigma-Aldrich, St. Louis, MO, USA
Ammonium peroxydisulfate (APS)	H: 272, 302, 315, 317, 319, 334, 335 P: 261, 280, 302+352, 305+351+338, 332+313, 337+313	Carl Roth, Karlsruhe, Germany
Ampicillin sodium salt	H: 317, 334 P: 261, 280, 342+311	Sigma-Aldrich, St. Louis, MO, USA
Angiotensin II, human	H: / P: /	Sigma-Aldrich, St. Louis, MO, USA
Azocarmine G	H: / P: /	Sigma-Aldrich, St. Louis, MO, USA
Azophloxine G	H: / P: /	Merck, Darmstadt, Germany
(-)-Blebbistatin	H: 332, 302, 312, 315, 319, 317, 335 P: 261, 264, 280, 362+364, 272, 304+340, 312, 301+312, 330, 302+352, 321, 332+313, 305+351+338, 337+313, 333+313, 309+311	Cayman Chemicals, Ann Arbor, MI, USA
Bromophenol blue	H: / P: /	Sigma-Aldrich, St. Louis, MO, USA
2,3-Butanedione monoxime (BDM)	H: / P: /	Sigma-Aldrich, St. Louis, MO, USA
Calcium chloride dihydrate ($CaCl_2$ x 2 H_2O)	H: 319 P: 305+351+388	Merck, Darmstadt, Germany
Carbon dioxide (CO_2)	H: 280 P: 202, 261, 262, 280.3, 410+403,	TMG, Krefeld, Germany

Chloroform	H: 302, 315, 319, 331, 351, 361d, 372 P: 202, 260, 302+352, 304+340, 305+351+338, 308+313	Carl Roth, Karlsruhe, Germany
Collagen, Type I solution from rat tail	H: / P: /	Sigma-Aldrich, St. Louis, MO, USA
Collagenase Type II 240U/mL	H: / P: /	Worthington, Lakewood, NJ, USA
cOmplete®, Mini, EDTA-free protease inhibitor cocktail	H: 315, 319 P: 264, 280, 302+352, 332+313, 337+313, 362+364	Roche Diagnostics, Mannheim, Germany
Coomassie® Brilliant Blue G250	H: / P: /	Serva Electrophoresis, Heidelberg, Germany
Cytosine β-D-arabino-furanoside (ara-C)	H: 317, 361 P: 280	Sigma-Aldrich, St. Louis, MO, USA
Deoxycholic acid, sodium salt	H: 302 P: 301+312, 330	Sigma-Aldrich, St. Louis, MO, USA
Dimethyl sulfoxide (DMSO)	H: / P: /	Thermo Scientific, Waltham, MA, USA
1,4-Dithiothreitol (DTT)	H: 302, 315, 319, 412 P: 264, 270, 273, 280, 337+313, 501	Sigma-Aldrich, St. Louis, MO, USA
DNA loading dye (6x)	H: / P: /	Thermo Scientific, Waltham, MA, USA
dNTP Mix, 10 mmol/L	H: / P: /	Thermo Scientific, Waltham, MA, USA
Dulbecco's Modified Eagle Medium (DMEM) High Glucose	H: / P: /	Invitrogen, Carlsbad, CA, USA

Dulbecco's Phosphate-Buffered Saline (DPBS) without Calcium and Magnesium	H: / P: /	Invitrogen, Carlsbad, CA, USA
Endothelin-1 human, porcine	H: / P: /	Sigma-Aldrich, St. Louis, MO, USA
Ethanol, absolute	H : 225, 319 P: 210, 240, 305+351+338, 403+233	Sigma-Aldrich, St. Louis, MO, USA
Ethanol 99% complete denatured	H : 225, 319 P: 210, 240, 305+351+338, 403+233	Th. Geyer, Renningen, Germany
Ethidium bromide	H: 331, 341 P: 261, 280, 304+340, 311, 403+233	AppliChem, Darmstadt, Germany
Ethylenediamine tetraacetic acid (EDTA)	H: 319 P: 305+351+338	Carl Roth, Karlsruhe, Germany
Ethylene glycol-bis(β-aminoethyl ether)-N,N,N',N'-tetraacetic acid (EGTA)	H: / P: /	Carl Roth, Karlsruhe, Germany
Fetal bovine serum (FBS) Superior	H: / P: /	Biochrom, Berlin, Germany
Formaldehyde 37%	H: 301+311+331, 314, 317, 335, 341, 350, 370 P: 303+361+353, 304+340, 305+351+338, 308, 310	Carl Roth, Karlsruhe, Germany
Formic acid	H: 226, 302, 314, 331 P: 210, 280, 303+361+353, 304+340, 310, 305+351+338, 403+233	Sigma-Aldrich, St. Louis, MO, USA
Forskolin	H: 312 P: 280	Sigma-Aldrich, St. Louis, MO, USA

Gelatin, from porcine skin, type A	H: / P: /	Sigma-Aldrich, St. Louis, MO, USA
D(+)-Glucose anhydrous	H: / P: /	Carl Roth, Karlsruhe, Germany
L-Glutamine 200MM	H: / P: /	Invitrogen, Carlsbad, CA, USA
Glycerol	H: / P: /	Carl Roth, Karlsruhe, Germany
Glycine ($C_2H_5NO_2$)	H: / P: /	Carl Roth, Karlsruhe, Germany
Glycogen 10 µg/µL	H: / P: /	AppliChem, Darmstadt, Germany
Glycylglycine	H: / P: /	Carl Roth, Karlsruhe, Germany
Heparin	H: / P: /	Rotexmedica, Trittau, Germany
Horse serum	H: / P: /	Sigma-Aldrich, St. Louis, MO, USA
Hydrochloric acid solution (HCl) 1 mol/L	H: 290 P: /	VWR International, Darmstadt, Germany
4-(2-Hydroxyethyl)-1-piperazineethanesulfonic acid (HEPES)	H: / P: /	Carl Roth, Karlsruhe, Germany
Insulin-Transferrin-Selenium-X (ITS)	H: / P: /	Invitrogen, Carlsbad, CA, USA
Iodoacetamide	H: 301, 317, 334 P: 261, 280, 301+310, 342+311	Sigma-Aldrich, St. Louis, MO, USA
Isoflurane	H: 336, 373 P: 304+340, 312	Abbott, Wiesbaden, Germany

Isoprenaline hydrochloride	H: 315, 319, 335 P: 261, 305+351+338	Sigma-Aldrich, St. Louis, MO, USA
Laminin, from mouse EHS-sarcoma	H: / P: /	Roche Diagnostics, Mannheim, Germany
Liberase TM Research Grade	H: 315, 319, 334, 335 P: 261, 280, 284, 304+340, 312, 337+313, 342+311	Roche Diagnostics, Mannheim, Germany
Lithium chloride (LiCl)	H: 302, 315, 319 P: 280, 302+352, 305+351+338	Carl Roth, Karlsruhe, Germany
D-Luciferin, potassium salt	H: / P: /	Promega, Mannheim, Germany
Lysyl Endopeptidase® (Lys C)	H: / P: /	Wako Chemicals, Neuss, Germany
Magnesium chloride ($MgCl_2$)	H: / P: /	Carl Roth, Karlsruhe, Germany
Magnesium chloride hexahydrate ($MgCl_2$ x 6 H_2O)	H: / P: /	Carl Roth, Karlsruhe, Germany
Magnesium sulfate ($MgSO_4$ x H_2O)	H: / P: /	Carl Roth, Karlsruhe, Germany
Magnesium sulfate heptahydrate ($MgSO_4$ x 7 H_2O)	H: / P: /	Merck, Darmstadt, Germany
Manganese dichloride tetrahydrate ($MnCl_2$ x 4 H_2O)	H: 302, 318, 373, 411 P: 273, 280, 301+312, 330, 305+351+338, 310, 391, 501	Sigma-Aldrich, St. Louis, MO, USA
Medium 199 (+ Earle's salts + L-Glutamine) (M199)	H: / P: /	Invitrogen, Carlsbad, CA, USA
2-mercaptoethanol	H: 301+331, 310, 315, 317, 318, 373, 410 P: 270, 280, 302+352, 330, 304+340, 305+351+338, 310	Carl Roth, Karlsruhe, Germany

Metafectene® PRO	H: / P: /	Biontex, München, Germany
Metamizole	H: 361 P: 281	Ratiopharm, Ulm, Germany
Methanol	H: 225, 301+311+331, 370 P: 210, 240, 280, 302+352, 304+340, 308, 310, 403+233	VWR International, Darmstadt, Germany
Milk powder	H: / P: /	Carl Roth, Karlsruhe, Germany
Minimum Essential Medium (MEM) + Earle's Salts	H: / P: /	Invitrogen, Carlsbad, CA, USA
Nitrogen, liquid (N2)	H: 281 P: 282, 336+315, 403	TMG, Krefeld, Germany
Nonidet P40	H: 302, 318, 411 P: 280, 301+312, 305+351+338	AppliChem, Darmstadt, Germany
Nuclease free dH_2O	H: / P: /	Thermo Scientific, Waltham, MA, USA
Orange G	H: / P: /	Sigma-Aldrich, St. Louis, MO, USA
Penicillin/streptomycin (10,000 U/10 mg/mL)	H: 317, 334, 360, 371 P: 302+352, 304+340, 201, 260, 333+313, 261	Sigma-Aldrich, St. Louis, MO, USA
(R)-(-)-Phenylephrine hydrochloride	H: 302, 315, 319, 335 P: 261, 305, 351, 338	Sigma-Aldrich, St. Louis, MO, USA
1,4-Piperazinediethanesulfonic acid (PIPES)	H: / P: /	Sigma-Aldrich, St. Louis, MO, USA
Phosphotungstic acid	H: 314 P: 280, 305, 338, 310	Sigma-Aldrich, St. Louis, MO, USA

PhosSTOP® phosphatase inhibitor	H: 302 P: 264, 270, 301+312, 330, 501	Roche Diagnostics, Mannheim, Germany
Ponceau 2R	H: / P: /	Sigma-Aldrich, St. Louis, MO, USA
Potassium chloride (KCl)	H: / P: /	Carl Roth, Karlsruhe, Germany
di-Potassium hydrogen phosphate (K_2HPO_4)	H: / P: /	Carl Roth, Karlsruhe, Germany
Potassium dihydrogen phosphate (KH_2PO_4)	H: / P: /	Carl Roth, Karlsruhe, Germany
Potassium hydrogen carbonate ($KHCO_3$)	H: / P: /	Merck, Darmstadt, Germany
2-Propanol (isopropanol)	H: 225, 319, 336 P: 210, 261, 305+351+338	Sigma-Aldrich, St. Louis, MO, USA
Protein A Agarose Fast Flow 50% (v/v)	H: / P: /	Sigma-Aldrich, St. Louis, MO, USA
Proteinase K (20 µg/µL)	H: 334 P: 304+340, 261, 342+311, 284	Thermo Scientific, Waltham, MA, USA
Protein A Sepharose CL-4B	H: / P: /	GE Healthcare Life Sciences, Freiburg, Germany
Restore™ PLUS Western Blot Stripping Buffer	H: 290 P: 390, 234	Thermo Scientific, Waltham, MA, USA
Roti®-Histofix 4%	H: 302, 317, 341, 350 P: 261, 280, 302+352, 308+313	Carl Roth, Karlsruhe, Germany
Roti® Phenol	H: 301+311+331, 314, 341, 373, 411 P: 201, 280, 304+340, 305+351+338, 308+313	Carl Roth, Karlsruhe, Germany

Sodium chloride (NaCl)	H: / P: /	Carl Roth, Karlsruhe, Germany
Sodium dodecyl sulfate (SDS)	H: 228, 302+332, 315, 318, 335, 412 P: 210, 261, 280, 302+352, 305+351+338, 312	Carl Roth, Karlsruhe, Germany
Sodium hydrogen carbonate ($NaHCO_3$)	H: / P: /	Carl Roth, Karlsruhe, Germany
di-Sodium hydrogen phosphate (Na_2HPO_4)	H: / P: /	Carl Roth, Karlsruhe, Germany
di-Sodium hydrogen phosphate dihydrate (Na_2HPO_4 x 2 H_2O))	H: / P: /	Merck, Darmstadt, Germany
Sodium hydroxide solution 1 mol/L (NaOH)	H: 314 P: 280, 303+361+353, 304+340, 310, 305+351+338	Carl Roth, Karlsruhe, Germany
Sodium orthovanadate (Na_3VO_4)	H: 302+312+332 P: 280	AppliChem, Darmstadt, Germany
Taurine ($H_2NCH_2CH_2SO_3H$)	H: / P: /	Merck, Darmstadt, Germany
N,N,N',N'-Tetramethyl ethylenediamine (TEMED)	H: 225, 332, 302, 314 P: 210, 233, 280, 301+330+331, 305+351+338, 308, 310	Merck, Darmstadt, Germany
Trifluoroacetic acid (TFA)	H314, 332, 413 P273, 280, 305+351+338, 310	Sigma-Aldrich, St. Louis, MO, USA
Triton X 100	H: 302, 318, 411 P: 273, 280, 305+351+338	Carl Roth, Karlsruhe, Germany
Trizma® base ($C_4H_{11}NO_3$)	H: / P: /	Sigma-Aldrich, St. Louis, MO, USA

Trypsin 1360 USP U/mg	H: 315, 319, 334, 335 P: 302+352, 305+351+338, 304+341, 342+311	Biochrom, Berlin, Germany
Trypsin-EDTA solution 10X 0.5% trypsin, 0.2% EDTA	H: / P: /	Sigma-Aldrich, St. Louis, MO, USA
Tryptone	H: / P: /	Carl Roth, Karlsruhe, Germany
Tween® 20	H: / P: /	Carl Roth, Karlsruhe, Germany
Xylene	H: 226, 332, 312, 315 P: 302+352	Th. Geyer, Renningen, Germany
Yeast extract	H: / P: /	Carl Roth, Karlsruhe, Germany

7.1.2 Kits

Amersham® ECL® Western Blotting Analysis System	GE Healthcare, Little Chalfont, UK
Bradford Protein assay	BioRad Laboratories, München, Germany
Colloidal Blue Staining Kit	Thermo Scientific, Waltham, MA, USA
Genopure® Plasmid Maxi Kit H: 225, 290, 315, 319 P: 210, 233, 362+364, 370+378	Roche Diagnostics, Mannheim, Germany
High-Capacity cDNA Reverse Transcription Kit H: 360, 351 P: 201, 202, 308+313, 314, 280	Applied Biosystems, Foster City, CA, USA
High Pure® Plasmid Isolation Kit H: 302+332, 315, 319 P: 261, 280, 362+364	Roche Diagnostics, Mannheim, Germany
Hot FirePol® DNA polymerase	SolisBioDyne, Tartu, Estonia

KAPA® Mouse Genotyping Hot Start Kit H: 301, 370; P: 270, 264, 310, 312, 330	KAPA Biosystems, Wilmington, MA, USA
Maxima® SYBR Green/ROX qPCR Master Mix (2x)	Thermo Scientific, Waltham, MA, USA
Pierce® BCA protein assay kit H: 400, 411; P: 273, 391, 501	Thermo Scientific, Waltham, MA, USA
RNAzol® B H: 302, 312+332, 314, 341, 373, 411 P: 201, 280, 303+361+353, 304+340, 310, 305+351+338, 501	WAK-Chemie Medical GmbH, Steinbach, Germany
Sirius Red/Fast Green Collagen Staining Kit	Chondrex Inc., Redmond, WA, USA
Weigert's iron hematoxylin solution H: 225, 315, 319; P: 210, 305+351+338	Sigma-Aldrich, St. Louis, MO, USA

7.1.3 Apparatus

ABI Prism 7900HT sequence detection system	Applied Biosystems, Foster City, CA, USA
Axioskop 2	Carl Zeiss Microscopy, Jena, Germany
Axiovert 25	Carl Zeiss Microscopy, Jena, Germany
Bio Rad PowerPac® basic	BioRad Laboratories, München, Germany
Bio Rad T100® Thermal Cycler	BioRad Laboratories, München, Germany
Bioruptor Plus® sonication device	Diagenode, Seraing (Ougrée), Belgium
Centro LB 960 Luminometer	Berthold Technologies, Bad Wildbad, Germany

Columbus™ Image Data Management and Analysis System	PerkinElmer, Waltham, MA, USA
Digital precision caliper (0-100 mm)	Pollin Electronic, Pförring, Germany
Eppendorf BioPhotometer	Eppendorf AG, Hamburg, Germany
Eppendorf Centrifuge 5424R	Eppendorf AG, Hamburg, Germany
Eppendorf Reference 2 pipette	Eppendorf AG, Hamburg, Germany
Eppendorf Thermomixer comfort 1,5 ml	Eppendorf AG, Hamburg, Germany
EVO 120 autoclave	Meditech, Henstedt-Ulzburg, Germany
FiveEasy pH FE20	Mettler-Toledo, Giessen, Germany
FluoroCount Microplate Fluorometer, halogen light source, 485 nm, 530 nm	Thermo Scientific, Waltham, MA, USA
Freezer (- 20 °C)	Liebherr, Biberach an der Riß, Germany
Freezer (- 80 °C)	Kryotec, Hamburg, Germany
Fridge, 4 °C	Liebherr, Biberach an der Riß, Germany
GFL 3006 Reciprocating Shaker	GFL Gesellschaft für Labor-technik, Burgwedel, Germany
Glass equipment of Langendorff perfusion system	W. Hassa Laborbedarf, Lübeck, Germany
Heraeus Function Line incubator	Thermo Fisher Scientific, Waltham, MA, USA

Heraeus Heracell incubator	Thermo Fisher Scientific, Waltham, MA, USA
Heraeus Multifuge X3R Centrifuge	Thermo Fisher Scientific, Waltham, MA, USA
HeraSafe sterile bench	Thermo Fisher Scientific, Waltham, MA, USA
HiSeq 2000®	Illumina®, San Diego, CA, USA
Horizontal gel system	PeqLab Technologies, Erlangen, Germany
Ice machine	Hoshizaki, Amsterdam, Netherlands
ImageQuant® LAS 4000 Luminescent Image Analyzer System	GE Healthcare, Little Chalfont, UK
Innova 4000 Incubator shaker	New Brunswick Scientific, Nürtingen, Germany
Leica RM 2125RT Mermaid microtome	Leica Biosystems, Nussloch, Germany
LTQ Orbitrap Discovery	Thermo Fisher Scientific, Waltham, MA, USA
NanoDrop® ND-1000 spectrophotometer	Thermo Fisher Scientific, Waltham, MA, USA
Peristaltic pump P-3	Pharmacia fine chemicals, Piscataway, NJ, USA
Pipet filler	Thermo Fisher Scientific, Waltham, MA, USA
RCT basic magnetic stirrer	IKA-Werke GmbH, Staufen im Breisgau, Germany
Rotina 35R centrifuge	Hetterich, Tuttlingen, Germany

RS-TR05 analog tuberoller	Phoenix Instrument, Garbsen, Germany
Sartorius laboratory scale BP 610	Sartorius laboratory, Göttingen, Germany
Sartorius laboratory scale MC 210 P	Sartorius laboratory, Göttingen, Germany
Speed Vac® vacuum concentrator	Thermo Fisher Scientific, Waltham, MA, USA
Surgical instruments	Fine Science Tools, Heidelberg, Germany Carl Roth, Karlsruhe, Germany
Ultra-pure water system Milli-Q	Merck-Millipore, Darmstadt, Germany
UltraTurrax® T8	IKA-Werke GmbH, Staufen im Breisgau, Germany
VacuGene® pump	Pharmacia fine chemicals, Piscataway, NJ, USA
Vevo® 2100 Imaging System	VisualSonics, Toronto, Canada
Water bath	GFT, Burgwedel, Germany Julabo, Seelbach, Germany

Software:	
ABI 7900HT SDS 2.4.1 software	Applied Biosystems, Foster City, CA, USA
DESeq2® for mRNA-Seq analysis	Bioconductor, open source software
GraphPad Prism 5	GraphPad Software, Inc., La Jolla, CA 92037 USA
Image J®	National Institute of Health, USA
MaxQuant® for proteomics analysis	Max Planck Institute of Biochemistry, Martinsried, Germany
Quantity One® 1-D analysis software	BioRad Laboratories, München, Germany
VevoLab 1.7.1 software for echocardiography analysis	Visualsonics, Amsterdam, Netherlands

7.1.4 Consumables

6-well culture plate	Greiner Bio One, Frickenhausen, Germany
10 cm petri dishes	Greiner Bio One, Frickenhausen, Germany
12-well cell culture plate	Greiner Bio One, Frickenhausen, Germany
96-well plate, black	Thermo Fisher Scientific, Waltham, MA, USA
96-well plate, white	Thermo Fisher Scientific, Waltham, MA, USA
384-well clear optical research plate	Applied Biosystems, Foster City, CA, USA

Alzet micro-osmotic pump (Model 1007D)	Durect Corporation, Cupertino, CA, USA
Bioruptor® Microtubes 0.65 mL	Diagenode, Seraing (Ougrée), Belgium
Cell scraper	Sarstedt, Nümbrecht, Germany
Cellstar tubes 15 mL	Greiner Bio One, Frickenhausen, Germany
Cellstar tubes 50 mL	Greiner Bio One, Frickenhausen, Germany
Cell strainer 100 µm nylon	Falcon, Durham, NC, USA
Conical flask	Falcon, Durham, NC, USA
Cover glasses	Marienfeld Superior, Lauda Königshofen, Germany
Cuvettes, polystyrene	Sarstedt, Nümbrecht, Germany
Dynabeads® Protein G	Thermo Fisher Scientific, Waltham, MA, USA
Fuchs-Rosenthal counting chamber	Assistent, Glaswarenfabrik Karl Hecht, Sondheim v. d. Rhön, Germany
Gel loadertips, Multiflex® 1-200 µL	A. Hartenstein, Würzburg, Germany
Glassware	Brand, Wertheim, Germany Schott, Mainz, Germany
Gloves, nitrile	VWR International, Darmstadt, Germany

Immuno-Blot® PVDF membrane, 0.2 µm	BioRad Laboratories, München, Germany
Inject 10 mL	B. Braun, Melsungen, Germany
Low DNA-binding tube	Sarstedt, Nümbrecht, Germany
Manual Phase Lock Gel(R) tubes	5 Prime, Hilden, Germany
Microscope slides	Assistent, Glaswarenfabrik Karl Hecht, Sondheim v. d. Rhön, Germany
Micro tubes (0.2, 1.5, 2.0 mL)	Sarstedt, Nümbrecht, Germany
Millex®-GV Syringe driven filter unit 0.22 µm	Merck-Millipore, Darmstadt, Germany
Neubauer counting, chamber depth 0.100 mm; 0.0025 mm^2	Marienfeld Superior, Lauda Königshofen , Germany
Nitrocellulose membrane, 0.45 µm	BioRad Laboratories, München, Germany
Parafilm	American National Can™, Greenwich, CA, USA
pipette tips 10 µL, 20 µL, 200 µL, 1000 µL	Sarstedt, Nümbrecht, Germany
Reflex 7 mm wound clips	Cell point scientific, Gaithersburg, MD, USA
Serological pipette 5 mL, 10 mL, 25 mL	Sarstedt, Nümbrecht, Germany
Serological pipette 10mL, wide tip	Becton Dickinson, Franklin Lakes, NJ, USA
TC flask T75	Sarstedt, Nümbrecht, Germany

7.1.5 Antibodies

Table 7.1: Primary antibodies.

Antibody	Application	Source	Clone	Company/ Reference
pAKT Ser473	Immunoblot	Rabbit	Polyclonal	Cell Signaling
AKT (pan)	Immunoblot	mouse	Monoclonal	Cell Signaling
Calsequestrin	Immunoblot	Rabbit	Polyclonal	Thermo Fisher
CRTC1	Immunoblot	Rabbit	Polyclonal	Cell Signaling
pERK Thr202/Tyr204	Immunoblot	Rabbit	Monoclonal	Cell Signaling
ERK1/2	Immunoblot	Rabbit	Monoclonal	Cell Signaling
Mouse IgG	ChIP	Mouse	Polyclonal	Sigma-Aldrich
pMybpC Ser282	Immunoblot	Rabbit	Polyclonal	Prof. Lucie Carrier
MybpC	Immunoblot	Rabbit	Polyclonal	Prof. Wolfgang Linke
pPKD Ser916	Immunoblot	Rabbit	Polyclonal	Cell Signaling
PKD	Immunoblot	Rabbit	Polyclonal	Santa Cruz
pPLN Ser16	Immunoblot	Rabbit	Polyclonal	Badrilla
PLN	Immunoblot	Mouse	Monoclonal	Badrilla
RGS2	Immunoblot	Chicken	Polyclonal	Sigma-Aldrich
RGS4	Immunoblot	Goat	Polyclonal	Santa Cruz
pTnI Ser23/24	Immunoblot	Rabbit	Polyclonal	Cell Signaling
TnI	Immunoblot	Rabbit	Polyclonal	Cell Signaling
TIMP4	Immunoblot	Rabbit	Polyclonal	Thermo Fisher
TORC1	ChIP	Rabbit	Monoclonal	Abcam

Table 7.2: Secondary antibodies, conjugated to horseradish peroxidase.

Antibody	Application	Source	Clone	Company
Anti-mouse	Immunoblot	Sheep	Polyclonal	Dianova
Anti-rabbit	Immunoblot	Goat	Polyclonal	Dianova
Anti-chicken	Immunoblot	Rabbit	Polyclonal	Sigma
Anti-goat	Immunoblot	Donkey	Polyclonal	Santa Cruz

7.1.6 Plasmids

7.1.6.1 Expression constructs

	Promoter	**Source**	**Vector**
CRTC1	CMV	Heinrich (2009a)	pcDNA3.1
CRTC2	CMV	Heinrich (2009a)	pcDNA3.1
GFPtpz	CMV	Canberra-Packard, Dreieich, Germany	
Bluescript	no promoter	Prof. Oetjen	pUC

7.1.6.2 Luciferase reporter gene constructs

	Source	**Vector**	**Region**	**Reference**
Rgs2-Luc WT	Mouse	PGL3 basic	-867 bp promoter	Xie et al. (2011)
Rgs2-Luc Mut	Mouse	PGL3 basic	-867 bp promoter (CRE mutated at bp 214-217)	
Rgs4-Luc-167	Rat	pGL4.11	-167 bp promoter	Davies et al. (2010)
Rgs4-Luc-167m	Rat	pGL4.11	-167 bp promoter (AP1R mutated)	
Rgs4-Luc-426	Rat	pGL4.11	-426 bp promoter	
Rgs4-Luc-426m	Rat	pGL4.11	-426 bp promoter (AP1F mutated)	

7.1.7 Restriction enzymes and buffers

Hind III FastDigest®	Fermentas
Kpn I	Fermentas
Sac I	Fermentas
Buffer Tango	Fermentas
FastDigest® Green buffer	Fermentas
Kpn I buffer	Fermentas

7.1.8 DNA and protein markers

For protein analysis on SDS-PAGE gels the PageRuler® Plus Prestained Protein Ladder from Thermo Fisher was used (Figure 7.1 A). For DNA analysis on agarose gels the GeneRuler® 100 bp or 1 kb DNA Ladders from Thermo Fisher were used (Figure 7.1 B and C).

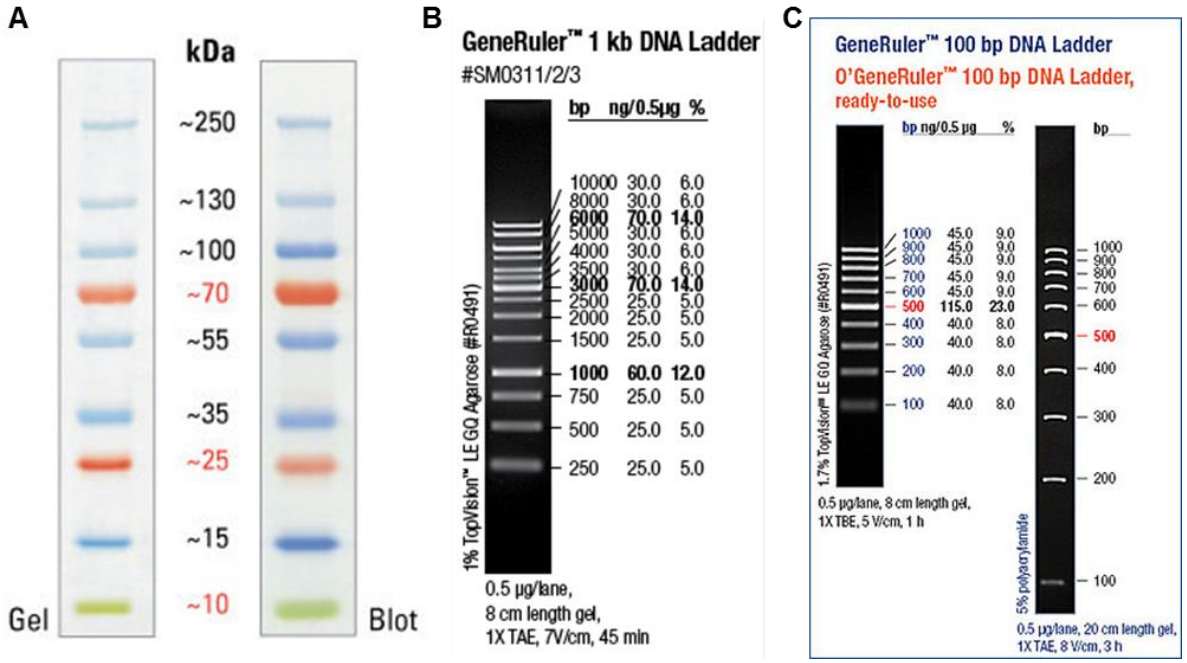

Figure 7.1: Protein and DNA ladders. A. PageRuler® Plus band profile from a 4-20% Tris-glycine gel (SDS-PAGE) and subsequent transfer to membrane. **B.** GeneRuler® 1 kb DNA ladder. **C.** GeneRuler® 100 bp DNA ladder. Images taken from www.thermofisher.com.

7.1.9 Stock solutions

APS 10%, stored at - 20 °C

APS	1 g
dH_2O	ad 10 mL

Gelatin solution, stored at 4 °C

Gelatin	10 mg
dH_20	2.95 mL

heated at 37 °C until completely dissolved

SDS 10%, stored at room temperature

SDS	10 g
dH_2O	100 mL

Tris 0.5 mol/L, pH 6.8, stored at room temperature

Tris	60.6 g
dH_2O	ad 1 L

Tris 1.5 mol/L, pH 8.8, stored at room temperature

Tris	181.7 g
dH_2O	ad 1 L

7.1.10 Cell lines and mouse strains

7.1.10.1 Bacteria

The heat competent *Escherichia coli* One Shot® Stbl3 strain from Invitrogen was used for plasmid amplification.

7.1.10.2 Primary cells and cell lines

Human embryonic kidney cells (HEK293T) from Cell Biolabs were cultured in Dulbecco's Modified Eagle Medium (DMEM) High Glucose containing 1% penicillin/streptomycin and 10% fetal bovine serum (FBS) (DMEM complete medium) at 37 °C, 95% humidity and 9% CO_2. Cells were split once a week by digestion for 3 to 5 min with trypsin/EDTA at 37 °C,

stopped by addition of DMEM complete medium. Cells were detached from the dish, centrifuged at 140 x *g* for 3 min, and washed with DMEM complete medium. The cells were seeded at a density of maximum 10,000 cells/cm^2. Medium was changed every three to four days. HEK293T cells were used for transient transfection assays.

After isolation (chapter 7.2.5.2), neonatal mouse cardiomyocytes were plated on collagen-coated (0.1 to 0.3 mg/mL) 12-well dishes at a density of 40,000 to 85,000 cells/cm^2 in 1 mL cardiomyocyte culture medium (DMEM:M199 3:1, 10% horse serum, 5% FBS, penicillin/streptomycin 100 U/100 µg/mL, HEPES 1 mmol/L, pH 7.4) and incubated at 37 °C and 10% CO_2. To inhibit proliferation of remaining fibroblasts, 25 µmol/L cytosine β-D-arabinofuranoside (ara-C) was added to the culture medium.

After isolation (chapter 7.2.6.2), adult mouse ventricular myocytes were cultured overnight in 1 mL cardiomyocyte culture medium (minimum essential medium (MEM) with penicillin/streptomycin 100 U/100 µg/mL, 2 mmol/L L-glutamine, 25 µmol/L (-)-blebbistatin, and 1x insulin-transferrin-selenium (ITS) at 37 °C and 9% CO_2 on laminin-coated (0.2 mg/mL) 12-well plates at a density of about 50,000 to 100,000 cells per well.

7.1.10.3 Animal model

All procedures involving experimental animals were performed in compliance with the german law for the protection of animals by the Bundesministerium für Ernährung, Landwirtschaft und Verbraucherschutz. Mice were bred in the animal facility of the University Medical Center and kept under standard caging conditions in open Makrolon® cages at a 12 h dark/light cycle with voluntary access to water and standard chow (Altromin GmbH & Co. KG, Lage, Germany) at 20 to 24 °C and 45 to 65% humidity.

7.1.10.4 Crtc1-deficient mice

Mice globally deficient in *Crtc1* (*Crtc1*$^{-/-}$) were previously generated by the group of Jean-René Cardinaux (University of Lausanne, Switzerland) and were given to us as a kind gift. *Crtc1*-deletion was obtained by insertion of the gene trap vector pGT01xf into the fourth intron of the *Crtc1* gene (Figure 7.2). Mice possessing the *Crtc1* gene with the inserted gene trap were maintained on a C57BL/6J background. *Crtc1*$^{-/-}$ mice are viable, fertile, and develop a depressive-like and hyperphagic phenotype with increased bodyweight at the age of 16 weeks (Breuillaud et al. 2009).

For experiments, *Crtc1*$^{-/-}$ mice and their wild-type littermates were used.

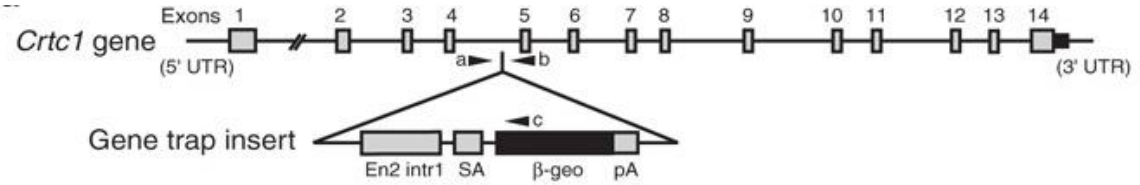

Figure 7.2: Schematic representation of the *Crtc1* gene with the insertion of the gene trap vector pGT01xf. Engrailed-2 intron 1 sequence (En2 intr1), splice acceptor (SA), β-galactosidase-neomycin resistance cassette (β-geo), polyadenylation sequence (pA), untranslated region (UTR). Primers used for genotyping (a, b and c; see chapter 7.2.2.6) are indicated by arrowheads. Figure taken from Breuil-laud et al. (2009).

7.2 Methods

If not otherwise stated, autoclaved, deionized water (dH_2O) was used for experiments. For adjustment of the pH value of buffers and solutions, 1 mol/L NaOH or 1 mol/L HCl were used.

7.2.1 Organ extraction

Organ extraction was authorized by the Behörde für Gesundheit und Verbraucherschutz der Freien und Hansestadt Hamburg (ORG 664).

Mice were sacrificed by cervical dislocation after CO_2 anesthesia and weighed. Hearts were quickly removed after median thoracotomy, rinsed in 0.9% NaCl solution to wash out remaining blood, shortly dried on a tissue paper and weighed before being frozen in liquid nitrogen. Tissue was either stored whole at - 80 °C or powdered with a steel mortar in liquid nitrogen and stored at - 80 °C.

Lung, liver and brain were excised, weighed, frozen in liquid nitrogen, and stored at - 80 °C. Tibia was extracted and measured with a digital precision caliper.

7.2.2 Working with RNA and DNA

7.2.2.1 Isolation of RNA

Total RNA was extracted from murine heart tissue or heart powder using the RNAzol® B Kit, according to the manufacturer's instructions. 1 mL of RNAzol® was added to 30 to 50 mg heart tissue and homogenized by an UltraTurrax®. The aqueous and organic phase were separated by addition of 0.2 mL chloroform per 1 mL RNAzol®. DNA and proteins remained in the organic phase while RNA could be precipitated from the aqueous phase by isopropanol. After two wash steps with 75% ethanol, RNA was solubilized in 15 µL nuclease free dH_2O.

7.2.2.2 Determination of RNA concentration

RNA concentration, purity, and quality were determined using the NanoDrop® ND-1000 spectrophotometer. RNA absorbance was measured at a wavelength of 260 nm. According to an extinction coefficient of 40 ng-cm/µL, it was assumed that 1 unit of absorbance corresponds to 40 ng/µL RNA. Absorbance was also determined at a wavelength of 230 nm and 280 nm. A ratio of A260/280 lower than 1.9 may indicate the presence of contaminants such as proteins or phenol. The ratio of A260/230 is a secondary measure of RNA purity and is commonly in the range of 1.8 to 2.2.

7.2.2.3 Reverse transcription

Total RNA was reverse transcribed using the High-Capacity cDNA Reverse Transcription Kit containing Random Primers, according to the manufacturer's instructions. 10 µL sample containing 0.5 to 1 µg total RNA was mixed with an equal amount of 10x RT master mix. Reverse transcription was performed at 25 °C for 10 min, 37 °C for 120 min, and 85 °C for 5 min. Samples were stored at - 80 °C until further use.

7.2.2.4 Quantitative Real Time PCR

Quantitative real time PCR (qPCR) was performed on the ABI Prism® 7900HT sequence detection system using the Maxima® SYBR Green/ROX qPCR Master Mix Kit according to the manufacturer's instructions. SYBR Green I is a DNA double-strand intercalating fluorescent dye. Fluorescent signal (excitation maximum at 494 nm and emission maximum

at 521 nm) increases proportionally to DNA concentration (Figure 7.3). The ROX passive reference dye (excitation maximum at 580 nm and emission maximum at 621 nm) serves as an internal reference for normalization of SYBR Green I fluorescent signal.

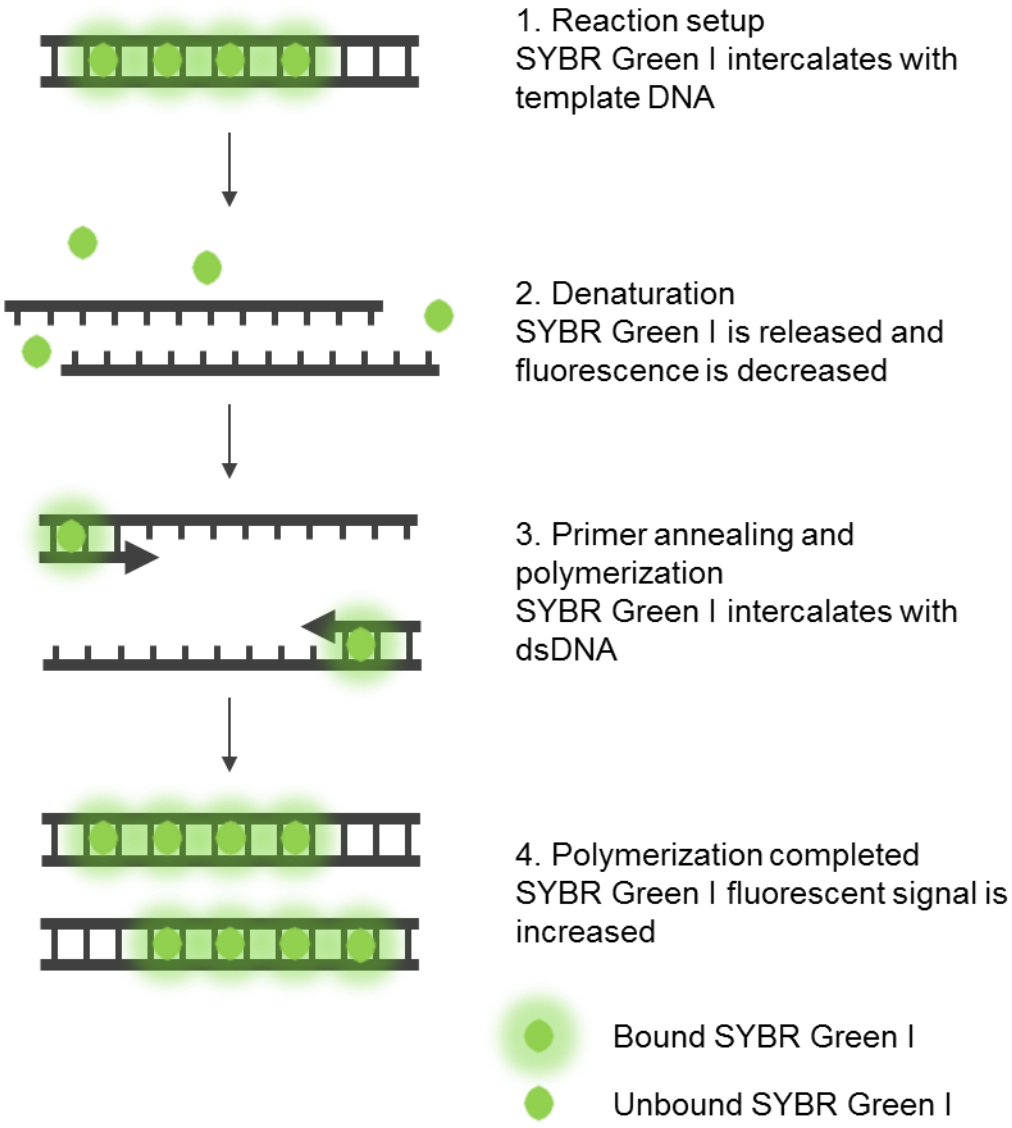

Figure 7.3: Schematic depiction of SYBR Green I DNA intercalating dye.

cDNA from reverse transcribed mRNA (chapter 7.2.2.3) or DNA from chromatin immunoprecipitation (chapter 7.2.2.11.2), diluted 1:10 in dH_2O, was amplified with primer pairs specified in table 7.3 at a concentration of 250 nmol/L. Samples were measured in triplets. The used PCR-program is mentioned in table 7.4. A dissociation curve analysis was run with each experiment to distinguish between mismatched products (e.g. primer-dimers) and well matched products. Furthermore, samples were run on an agarose gel containing 0.04% ethidium bromide after qPCR to detect possible side products of amplification. Data

was normalized to the endogenous control *GαS*; a no template control and a reverse transcriptase minus control missing the RT enzyme were included in all experimental runs. For evaluation of relative mRNA expression, the cycle threshold (Ct), indicating the beginning of exponential increase in fluorescence, was compared using the $2^{-\Delta\Delta Ct}$ formula. For calculations, the mean Ct value of triplet measurements was used. ΔCt was obtained by subtracting the mean Ct value of the endogenous control gene from the mean Ct value of the gene of interest. ΔΔCt was obtained by calculating the mean value of ΔCt from the reference group and subtracting it from the ΔCt value of each sample. Assuming that with every cycle, amplicon concentration is doubled, the $2^{-\Delta\Delta Ct}$ formula provides the relative amount of mRNA in each sample expressed to controls, which were set to 1 (Livak and Schmittgen 2001).

Before use, primer pair efficiency was tested. Five 1:5 step-dilutions of initial 500 ng cDNA were amplified with 250 nmol/L primer concentration. Primers with an efficiency greater than 85% and smaller than 115% and a correlation coefficient (R^2) greater 0.85 were considered for experimental use. Analysis was performed using the ABI 7900HT SDS 2.4 software.

Table 7.3: qPCR primer pairs.

Primer name	Primer sequence (5'→3')	Expected fragment length (bp)
Acta1 Forw #	CCCCTGAGGAGCACCCGACT	198
Acta1 Rev #	CGTTGTGGGTGACACCGTCCC	
Crtc1 Forw *	AGACAGACAAGACCCTTTCTAAGCA	67
Crtc1 Rev *	CAGGACTTGGGCCTGGAA	
Crtc2 Forw *	GGCCTTCGAGGAGGTGATG	71
Crtc2 Rev *	TATAAGCCAGTCGCAGTTTTTGG	
Crtc3 Forw *	ACACCTGTGGGAGAGCAAGG	216
Crtc3 Rev *	CCAAAGAGGTGGTCGCTGGT	
Col1α1 Forw #	TGGAGATGATGGGGAAGCTG	151
Col1α1 Rev #	ATCTCCTTTGGCACCATCCA	
Col3α1 Forw #	ATGAGGAGCCACTAGACTGC	165
Col3α1 Rev #	GGTCACCATTTCTCCCAGGA	
Ctgf Forw	CCGGGTTACCAATGACAATA	204
Ctgf Rev	CACACCCCACAGAACTTAGC	
GαS Forw #	CAAGGCTCTGTGGGAGGAT	147
GαS Rev #	CGAAGCAGGTCCTGGTCACT	
Myh7 Forw#	GAGGAGAGGGCGGACATC	110
Myh7 Rev#	GGAGCTGGGTAGCACAAGAG	
Nppa Forw #	ATCTGCCCTCTTGAAAAGCA	213
Nppa Rev #	ACACACCACAAGGGCTTAGG	
Nppb Forw #	CCAGTCTCCAGAGCAATTCAA	81
Nppb Rev #	AGCTGTCTCTGGGCCATTTC	

Primer name	Primer sequence (5'→3')	Expected fragment length (bp)
Rgs2 Forw	ACCACCACTGACAGTTCAAAG	369
Rgs2 Rev	GAGGCGCCTGTCTTCTTACC	
Rgs2 promoter Forw	CCACCTCCCACCCTGTGT	240
Rgs2 promoter Rev	CCACCGCAGCTGTTTGAG	
Rgs3 Forw [+]	TCACACGCAATGGGAACCT	70
Rgs3 Rev [+]	GCCAGCTTATTCTTCATGTCCTT	
Rgs4 Forw [+]	GGGCTGAATCGTTGGAAAAC	75
Rgs4 Rev [+]	ATTCCGACTTCAGGAAAGCTTT	
Rgs5 Forw [x]	ATCAAGATCAAGTTGGGAATTCTCCTCCAG	480
Rgs5 Rev [x]	GCTCCTTATAAAATTCAGAGCGCACAAAGC	
Rgs6 Forw	CGGAGCGAGTCGAGACAAT	62
Rgs6 Rev	TGAGCCATCCTGAGTGTCTTC	
Timp4 Forw	GCTCTAGTGATACGGGCCAA	99
Timp4 Rev	CTGTTTGATTTCATACCGGATCAGT	

[#] primer designed by the group of L. Carrier (University Medical Center Hamburg-Eppendorf, Germany) * primer designed by the group of J.R. Cardinaux (University of Lausanne, Switzerland); [+] primer published by Kurrasch et al. (2004), (Kurrasch et al. 2004); [x] primer published by Zhang et al., (2006) (Zhang et al. 2006)

Table 7.4: Program for qPCR.

Step	*Temperature, °C*	*Time, mm:ss*	
Initial denaturation	95	10:00	
Denaturation	95	00:15	45 cycles
Annealing/Extension	60	01:00	
Denaturation	95	00:15	
Dissociation curve	60	01:00	
	95	00:15	

7.2.2.5 Micro-array based mRNA expression analysis

mRNA sequencing (mRNA-Seq) is a deep-sequencing technology revealing levels of transcripts and their isoforms. In cooperation with the laboratory of Prof. Norbert Hübner (Max-Delbrück Center, Berlin), a mRNA-Seq analysis was conducted using the Illumina® sequencing approach on the HiSeq 2000® apparatus. mRNA was isolated from murine heart tissue as described in chapter 7.2.2.1. At least 0.02 µg/µL mRNA with a RIN score > 8 was further processed by the laboratory of Prof. Hübner. In general, mRNA was selected for polyadenylated RNAs to remove rRNA. mRNA was transcribed to cDNA and an adapter region was added to the 5'- and 3'-end of the strand. Via the adapter region, the strands attach to complementary oligonucleotides on a flow cell where they are amplified. The sequence by synthesis approach was used. Nucleotides tagged with a fluorescent marker generate a specific base-by-base color code for each sequence (Illumina ; van Dijk et al. 2014; Kukurba and Montgomery 2015). DESeq2® was used for differential analysis of obtained count data (Love et al. 2014).

7.2.2.6 Genotyping

To distinguish between *Crtc1*$^{-/-}$, wild-type, and heterozygous mice, DNA from tail tips was analyzed by PCR.

To extract DNA from the tissue, KAPA® Mouse Genotyping Hot Start Kit was used according to the manufacturer's instruction. Tissue was digested with KAPA® express extract enzyme and KAPA® express extract buffer at 75 °C for 10 min; digestion enzyme was

inactivated at 95 °C for 5 min. PCR samples were prepared using the following components per reaction with the primers shown in table 7.5:

DNA obtained from digest	1 µL
KAPA2G Fast Genotyping Mix	12.5 µL
dH_2O	9.875 µL
DMSO	1.25 µL
Primer a “Intron 4-5 gen new” 100 mmol/L	0.125 µL
Primer b “TORC1 Exon 5-3’” 100 mmol/L	0.125 µL
Primer c “GT-Beta-gal” 100 mmol/L	0.125 µL

Table 7.5: Primer pairs for PCR genotyping.

Primer name	Primer sequence (5’→3’)
Primer a “Intron 4-5 gen new”	GGCAGTACATAGCTTCTCTGGTGA
Primer b “TORC1 Exon 5-3’”	TGCAGGGCAGAGTCAGACTTGGT
Primer c “GT-Beta-gal”	GACAGTATCGGCCTCAGGAAGATCG

PCR was conducted in the Bio Rad T100® thermal cycler using the protocol listed in table 7.6.

Table 7.6: Program for PCR genotyping.

Step	*Temperature, °C*	*Time, mm:ss*	
Initial denaturation	94	03:00	
Denaturation	94	00:15	11 cycles
Annealing	65 - 0.5 °C/cycle	00:15	
Elongation	72	00:30	
Denaturation	94	00:15	24 cycles
Annealing	60	00:15	
Elongation	72	00:30	
Final Elongation	72	10:00	

PCR products were separated by size in an electric field on a 1% agarose gel containing 0.04% ethidium bromide. The GeneRuler® 1 kb DNA ladder was used as a molecular weight marker. The primers a “Intron4-5 gen new” and b “TORC1exon5-3’” amplify a 670 bp fragment from the wild-type allele, the primers a “Intron4-5 gen new” and c “GT-Beta gal” amplify a 1197 bp fragment from the *Crtc1*-deficient allele. In heterozygous mice, both fragments are amplified (Figure 7.4).

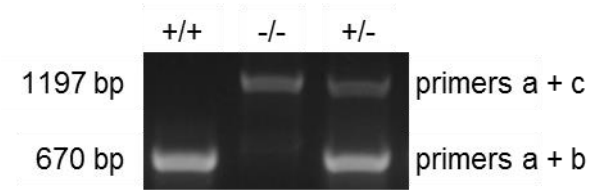

Figure 7.4: PCR genotyping. Typical agarose gel from electrophoretic analysis. The 670-basepair (bp) and 1179-bp bands correspond to the WT (+/+) allele and the *Crtc1*$^{-/-}$ allele (-/-), respectively.

7.2.2.7 Amplification of plasmid DNA

7.2.2.7.1 Buffers and solutions

Transformation buffer

$MnCl_2$ x 4 H_2O	55 mmol/L
$CaCl_2$ x 2 H_2O	15 mmol/L
KCl	250 mmol/L
PIPES	10 mmol/L
In dH_2O	

Super optimal broth (SOB) medium, pH 7.0, autoclaved, stored at 4 °C

Tryptone	2% (w/v)
Yeast extract	0.5% (w/v)
NaCl	8.56 mmol/L
KCl	2.5 mmol/L
$MgCl_2$	10 mmol/L
In dH_2O	

SOB with catabolite repression (SOC) medium, stored at 4 °C

D-Glucose	20 mmol/L
$MgSO_4$	10 mmol/L
In SOB	

Lysogeny broth (LB) medium, autoclaved, stored at 4 °C

NaCl	85.6 mmol/L
Tryptone	1% (w/v)
Yeast extract	0.5% (w/v)
In dH_2O	

Tris-EDTA (TE) buffer, pH 8, stored at room temperature

Tris	10 mmol/L
EDTA	1 mmol/L

7.2.2.7.2 Transformation in chemically competent E.coli

One Shot Stbl3® *E. coli* were mixed with 25 mL SOB medium and incubated at 37 °C for 6 to 8 h, constantly shaking. From this culture, 2 mL, 4 mL, and 10 mL were each mixed with 250 mL SOB medium and incubated overnight at 18 °C, constantly shaking. The culture with a maximal optical density of 0.6 A_{600} units/mL was further used. The solution was kept on ice for 10 min before centrifugation for 10 min at 1000 x *g* at 4 °C. The supernatant was discarded, the pellet was resuspended in 20 mL ice-cold transformation buffer and 1.5 mL DMSO and kept on ice for 10 min. The bacteria solution was aliquoted, frozen in liquid nitrogen and stored at - 80 °C until further use. For the transformation, the chemically competent *E.coli* were thawed on ice and mixed with the plasmid DNA. 30 min incubation on ice led to an uptake of DNA into the bacteria. A 90 sec heat shock at 42 °C increased efficiency. The mixture was kept on ice for 60 to 120 sec before being added to 500 µL SOC medium. The mixture was heated for 45 min at 37 °C for bacteria to express their antibiotic resistance. After centrifugation at 1000 x *g* for 1 min at room temperature, all but 100 µL supernatant was discarded, the pellet was resuspended in the remaining supernatant, plated on an agar plate containing ampicillin (50 µg/mL) and incubated overnight at 37 °C. One isolated growing clone was picked and cultured in 3 mL LB medium with 0.1% ampicillin in a 15 mL reaction tube at 22 °C gently rotating overnight until a density of 2 to 6 A_{600} units/mL was reached.

7.2.2.7.3 Mini preparation

Mini preparation was conducted with the High Pure® Plasmid Isolation Kit according to manufacturer's instructions. Shortly, pelleted bacteria were resuspended in 250 µL suspension buffer. 250 µL lysis buffer was added and incubated for 5 min at room temperature. 350 µL binding buffer was added to lysed solutions, gently mixed and incubated on ice for 5 min before centrifugation at 13,000 x *g* for 10 min. Supernatant was transferred into a filter tube and centrifuged at 13,000 x *g* for 1 min. The filter was washed with 700 µL wash buffer II before 100 µL elution buffer was added. After centrifugation at 13,000 x *g* for 1 min, the eluted plasmid was stored at - 20 °C.

7.2.2.7.4 Maxi preparation

Maxi preparation was carried out with the Genopure® Plasmid Maxi Kit according to manufacturer's instructions. Briefly, pelleted bacteria were resuspended in 12 mL suspension

buffer before addition of 12 mL lysis buffer and incubation for 2 to 3 min at room temperature. 12 mL neutralization buffer was added, gently mixed, and incubated for 5 min on ice. The lysate was cleared by centrifugation and added onto an equilibrated column. After the column was washed with 16 mL wash buffer, the plasmid was eluted from the column with 15 mL elution buffer. 11 mL isopropanol was added for precipitation and the sample was centrifuged at 15,000 x *g* for 10 min at 2 to 8 °C. The plasmid DNA pellet was resuspended in 100 µL TE buffer and stored at - 20 °C.

7.2.2.8 Determination of DNA concentration

DNA concentration was determined using the NanoDrop® ND-1000 spectrophotometer. DNA absorbance was measured at a wavelength of 260 nm.
According to an extinction coefficient of 50 ng-cm/µL, it was assumed that 1 unit of absorbance corresponds to 50 ng/µL DNA.

7.2.2.9 Restriction enzyme digest of plasmid DNA

To confirm the proper insert of the construct DNA, plasmid DNA was digested with restriction enzymes in the supplied buffer according to manufacturer's instructions. DNA was digested with enzymes for 2 h at 37 °C. *Rgs2* promoter plasmids were digested with 1x Kpn I and 4x Hind III in 9x Kpn I buffer for 2 h at 37 °C. *Rgs4* promoter plasmids were first digested with FastDigest Hind III in FastDigest Green buffer for 10 min followed by a digest with Sac I in Tango buffer a for 2 h at 37 °C. DNA was mixed with DNA loading dye and separated by size on a 1% agarose gel containing 0.04% ethidium bromide. The GeneRuler® 1 kb DNA ladder was used for size estimation.

7.2.2.10 Luciferase reporter gene assay

7.2.2.10.1 Buffers and solutions

Scraping buffer, pH 7.6, stored at room temperature

NaCl	150 mmol/L
EDTA	1 mmol/L
Tris	40 mmol/L
In dH_2O	

Potassium phosphate buffer, pH 7.8, stored at room temperature

K_2HPO_4	100 mmol/L
KH_2PO_4	100 mmol/L
DTT	1 mmol/L

Glycylglycine buffer, pH 7.8, stored at 4 °C

Glycylglycine	25 mmol/L
$MgSO_4$	15 mmol/L
EGTA	4 mmol/L
In dH_2O	

Luciferin stock, stored at - 80 °C

DTT	10 mmol/L
D-Luciferin	1 mmol/L
In glycylglycine buffer	

Luciferase assay mix, prepared fresh before use

Glycylglycine buffer	7.8 mL
Potassium phosphate buffer	1.56 mL
ATP 200 mmol/L	104 µL
DTT 1 mol/L	10.4 µL

Luciferin buffer, prepared fresh before use

Glycylglycine buffer	2 mL
Luciferin stock	500 µL
DTT 1 mol/L	20 µL

7.2.2.10.2 Transient transfection

For studying CRE-dependent gene transcription, HEK293T cells were transiently transfected with different luciferase reporter gene constructs. HEK293T cells were cultured in 6-well culture plates and seeded at a density of about 110,000 cells/cm^2 in 2 mL DMEM. 0.5 µg/mL luciferase reporter gene vector was cotransfected with 0.5 µg/mL expression vector for CRTC1, CRTC2 or the empty vector pBluescript to equalize the amount of DNA transfected. The green fluorescent protein (GFP)-reporter gene GFP topaz was cotransfected (0.1 µg/mL) to correct for transfection efficiency. Metafectene® Pro (2 µg/mL) was

used as transfection reagent according to the manufacturer's instructions. Cells were cultured for 48 h in DMEM at 37 °C, 95% humidity and 9% CO_2.

7.2.2.10.3 Treatment of cells and harvest

Transfected HEK293T cells were treated with isoprenaline (1 µmol/L) or forskolin (10 µmol/L) 6 h before harvest. Medium was discarded, cells were washed with 2 mL PBS and harvested mechanically with a cell scraper in 1 mL scraping buffer. Cells were pelleted at 3380 x *g* for 3 min at 4 °C, and resuspended in 150 µL potassium phosphate buffer. To destroy the cell membranes, cells were frozen in liquid nitrogen and thawed at 37 °C in a waterbath for three times. After centrifugation at 18,400 x *g* for 3 min at 4 °C the supernatant was further used or stored at - 80 °C.

7.2.2.10.4 Measurement of luciferase activity

Using luciferase reporter gene assays, promoter activity can be determined by luciferase activity. Increase of transcriptional activity results in proportional increased expression of the reporter protein luciferase, whose enzymatic activity can be determined. North American firefly (*Photinus pyralis*) luciferase is an enzyme that catalyzes the reaction of its substrate luciferin to an instable dioxetane under use of O_2 and ATP. Decarboxylation leads to an excited state which relaxes to its ground state by emission of light at 560 nm wavelength.

To measure luciferase activity, 20 µL of sample was mixed with 145 µL luciferase assay mix on a black 96 well plate. After addition of 80 µL luciferin buffer, light emission was measured at 560 nm by the Centro LB 960 Luminometer for 10 sec. Background signal was measured using potassium phosphate buffer without cell extracts.

7.2.2.10.5 Measurement of GFP fluorescence

To estimate transfection efficiency, cotransfection of a GFP control vector is a useful method. It is assumed that HEK293T cells take up different plasmids with the same probability (Reid and Flynn 1997). GFP, isolated from the jellyfish *Aequorea Victoria*, contains a fluorescent chromophore. The GFP variant GFP topaz (GFPtpz) contains 4 point mutations resulting in a change in the emission spectrum to 530 nm (Tsien 1998). The GFPtpz under control of a CMV-promoter (pGFPtpz-cmv) was cotransfected and fluorescence was detected in 30 µL sample for 1 sec on a white 96-well plate by the FluoroCount® Microplate

Fluorometer with a halogen light source with filters for 485 nm (excitation) and 530 nm (emission). Background signal was measured from 30 µL potassium phosphate buffer.

7.2.2.11 Chromatin immunoprecipitation

7.2.2.11.1 Buffers and solutions

Protease inhibitors were stored at - 20 °C and added to the buffers before use.

Cell lysis buffer, pH 8.0, stored at 4 °C

Tris	10 mmol/L
NaCl	10 mmol/L
Nonidet P40	0.2% (v/v)
Protease inhibitors	1x
In dH_2O	

Nuclei lysis buffer, stored at 4 °C

Tris, pH 8	50 mmol/L
EDTA	10 mmol/L
SDS	1% (w/v)
Protease inhibitors	1x
In dH_2O	

Dilution buffer

Tris, pH 8	20 mmol/L
EDTA	2 mmol/L
NaCl	150 mmol/L
Triton X100	1% (v/v)
SDS	0.01% (w/v)
Protease inhibitors	1x
In dH_2O	

Wash buffer I

Tris, pH 8	20 mmol/L
NaCl	150 mmol/L
EDTA	2 mmol/L
SDS	0.1% (w/v)
Triton X100	1% (v/v)
In dH_2O	

Wash buffer II

Tris, pH 8	20 mmol/L
NaCl	500 mmol/L
EDTA	2 mmol/L
SDS	0.1% (w/v)
Triton X100	1% (v/v)
In dH_2O	

Wash buffer III

Tris, pH 8	10 mmol/L
LiCl	250 mmol/L
EDTA	1 mmol/L
Nonidet P40	1% (v/v)
Deoxycholic acid	1% (w/v)
In dH_2O	

Tris-EDTA (TE) buffer

Tris, pH 8	10 mmol/L
EDTA	1 mmol/L
In dH_2O	

Elution buffer I

Tris, pH 8	10 mmol/L
EDTA	1 mmol/L
SDS	1% (w/v)
In dH_2O	

Elution buffer II

Tris, pH 8	10 mmol/L
EDTA	1 mmol/L
SDS	0.67% (w/v)
In dH_2O	

7.2.2.11.2 Procedure

To investigate the recruitment of CRTC1 to promoter regions containing a CRE-site, chromatin immunoprecipitation (ChIP) was conducted. ChIP is a method where protein:DNA interactions are crosslinked and precipitated by specific antibodies. Using PCR analysis with specific primers, CRTC1-bound promoter regions can be identified (Figure 7.5).
Chromatin immunoprecipitation was performed according to Heinrich et al. (Heinrich 2009a). Ventricular heart tissue from C57BL/6J mice, shred into pieces by a scalpel, neonatal mouse cardiomyocytes or peripheral blood monocytes were agitated for 20 minutes in 1 mL 0.9% NaCl with 1% formaldehyde. Cross-linking by formaldehyde was stopped by 125 mmol/L glycine for 5 min. Cells were pelleted by centrifugation at 1500 x *g* for 2 min at 4 °C and lysed in 800 µL cell lysis buffer. Lysis was supported by three freeze (liquid nitrogen) and thaw (37 °C water bath) cycles. After homogenization in a 5 mL dounce homogenizer, cell debris was kept on ice for 10 min before being pelleted at 2350 x *g* for 5 min at 4 °C. Nuclei were lysed by addition of 600 µL nuclei lysis buffer to the pellet, samples were transferred to Bioruptor® microtubes and kept on ice for 10 min. Extracted DNA was sonicated briefly to shear the DNA in the Bioruptor Plus® sonication device (5 x 5 sec, 30 sec break, low). Samples were transferred to a 1.5 mL reaction tube and centrifuged at 15870 x *g* for 10 min at 4 °C. For preclearing, 2.4% Protein A Sepharose CL-4B was added to the sample and rotated for 1 h at 4 °C. Samples were centrifuged for 2 min at 15870 x *g* at 4 °C. A 5% input control was taken from the supernatant and stored in a low DNA-binding tube at 4 °C overnight. To the remaining supernatant, 3 µg TORC1 antibody (0.618 µg/µL) or IgG antibody bound to 30 µL protein A agarose (1 µg/µL) was added and incubated overnight on a rotating platform. Samples were washed twice with 1 mL wash buffer I, once with 1 mL wash buffer II, once with 1 mL wash buffer III, and once with 1 mL TE buffer. After each step, the samples were centrifuged at 1500 x *g* for 2 min at 4 °C and the supernatant was discarded. Samples were transferred to low DNA-binding tubes, protein:DNA complexes were eluted from the agarose in 100 µL elution buffer I for 15 min at 65 °C (Eppendorf Thermomixer comfort) and centrifuged at 15870 x *g* for 5 min at 4 °C. The resulting pellet was treated with 150 µL elution buffer II for 15 minutes at 65 °C

(Eppendorf Thermomixer comfort) and centrifuged at 15870 x *g* for 5 min at 4 °C. Supernatants from the two centrifugation steps were combined in a low DNA-binding tube. The volume of the input control samples was adjusted by addition of 0.8% SDS (w/v) and 200 µL TE buffer. All samples were incubated overnight at 65 °C (Eppendorf thermomixer comfort) to reverse the cross-link. To digest the proteins in the sample, 100 µg proteinase K and 250 µL TE buffer were added and samples were incubated at 37 °C for 2 h (Eppendorf thermomixer comfort). To precipitate high molecular RNA, 400 mmol/L LiCl was added. DNA was purified by a phenol/chloroform extraction using Manual Phase Lock Gel® tubes according to manufacturer's instructions. The sample and 500 µL phenol were added to the tube, thoroughly mixed and centrifuged at 15870 x *g* for 2 min. The resulting upper, liquid phase was again mixed with 500 µL phenol in a Manual Phase Lock Gel® tube and centrifuged at 15870 x *g* for 2 min. The upper phase was mixed with 500 µL chloroform and centrifugation at 15870 x *g* for 2 min at room temperature. The supernatant was transferred to a low DNA-binding reaction tube and DNA was precipitated by 1 µL glycogen (10 µg/µL) in 900 µL 100% ethanol for 35 minutes at 15870 x *g* at 4 °C. After washing with 500 µL 70% ethanol, DNA was eluted in 20 µL TE buffer. Samples were analyzed by PCR, qPCR or stored at - 80 °C until further use.

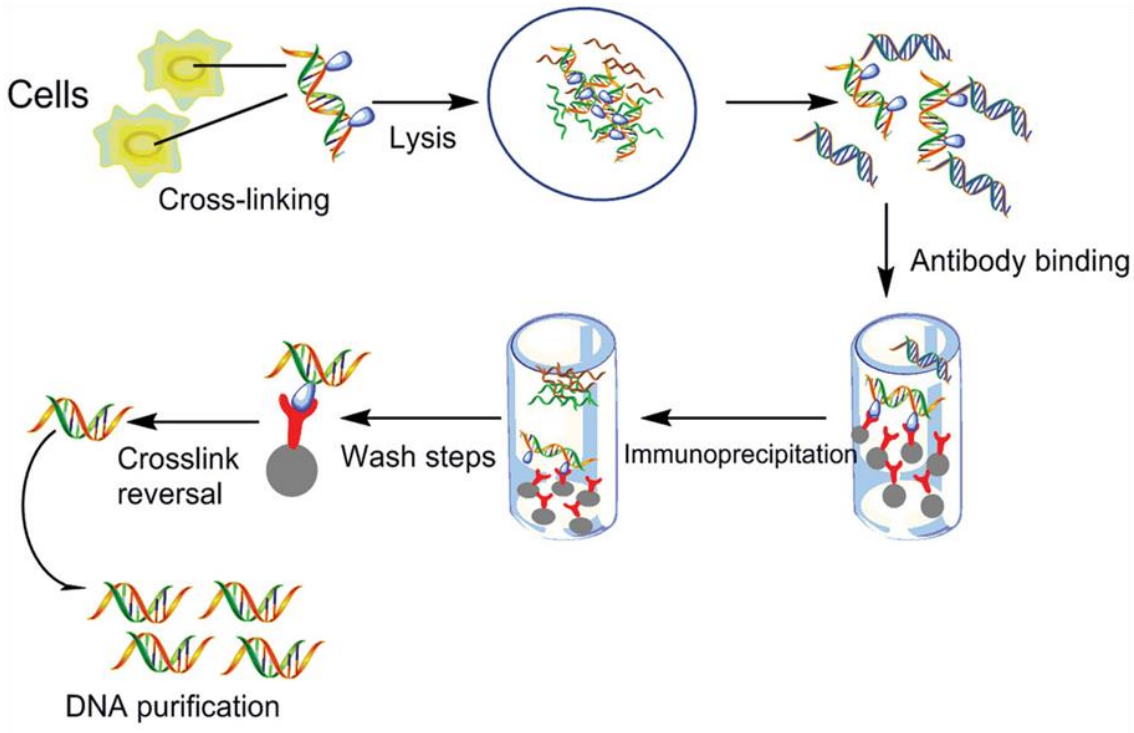

Figure 7.5: Schematic representation of the chromatin immunoprecipitation procedure. Figure was taken from Song et al. (2015).

7.2.2.11.3 Procedure using magnetic beads

The method was performed as previously described, but instead of protein A agarose, magnetic Dynabeads® were used according to the manufacturer's instructions. Per sample, 30 µL Dynabeads® in dilution buffer were pre-bound to 3 µg TORC1 antibody (0.618 µg/µL), rotating at 4 °C for 1 h. A magnet, applied to the side of the tube, held the magnetic beads in place while the supernatant was removed. Beads were washed with 200 µL dilution buffer. Magnet was applied again, dilution buffer was removed, sample was added, and incubated rotating overnight at 4 °C. For the wash steps, a magnet was applied to the side of the tube, supernatant was removed, wash buffer was added, and rotated for 5 min. Elution from the Dynabeads® was performed as described for protein A agarose beads. This procedure was used for chromatin immunoprecipitation performed to detect CRTC1 recruitment to the *Rgs2* and the *Rgs4* promoter.

7.2.2.11.4 Analysis by PCR

DNA obtained from ChIP was amplified using promoter-specific primers flanking the CRE region (Table 7.8). PCR reaction was carried out using the Hot FirePol® DNA polymerase in a T100® Thermal Cycler. PCR samples were prepared using the following components in dH_2O:

Hot FirePol® polymerase	2.5 U
Hot FirePol® BD buffer	1x
$MgCl_2$	1.25 mmol/L
dNTPs	200 µmol/L
forward primer	250 nmol/L
reverse primer	250 nmol/L
DNA	0.02x

PCR was conducted using the following PCR protocol:

Table 7.7: PCR protocol.

Step	*Temperature, °C*	*Time, mm:ss*	
Initial denaturation	95	12:00	
Denaturation	95	00:15	40 cycles
Annealing	50	00:20	
Elongation	75	00:15	
Final Elongation	75	10:00	

Table 7.8: ChIP analysis primer pairs.

Primer name	Primer sequence (5'-3')	Fragment length (bp)
Rgs2 promoter Forw	CCACCTCCCACCCTGTGT	240
Rgs2 promoter Rev	CCACCGCAGCTGTTTGAG	
Rgs4 promoter Forw	GCCGCGGTGGTTTCTATTTT	505
Rgs4 promoter Rev	CTGCCTCACACTACCCAGAATGC	
NR4A2 promoter Forw	AGAGCGGTTCCCACCTTAAA	69
NR4A2 promoter Rev	CGCGCTCGCTTTGGTATATT	

Amplified DNA after PCR was mixed with DNA loading dye and separated by size on a 2% agarose gel containing 0.04% ethidium bromide. The GeneRuler® 100 bp DNA ladder was used for size estimation.

7.2.3 Working with proteins

7.2.3.1 Protein extraction

7.2.3.1.1 Buffers and solutions

Lysis buffer, stored at 4 °C, inhibitors were stored at - 20 °C and added fresh before use

Tris, pH 8.8	40 mmol/L
Glycerol	13% (v/v)
EDTA	5 mmol/L
Na_3VO_4	1 mmol/L
SDS	4% (w/v)
DTT	1 mmol/L
Protease Inhibitors	1x
Phosphatase Inhibitors	1x
In dH_2O	

Loading buffer, pH 6.8, stored at - 20 °C

Tris	130 mmol/L
SDS	4% (w/v)
Bromophenol blue	0.02% (w/v)
Glycerol	50% (v/v)
In dH_2O	

Running buffer, stored at room temperature

Tris	25 mmol/L
Glycine	192 mmol/L
SDS	3.5 mmol/L
In dH_2O	

Transfer buffer, stored at room temperature

Tris	25 mmol/L
Glycine	192 mmol/L
Methanol	20% (v/v)
In dH_2O	

Tris-buffered saline (TBS) buffer, pH 7.6, stored at room temperature

Tris	50 mmol/L
NaCl	150 mmol/L
In dH_2O	

TBS with Tween 20 (TBS-T) buffer, stored at room temperature

TBS buffer	99.9% (v/v)
Tween 20	0.1% (v/v)

Stacking gel

Acrylamide/Bis 37.5:1 30%	400 µL
Tris 0.5 mol/L, pH 6.8	750 µL
SDS 10%	30 µL
TEMED	3 µL
APS 10%	30 µL
dH_2O	1.8 mL

Separation gel	6%	10%	15%
Acrylamide/Bis 37.5:1 30%	1 mL	1.67 mL	2.5 mL
Tris 1.5 mol/L, pH 8.8	1.25 mL	1.25 mL	1.25 mL
SDS 10%	50 µL	50 µL	50 µL
TEMED	5 µL	5 µL	5 µL
APS 10%	50 µL	50 µL	50 µL
dH_2O	2.6 mL	2 mL	1.1 mL

7.2.3.1.2 Procedure

Total protein was extracted from murine heart tissue by addition of 50 to 500 µL lysis buffer (depending on the size of the tissue) and homogenization with the UltraTurrax®. Total protein was extracted from cells by addition of 30 to 50 µL lysis buffer, three freeze (liquid nitrogen) and thaw (room temperature) cycles, and homogenization by pipetting up and down. After centrifugation at 15000 x *g* for 1 min at 4 °C, the supernatant was used or stored at - 80 °C.

7.2.3.2 Bicinchoninic acid (BCA) -test

For immunoblot analysis total protein content was determined by Pierce® BCA protein assay kit according to the manufacturer's instructions. Cu^{2+} is reduced quantitatively to Cu^{+} by proteins in an alkaline medium (biuret reaction). A purple-colored complex is formed by the chelation of one Cu^{+}-ion and two bicinchoninic acid molecules. This complex exhibits an absorbance at a wavelength of 562 nm that is linear with increasing protein concentrations in a range of 20 to 2000 µg/mL.
50 parts of reagent A were mixed with 1 part of reagent B to obtain the working reagent. 480 µL of working reagent were added to 24 µL of sample diluted 1:20 with dH_2O. After incubation at 37 °C for 30 min in a water bath, absorbance was measured in a spectrophotometer. Background signal was measured using a sample containing lysis buffer instead of protein sample.

7.2.3.3 Bradford protein assay

For zymography, protein content was determined using the Bio-Rad protein assay dye reagent. The assay is based on the color change of Coomassie brilliant blue G-250 from red to blue upon binding of protein, which can be measured at a wavelength of 595 nm (Bradford 1976). The assay has a linear range of 0.2 to 1.5 mg/mL. 800 µL protein sample, diluted 1:800 with dH_2O, were mixed with 200 µL Bio-Rad protein assay dye reagent and incubated for 5 min. Absorbance was measured at 595 nm. Background signal was measured using a sample containing dH_2O instead of a protein sample.

7.2.3.4 Immunoblot

To quantify the content of a specific protein, denatured proteins can be separated by size in an electric field on a sodium dodecyl sulfate (SDS)-polyacrylamide gel. SDS coats the proper charge of the protein resulting in a total negative charge which leads to a migration towards the anode. After separation, proteins can be transferred onto a membrane in an electric field and detected by specific antibodies. A primary antibody is targeted against the antigen while a secondary antibody is directed against the first antibody. The secondary antibody is conjugated to a horseradish peroxidase. Addition of enhanced chemiluminescence (ECL) detection reagent results in a chemiluminescent signal that can be detected with a charge-coupled device (CCD) camera (Figure 7.6).

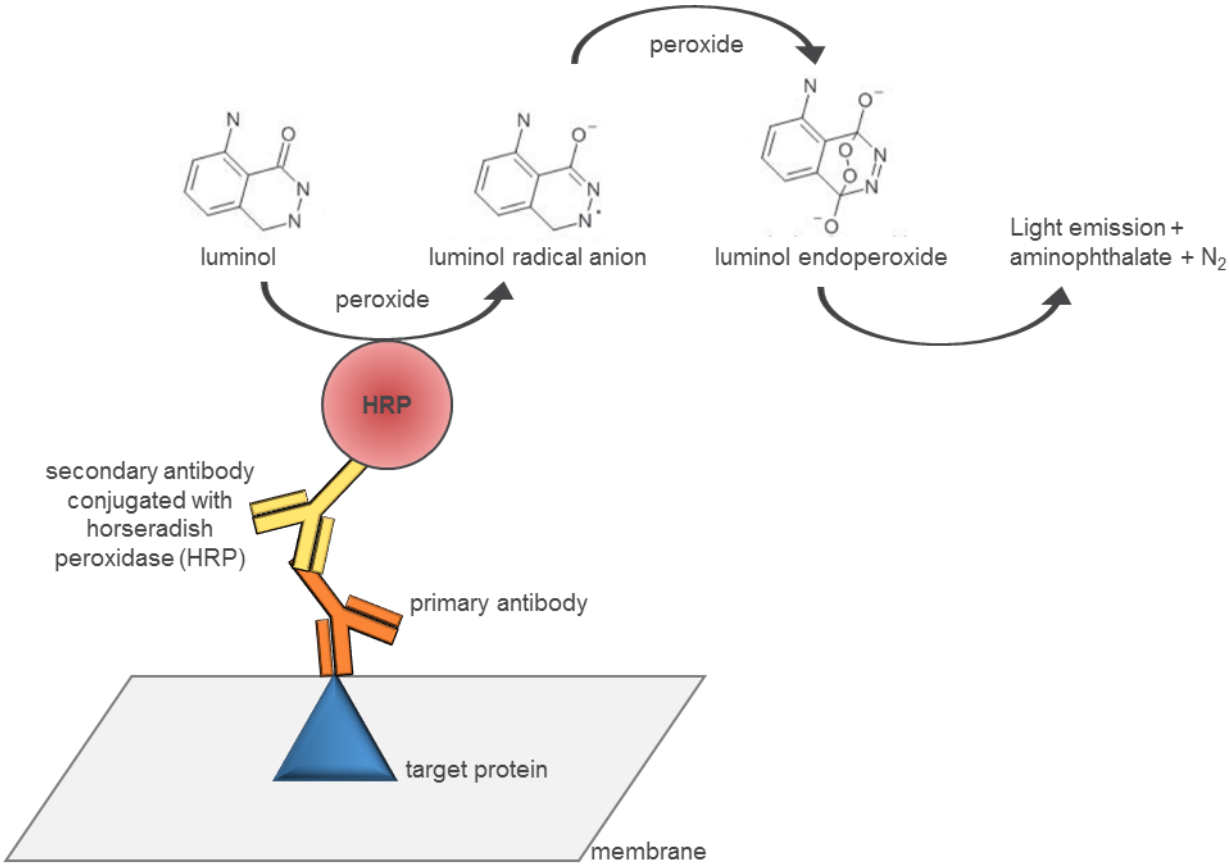

Figure 7.6: Immunoblot detection via ECL reagent. The primary antibody recognizes proteins bound to the membrane. The secondary antibody, conjugated with horseradish peroxidase (HRP), recognizes the primary antibody. HRP catalyzes the reaction of luminol and peroxide to aminophtalates and nitrogen (N_2) under light emission. Chemical formulas taken from the Amersham™ECL™ Prime Western Blotting Detection Reagent Product booklet.

Equal amounts of protein (20, 50, or 75 µg) were adjusted to the same volume with lysis buffer. 0.57 µL 2-mercaptoethanol and 9.43 µL loading buffer were added and the samples were heated at 95 °C for 5 min to denature the proteins. Samples were separated by size on a 6%, 10%, or 15% (depending on the target protein size; see table 7.9) polyacrylamide gel in running buffer at 80 V for the first 10 min followed by 100 V until the end of the run using the Bio Rad PowerPac® Basic power supply. The PageRuler® Plus Protein ladder was used for size estimation. Proteins were transferred onto a nitrocellulose (NC) or polyvinylidene fluoride (PVDF) membrane, depending on the target protein (see table 7.9), at 400 mA for 2 h in transfer buffer. After three wash steps with TBS buffer, the membrane was incubated in 5% milk in TBS-T buffer for 2 h at room temperature to block unspecific binding sites on the membrane. After three wash steps with TBS-T buffer, primary antibody (Table 7.9) was applied overnight at 4 °C. After three wash steps with TBS-T buffer, secondary antibody (Table 7.9) was applied for 2 h at room temperature followed by three wash steps with TBS-T buffer. To detect the chemiluminescence, the Amersham® ECL®

Western Blotting Analysis System was used according to manufacturer's instructions for detection with the ImageQuant® LAS 4000 Luminescent Image Analyzer. Quantification of optical density of the signals was performed using Quantity One® 1-D analysis software 4.6.5. Quantified protein content was normalized to calsequestrin or total protein as loading control. To quantify total protein content after phosphorylated protein was quantified antibodies were removed from the membrane by incubation for 3 min in 2 mL Restore™ Plus Western Blot Stripping buffer. The membrane was then washed three times in TBS buffer and incubated in 5% milk in TBS-T buffer for 2 h. After three wash steps with TBS-T buffer, the primary antibody for total protein was applied and detection was continued as described before.

Table 7.9: Primary antibodies for immunoblot analysis.

Antibody	Gel (%)	Dilution	Membrane	Secondary Antibody
pAKT Ser473	10	1:1000	NC	Anti-rabbit
AKT (pan)	10	1:2000	NC	Anti-mouse
Calsequestrin	6-15	1:5000	NC	Anti-rabbit
CRTC1	10	1:1000	NC	Anti-rabbit
pERK Thr202/Tyr204	10	1:2000	NC	Anti-rabbit
ERK1/2	10	1:1000	NC	Anti-rabbit
pMybpC Ser282	6	1:5000	NC	Anti-rabbit
MybpC	6	1:5000	NC	Anti-rabbit
pPKD Ser916	10	1:500	NC	Anti-rabbit
PKD	10	1:1000	NC	Anti-rabbit
pPLN Ser16	15	1:2500	PVDF	Anti-rabbit
PLN	15	1:5000	PVDF	Anti-mouse
RGS2	10	1:500	PVDF	Anti-chicken
RGS4	10	1:500	PVDF	Anti-goat
pTnI Ser23/24	15	1:1500	PVDF	Anti-rabbit
TnI	15	1:1500	PVDF	Anti-rabbit
Timp4	10	1:1000	NC	Anti-rabbit

7.2.3.5 Zymography

7.2.3.5.1 Buffers and solutions

Lysis buffer, pH 7.4, stored at 4 °C

Tris	50 mmol/L
NaCl	100 mmol/L
$MgCl_2$ x 6 H_2O	4 mmol/L
Glycerol	10% (v/v)
Nonidet P40	10% (v/v)
In dH_2O	

Laemmli buffer 4x, stored at - 20 °C

Glycerol	40% (v/v)
SDS	8% (v/v)
Tris pH 6.8	250 mmol/L
Bromophenol blue	1% (v/v)

Separation gelatin gel, 10%

Gelatin solution (3.4 mg/mL)	2.95 mL
Tris 1.5 M, pH 8.8	1.9 mL
Acrylamide/Bis 37.5:1 30%	2.5 mL
SDS 10%	75 µL
TEMED	6 µL
APS 10%	37.5 µL

Stacking gel

Acrylamide/Bis 37.5:1 30%	635 µL
Tris 0.5 M, pH 6.8	1.252 mL
SDS 10%	50 µL
TEMED	5 µL
APS 10%	40 µL
dH_2O	3.061 mL

Running buffer, stored at room temperature

Tris	25 mmol/L
Glycine	192 mmol/L
SDS	3.5 mmol/L
In dH_2O	

Wash buffer, pH 7.4, stored at room temperature

Triton X100	2.5% (v/v)
Tris	50 mmol/L
$CaCl_2$	5 mmol/L

Incubation buffer, pH 7.4, stored at room temperature

Tris	50 mmol/L
$CaCl_2$	1 mmol/L

Coomassie-blue solution, stored at room temperature

Coomassie G250	5.85 mmol/L
Ethanol	30% (v/v)
Acetic acid	10% (v/v)
dH_2O	60% (v/v)

Destain solution, stored at room temperature

Ethanol	30% (v/v)
Acetic acid	10% (v/v)
dH_2O	60% (v/v)

7.2.3.5.2 Procedure

To analyze enzymatic activity of metalloproteinases, a zymography was performed. Proteins were separated by size in an electric field on a gelatin/SDS gel. Gelatin serves as a substrate for metalloproteinases. Staining with Coomassie blue makes the areas visible where gelatin has been digested by metalloproteinases.

Powder from heart tissue was lysed by addition of 200 µL lysis buffer and pipetting up and down. To activate the metalloproteinases, 10 µg of total protein in 12 µL lysis buffer was mixed with 3 µL 5 mmol/L APMA and incubated for 10 min at 37 °C (waterbath). After

addition of 3.75 µL Laemmli buffer, samples were incubated for 30 min at 37 °C (water-bath). Samples were pipetted onto the gelatin/SDS gel and an electric potential of 80 V was applied. The electrophoresis chamber was kept on ice during the run for inactivation of the metalloproteinases. The gel was washed twice with wash buffer for 1 h at room temperature, gently shaking. To activate the metalloproteinases, the gel was incubated overnight in incubation buffer at 37 °C. The gel was stained with Coomassie-blue solution for about 1 h until the entire gel was dark blue. Destaining in in destain solution was performed until clear bands appeared. Destaining was stopped by 2% acetic acid.

7.2.3.6 Proteomics

Proteomics analysis is used to quantify protein expression between samples. Proteins are isolated from cells and separated by molecular mass using gel electrophoresis. Since the extraction of whole proteins from gels is insufficient, proteins are digested “in-gel” and afterwards extracted. For analysis by mass spectrometry (MS) samples are ionized, for this thesis by electrospray ionization (ESI), and mass to charge ratio was measured by a quadrupole mass analyzer (Graves and Haystead 2002).
Proteomics analysis was performed in cooperation with the group of Prof. Markus Krüger (CECAD, Cologne). 50 µg total protein from heart powder in 4% SDS/Tris buffer at pH 7.6 was separated according to molecular weight on a 10% polyacrylamide gel at 100 V. The gel was stained with the Colloidal Blue Staining Kit according to manufacturer’s instructions and evenly sized gel pieces (about 1 mm^2) were excised. Gel pieces were washed twice with 100 µL 50 mmol/L ammonium bicarbonate (ABC)/50% ethanol for 20 min at room temperature and solutions were discarded. Gel pieces were dehydrated for 10 min in 100 µL absolute ethanol and dried for 5 min in a SpeedVac® vacuum concentrator. For reduction of the proteins, the gel pieces were incubated in 100 µL 10 mmol/L DTT (in 50 mmol/L ABC) for 45 min at 56 °C. To alkylate and thereby block free sulfhydryl groups, gel pieces were incubated in 100 µL 55 mmol/L iodoacetamide for 30 min at room temperature in darkness. Gel pieces were washed in 100 µL 50 mmol/L ABC for 15 min at room temperature and dehydrated with 100 µL 100% ethanol for 15 min at room temperature. They were washed again in 100 µL 50 mmol/L ABC for 15 min at room temperature and dehydrated twice in 100 µL 100% ethanol for 15 min. To digest the proteins, 40 µL of 90% Trypsin/10% Lys-C (Trypsin: 0.5 µg in 1 µL 1mmol/L HCl, Lys-C: 0.5 µg in 1 µL dH_2O) was added to the gel pieces and incubated for 15 min at 4 °C before addition of 50 mmol/L ABC. Proteins in the gel pieces were left to digest overnight. To extract the proteins from the gel pieces, they were incubated in 100 µL 30% acetonitrile/0.3% trifluoroacetic acid

(TFA) for 20 min at room temperature. Gel pieces were incubated twice in 100 µL 70% acetonitrile and twice in 100% acetonitrile for 20 min. The supernatants were collected and dried in a SpeedVac® vacuum concentrator to a volume of about 80 µL. Samples were mixed with an equal amount of 5% acetonitrile/1% TFA and loaded on StageTips (2 layers of C18 material in a 0.2 mL pipette tip). Before the sample was loaded on the StageTips, the StageTips were washed once with 20 µL methanol, once with 20 µL 80% acetonitrile/0.1% formic acid, and twice with 20 µL 0.1% formic acid in dH_2O, each wash step followed by 2 min centrifugation at 630 x *g*. After centrifugation at 630 x *g* for 4 min at room temperature, the StageTips were washed with 20 µL 0.1% formic acid in dH_2O, centrifuged at 630 x *g* for 2 min at room temperature, and air dried before being stored at 4 °C.
The peptide fragments were analyzed by mass spectrometry performed by the group of Prof. Markus Krüger using the Easy nanoflow® HPLC system coupled via a nano-ESI source to a QExactive® Plus mass spectrometer. For quantification the proteomics software MaxQuant® and the implemented Andromeda search engine were used.

7.2.4 Histological analysis

7.2.4.1 Solutions

Masson solution

Ponceau 2R	0.2 g
Acid fuchsin	0.1 g
Acetic acid	0.6 mL
dH_2O	300 mL

Azophloxine solution

Azophloxine	0.5 g
dH_2O	100 mL
Acetic acid	0.2 mL

Ponceau - acid fuchsin - azophloxine solution

Acetic acid 0.2%	88 mL
Masson solution	7 mL
Azophloxine solution	2 mL

Phosphotungstic acid solution

Phosphotungstic acid	5 g
Orange G	2 g
dH_2O	100 mL

Aniline blue solution

Azocarmine G	0.1 g
Acetic acid	1 mL
dH_2O	100 mL

7.2.4.2 Stainings

Formalin-fixed (Roti®-Histofix 4%), paraffin-embedded ventricular cross sections of hearts were used for staining. Paraffin embedding and dystrophin staining was performed by the Mouse Pathology of the University Medical Center Hamburg-Eppendorf using standard techniques.

Masson's trichrome staining was performed using standard techniques. 4 µm thick tissue sections were deparaffinized by bathing in xylene for 15 min at 37 °C, in xylene for 15 min at room temperature, twice in 100% ethanol, twice in 96% ethanol, once in 80% ethanol, once in 70% ethanol and once in dH_2O for 2 min each. The trichrome stain was applied by immersion in Weigert's iron hematoxylin solution (1:1 hematoxylin solution:hematoxylin solution B) for 1 to 2 min to stain the nuclei. After washing with dH_2O for 10 min, tissue was immersed in Ponceau - acid fuchsin - azophloxine solution for 5 to 7 min to stain the plasma followed by 5 sec in 1% acetic acid and dH_2O. 7 min in phosphotungstic acid solution followed by 5 sec in 1% acetic acid and washing with dH_2O stains collagen and connective tissues. 20 min immersion in aniline blue solution followed by 5 sec in 1% acetic acid and washing with dH_2O is used to stain for fibre. After dehydration by immersion for twice 1 min in 100% ethanol and twice 1 min in xylene, tissue was covered with cover slips.

Sirius Red/Fast Green Collagen Staining Kit was used according to manufacturer's instructions. In short, 10 µm thick paraffin-embedded tissue sections were deparaffinized, completely immersed in dye solution and incubated for 30 minutes. Excessive dye was removed by repeated rinsing with dH_2O.

Stained tissue was observed with a Zeiss Axioskop 2 at 1.25x, 10x and 20x magnification.

7.2.4.3 Cell size analysis

Cross-section area in dystrophin stained tissue was determined at a 10x magnification. Using the program Image J® cell borders were marked and the cell area was calculated by the program. Cells with an area greater 155 µm², smaller 1455 µm², and with a ratio of smaller feret diameter/greater feret diameter greater 0.45 were taken into account.

7.2.5 Neonatal mouse cardiomyocytes

Extraction of hearts from neonatal mice was authorized by the Behörde für Gesundheit und Verbraucherschutz der Freien und Hansestadt Hamburg (org 704).

7.2.5.1 Buffers

Hank's Balanced Salt Solution (HBSS), pH 7.31, stored at 4 °C

KCl	5.33 mmol/L
KH_2PO_4	0.44 mmol/L
$NaHCO_3$	4.17 mmol/L
NaCl	137.93 mmol/L
Na_2HPO_4	0.34 mmol/L
D-Glucose	5.56 mmol/L

Light medium pH 7.4, prepared fresh before use

DMEM:M199	3:1
Penicillin/streptomycin	100 U/100 µg/mL
HEPES	1 mmol/L

Dark medium, prepared fresh before use

Light medium	85% (v/v)
Horse serum	10% (v/v)
FBS	5% (v/v)

7.2.5.2 Isolation

Neonatal mouse cardiomyocytes (NMCM) were isolated according to a protocol adapted from Laugwitz et al. (2005).

NMCM were extracted from at least 25 1- to 3-day-old mice. Mice were sacrificed by cervical dislocation. Hearts were extracted aseptically, washed in cold HBSS buffer and cut into small pieces. Heart tissue was predigested overnight at 4 °C in 0.5 mg/mL trypsin/HBSS, gently rotating. The predigested tissue was washed and warmed up in 20 mL light medium at 37 °C followed by a 2 min digestion in 10 mL collagenase type II/HBSS (90 µg/mL) at 37 °C under constant shaking. The supernatant was discarded. This predigestion was followed by five 9-minute digestion steps with 5 mL collagenase type II/HBSS (90 µg/mL) at 37 °C under constant shaking. After each digestion step, the supernatant was mixed with 5 mL cold dark medium and kept on ice to stop the digest. After isolation, cells were filtered through a 100 µm cell strainer and pooled in two 50 mL flasks. Cells were once centrifuged at 100 x *g* for 8 min at room temperature and a second time at 100 x *g* for 5 min before being resuspended in 20 to 25 mL dark medium. To sort out non-cardiomyocytes, cells were pre-plated twice for 75 min in T75 flasks at 37 °C and 10% CO_2. After two-time centrifugation at 40 x *g* for 5 min at room temperature, cells were counted using a Neubauer counting chamber. NMCM were plated on collagen-coated (0.1 to 0.3 mg/mL) 12-well dishes at a density of 40,000 to 85,000 cells/cm^2 in 1 mL medium and incubated at 37 °C and 10% CO_2. To inhibit proliferation of remaining fibroblasts, 25 µmol/L cytosine β-D-arabinofuranoside (ara-C) was added to the culture medium.

7.2.5.3 NMCM treatment

NMCM were treated two days after isolation with isoprenaline (1 µmol/L) for 30 min for ChIP experiments. NMCM were treated with endothelin-1 (100 nmol/L) for 10 min for immuno-blot experiments.

7.2.5.4 Cell harvest

For protein extraction, medium was removed and NMCM were washed with PBS. Cells were mechanically removed from the plate with a cell scraper and transferred to a 1.5 mL reaction tube. After centrifugation at 375 x *g* for 1 min at 4 °C, supernatant was removed and cells were stored at - 80 °C until further use.

7.2.6 Adult mouse ventricular cardiomyocytes

Extraction of hearts for the isolation of adult mouse ventricular myocytes was authorized by the Behörde für Gesundheit und Verbraucherschutz der Freien und Hansestadt Hamburg (org 664).

7.2.6.1 Buffers

Perfusion buffer, pH 7.6, prepared fresh before use

NaCl	113 mmol/L
KCl	4.7 mmol/L
KH_2PO_4	0.6 mmol/L
Na_2HPO_4 x 2 H_2O	0.6 mmol/L
$MgSO_4$ x 7 H_2O	1.2 mmol/L
$NaHCO_3$	12 mmol/L
$KHCO_3$	10 mmol/L
HEPES	10 mmol/L
Taurine	30 mmol/L
D-Glucose	5.55 mmol/L
BDM	10 mmol/L
Penicillin/streptomycin	100 U/100 µg/mL
In dH_2O	

Digestion buffer, prepared fresh before use

$CaCl_2$ x 2 H_2O	0.0125 mmol/L
Liberase TM	0.075 mg/mL
In perfusion buffer	

Stop solution I, prepared fresh before use

FBS	10% (v/v)
$CaCl_2$ x 2 H_2O	0.0125 mmol/L
In perfusion buffer	

Stop solution II, prepared fresh before use

FBS	5% (v/v)
$CaCl_2$ x 2 H_2O	0.0250 mmol/L
In perfusion buffer	

Cardiomyocyte culture medium, prepared fresh before use

BSA	1 mg/mL
Penicillin/streptomycin	100 U/100 µg/mL
L-Glutamine	2 mmol/L
(-)-Blebbistatin	25 µmol/L
ITS	1x

In Minimum Essential Medium (MEM)

7.2.6.2 Isolation

Adult mouse ventricular cardiomyocytes (AMVM) were isolated from 10 to 13 week old *Crtc1*$^{-/-}$ mice or their wild-type littermates according to a protocol adapted from O'Connell et al. (O'Connell et al. 2007). Heparinized mice (10 U heparin/mouse) were anaesthetized with CO_2 and sacrificed by cervical dislocation. Hearts were cannulated through the aorta and perfused with Ca^{2+}-free perfusion buffer for 6 min in a temperature controlled perfusion system at 37 °C at 3 mL/min flow rate. Hearts were digested with 0.075 mg/mL Liberase TM in perfusion buffer for 5.5 (*Crtc1*$^{-/-}$) or 7 min (WT). Ventricles were separated from the atria in 2.5 mL digestion buffer, collagenase activity was stopped by addition of 2.5 mL stop solution I and cells were carefully dissociated. Cell suspension was transferred to a flask where cells were left to sediment by gravity for 10 min. The supernatant was discarded and the pellet was resuspended in 10 mL stop solution II. Ca^{2+} was added stepwise to a final concentration of 900 µmol/L. Cell number was counted in a Fuchs-Rosenthal counting chamber. Isolated cardiomyocytes were either treated subsequent to isolation or cultured overnight in 1 mL cardiomyocyte culture medium at 37 °C and 9% CO_2 on laminin-coated (0.2 mg/mL) 12-well plates at a density of about 50,000 to 100,000 cells per well.

7.2.6.3 AMVM treatment

AMVM were either treated subsequent to isolation or after overnight culture. Cardiomyocytes were treated with isoprenaline (10 nmol/L or 100 nmol/L), phenylephrine (100 µmol/L), endothelin-1 (100 nmol/L), or angiotensin II (1 µmol/L) 10 min before harvest.

7.2.6.4 Cell harvest

Medium containing non-attached cells was transferred to a 1.5 mL reaction tube. Cells attached to the plate were mechanically detached with a cell scraper and transferred to the same reaction tube. Cells were pelleted at 375 x *g* for 2 min at 4 °C, supernatant was removed, cells were washed with 1 mL DPBS and pelleted again at 375 x *g* for 2 min at 4 °C. Supernatant was removed and cells were stored at - 80 °C.

7.2.6.5 Cell size analysis

For cell size measurements freshly isolated mouse cardiomyocytes were plated on 96-well plates at cell densities of 5,000 cells per well. 96-well plates were previously coated with laminin (0.2 mg/mL). Mouse cardiomyocytes were cultured in 500 µL cardiomyocyte culture medium and incubated at 37 °C with 9% CO_2 overnight. Immunofluorescence analysis was carried out by Maksymilian Prondzynski (University Medical Center, Hamburg-Eppendorf). Cells were stained for α-actinin and images were taken at 10x magnification. Images were transferred to the Columbus™ Image Data Management and Analysis System. Columbus™ delivered pre-tested scripts, which were modified according to the characteristics of mouse cardiomyocytes. In this process single building blocks were defined and two filters were developed: a first filter included cell sizes ≥ 1000 µm^2, to exclude possible staining artefacts and a second filter excluded border cells, which were not fully imaged. Using the customized script, bulk analysis of AMCM was performed and cell size was obtained.

7.2.7 Implantation of micro-osmotic pumps

For a continuous 7-day isoprenaline administration, Alzet® Micro-osmotic pumps were implanted into 7- to 8-week-old mice. Animal experiments including implantation of micro-osmotic pumps were authorized by the Behörde für Gesundheit und Verbraucherschutz der Freien und Hansestadt Hamburg (TVA Nr. 72/12).
Pumps were prepared 1 day before implantation according to manufacturer's instructions under sterile conditions. Isoprenaline solution stabilized with 2 µL/mL 1 mol/L HCl was adjusted with 0.9% NaCl to a desired concentration of 2.5 µg/µL per gram bodyweight. This led to a diffusion rate of 30 µg isoprenaline per day per gram bodyweight. Pumps were carefully filled with 200 µL isoprenaline or 0.9% NaCl solution avoiding remains of air

in the pump. Pumps were activated by overnight incubation at 37 °C in sterile 0.9% NaCl solution.

Mice were anesthetized with isoflurane (1-2%) and fixed on a warming platform in prone position. Hair was removed from the neck area and a small incision was made. The osmotic pump was inserted subcutaneously and the incision was closed with 3 sterile suture clips. Mice received 1.33 mg/mL metamizole in the drinking water for 7 days post-surgery.

7.2.8 Echocardiography

Transthoracic echocardiography was performed by Birgit Geertz (University Medical Center, Hamburg-Eppendorf) using the Vevo® 2100 System. Animals were anesthetized with isoflurane (1–2%) and fixed to a warming platform in a supine position. Anesthesia was maintained at 0.5-1% isoflurane via a face mask and anesthetic depth was monitored by an electrocardiogram and respiration rate. Hair was carefully removed from the chest and an ultrasound transmission gel was applied. B-mode images were obtained using a MS 400 transducer with a bandwidth of 18 to 38 MHz and a frame rate of 230 to 400 frames/sec. Two-dimensional short axis views were recorded at the mid-papillary muscle level. The dimensions of the left ventricle were measured in a short axis view in diastole and systole. All images were recorded digitally and off-line analysis was performed using the Vevo® LAB 1.7.1 software.

The left ventricular (LV) inner diameter (LVID, mm), the LV posterior wall (LVPW, mm), the LV anterior wall (LVAW, mm), and the LV epicardial and endocardial area (mm) were measured in end-systolic (s) and end-diastolic (d) states. The diameter of the pulmonary artery (PA diam), the pulmonary velocity time integral (VTI), and the heart rate were measured. LV mass was calculated as $[(\text{LVID d} + \text{LVPW d} + \text{LVAW d})^3 - \text{LVID d}^3] \times 1.053$ mg/mm^3 and expressed in mg. 1.053 mg/mL represents the density of the myocardium. Fractional shortening (FS) was calculated as [(LVID d – LVID s) / LVID d] x 100 and expressed in % (Gardin et al. 1995). LV volume (LV Vol) was calculated as [7.0 / (2.4 + LVID)] x LVID^3 and expressed in mL. Ejection fraction (EF) was calculated as [(LV Vol d – LV Vol s) / LV Vol d] x 100 and expressed in % (Gao et al. 2011). Cardiac output (CO) was calculated as $(\pi \times (\text{PA diam (mm)} / 2)^2 \times \text{VTI (mm)} \times \text{HR (bpm)}) / 100$ and expressed as mL/min.

7.2.9 Statistical analysis

Analysis was carried out using the Graph Pad Prism 5 software. Data were expressed as mean±SEM. Comparison of two groups was performed by Student's t-test, multiple comparison was performed by one-way analysis of variances (ANOVA) followed by Bonferroni's post hoc test. A p-value < 0.05 was considered statistically significant.

8 References

Aktories K, Förstermann U, Hofmann FB and Starke K (2013). Allgemeine und spezielle Pharmakologie und Toxikologie.15-18.

Altarejos JY, Goebel N, Conkright MD, Inoue H, Xie J, Arias CM, Sawchenko PE and Montminy M (2008). The Creb1 coactivator Crtc1 is required for energy balance and fertility. Nat Med **14**: 1112-1117.

Altarejos JY and Montminy M (2011). CREB and the CRTC co-activators: sensors for hormonal and metabolic signals. Nat Rev Mol Cell Biol **12**: 141-151.

Barry SP and Townsend PA (2010). What causes a broken heart--molecular insights into heart failure. Int Rev Cell Mol Biol **284**: 113-179.

Beca S, Ahmad F, Shen W, Liu J, Makary S, Polidovitch N, Sun J, Hockman S, et al. (2013). Phosphodiesterase type 3A regulates basal myocardial contractility through interacting with sarcoplasmic reticulum calcium ATPase type 2a signaling complexes in mouse heart. Circ Res **112**: 289-297.

Bernardo BC, Weeks KL, Pretorius L and McMullen JR (2010). Molecular distinction between physiological and pathological cardiac hypertrophy: experimental findings and therapeutic strategies. Pharmacol Ther **128**: 191-227.

Bittinger MA, McWhinnie E, Meltzer J, Iourgenko V, Latario B, Liu X, Chen CH, Song C, et al. (2004). Activation of cAMP response element-mediated gene expression by regulated nuclear transport of TORC proteins. Curr Biol **14**: 2156-2161.

Blendy JA (2006). The role of CREB in depression and antidepressant treatment. Biol Psychiatry **59**: 1144-1150.

Bradford MM (1976). A rapid and sensitive method for the quantitation of microgram quantities of protein utilizing the principle of protein-dye binding. Anal Biochem **72**: 248-254.

Breuillaud L, Halfon O, Magistretti PJ, Pralong FP and Cardinaux JR (2009). Mouse fertility is not dependent on the CREB coactivator Crtc1. Nat Med **15**: 989-990; author reply 991.

Breuillaud L, Rossetti C, Meylan EM, Merinat C, Halfon O, Magistretti PJ and Cardinaux JR (2012). Deletion of CREB-regulated transcription coactivator 1 induces pathological aggression, depression-related behaviors, and neuroplasticity genes dysregulation in mice. Biol Psychiatry **72**: 528-536.

Bristow MR, Ginsburg R, Minobe W, Cubicciotti RS, Sageman WS, Lurie K, Billingham ME, Harrison DC, et al. (1982). Decreased catecholamine sensitivity and beta-

adrenergic-receptor density in failing human hearts. N Engl J Med **307**: 205-211.

Canettieri G, Coni S, Della Guardia M, Nocerino V, Antonucci L, Di Magno L, Screaton R, Screpanti I, et al. (2009). The coactivator CRTC1 promotes cell proliferation and transformation via AP-1. Proc Natl Acad Sci U S A **106**: 1445-1450.

Chakir K, Zhu W, Tsang S, Woo AY, Yang D, Wang X, Zeng X, Rhee MH, et al. (2011). RGS2 is a primary terminator of beta(2)-adrenergic receptor-mediated G(i) signaling. J Mol Cell Cardiol **50**: 1000-1007.

Choong E, Quteineh L, Cardinaux JR, Gholam-Rezaee M, Vandenberghe F, Dobrinas M, Bondolfi G, Etter M, et al. (2013). Influence of CRTC1 polymorphisms on body mass index and fat mass in psychiatric patients and the general adult population. JAMA Psychiatry **70**: 1011-1019.

Chung E and Leinwand LA (2014). Pregnancy as a cardiac stress model. Cardiovasc Res **101**: 561-570.

Chung E, Yeung F and Leinwand LA (2012). Akt and MAPK signaling mediate pregnancy-induced cardiac adaptation. J Appl Physiol (1985) **112**: 1564-1575.

Conkright MD, Canettieri G, Screaton R, Guzman E, Miraglia L, Hogenesch JB and Montminy M (2003). TORCs: transducers of regulated CREB activity. Mol Cell **12**: 413-423.

Cotecchia S, Del Vescovo CD, Colella M, Caso S and Diviani D (2015). The alpha1-adrenergic receptors in cardiac hypertrophy: signaling mechanisms and functional implications. Cell Signal **27**: 1984-1993.

Daaka Y, Luttrell LM and Lefkowitz RJ (1997). Switching of the coupling of the beta2-adrenergic receptor to different G proteins by protein kinase A. Nature **390**: 88-91.

Davies JS, Klein DC and Carter DA (2011). Selective genomic targeting by FRA-2/FOSL2 transcription factor: regulation of the Rgs4 gene is mediated by a variant activator protein 1 (AP-1) promoter sequence/CREB-binding protein (CBP) mechanism. J Biol Chem **286**: 15227-15239.

Dentin R, Hedrick S, Xie J, Yates J, 3rd and Montminy M (2008). Hepatic glucose sensing via the CREB coactivator CRTC2. Science **319**: 1402-1405.

Dentin R, Liu Y, Koo SH, Hedrick S, Vargas T, Heredia J, Yates J, 3rd and Montminy M (2007). Insulin modulates gluconeogenesis by inhibition of the coactivator TORC2. Nature **449**: 366-369.

Dhar AK and Barton DA (2016). Depression and the Link with Cardiovascular Disease. Front Psychiatry **7**: 33.

Dorn GW, 2nd, Robbins J and Sugden PH (2003). Phenotyping hypertrophy: eschew obfuscation. Circ Res **92**: 1171-1175.

Eckel RH (1997). Obesity and heart disease: a statement for healthcare professionals from the Nutrition Committee, American Heart Association. Circulation **96**: 3248-3250.

Eferl R and Wagner EF (2003). AP-1: a double-edged sword in tumorigenesis. Nat Rev Cancer **3**: 859-868.

Eghbali M, Deva R, Alioua A, Minosyan TY, Ruan H, Wang Y, Toro L and Stefani E (2005). Molecular and functional signature of heart hypertrophy during pregnancy. Circ Res **96**: 1208-1216.

El-Armouche A and Eschenhagen T (2009). Beta-adrenergic stimulation and myocardial function in the failing heart. Heart Fail Rev **14**: 225-241.

Engelhardt S, Hein L, Wiesmann F and Lohse MJ (1999). Progressive hypertrophy and heart failure in beta1-adrenergic receptor transgenic mice. Proc Natl Acad Sci U S A **96**: 7059-7064.

Fentzke RC, Korcarz CE, Lang RM, Lin H and Leiden JM (1998). Dilated cardiomyopathy in transgenic mice expressing a dominant-negative CREB transcription factor in the heart. J Clin Invest **101**: 2415-2426.

Ganau A, Devereux RB, Roman MJ, de Simone G, Pickering TG, Saba PS, Vargiu P, Simongini I, et al. (1992). Patterns of left ventricular hypertrophy and geometric remodeling in essential hypertension. Journal of the American College of Cardiology **19**: 1550-1558.

Gao S, Ho D, Vatner DE and Vatner SF (2011). Echocardiography in Mice. Curr Protoc Mouse Biol **1**: 71-83.

Gardin JM, Siri FM, Kitsis RN, Edwards JG and Leinwand LA (1995). Echocardiographic assessment of left ventricular mass and systolic function in mice. Circ Res **76**: 907-914.

Gaudin C, Ishikawa Y, Wight DC, Mahdavi V, Nadal-Ginard B, Wagner TE, Vatner DE and Homcy CJ (1995). Overexpression of Gs alpha protein in the hearts of transgenic mice. J Clin Invest **95**: 1676-1683.

Graves PR and Haystead TA (2002). Molecular biologist's guide to proteomics. Microbiol Mol Biol Rev **66**: 39-63; table of contents.

Gu S, Cifelli C, Wang S and Heximer SP (2009). RGS proteins: identifying new GAPs in the understanding of blood pressure regulation and cardiovascular function. Clin Sci (Lond) **116**: 391-399.

Hao J, Michalek C, Zhang W, Zhu M, Xu X and Mende U (2006). Regulation of cardiomyocyte signaling by RGS proteins: differential selectivity towards G proteins and susceptibility to regulation. J Mol Cell Cardiol **41**: 51-61.

Harris IS, Zhang S, Treskov I, Kovacs A, Weinheimer C and Muslin AJ (2004). Raf-1 kinase is required for cardiac hypertrophy and cardiomyocyte survival in response to pressure overload. Circulation **110**: 718-723.

Harvey PA and Leinwand LA (2011). The cell biology of disease: cellular mechanisms of cardiomyopathy. J Cell Biol **194**: 355-365.

Haworth RS, Cuello F and Avkiran M (2011). Regulation by phosphodiesterase isoforms of protein kinase A-mediated attenuation of myocardial protein kinase D activation. Basic Res Cardiol **106**: 51-63.

Heineke J and Molkentin JD (2006). Regulation of cardiac hypertrophy by intracellular signalling pathways. Nat Rev Mol Cell Biol **7**: 589-600.

Heinrich A (2009a). Molecular mechanism of the effect of the mood stabilizer lithium on cAMP-induced CREB transcriptional activity. doctoral thesis, Georg August Univeristy.

Heinrich A, Boer U, Tzvetkov M, Oetjen E and Knepel W (2009b). Stimulation by lithium of the interaction between the transcription factor CREB and its co-activator TORC. Biosci Rep **29**: 77-87.

Heinrich A, von der Heyde AS, Boer U, Phu do T, Tzvetkov M and Oetjen E (2013). Lithium enhances CRTC oligomer formation and the interaction between the CREB coactivators CRTC and CBP--implications for CREB-dependent gene transcription. Cell Signal **25**: 113-125.

Heinzel FR, Hohendanner F, Jin G, Sedej S and Edelmann F (2015). Myocardial hypertrophy and its role in heart failure with preserved ejection fraction. J Appl Physiol (1985) **119**: 1233-1242.

Herzig S, Hedrick S, Morantte I, Koo SH, Galimi F and Montminy M (2003). CREB controls hepatic lipid metabolism through nuclear hormone receptor PPAR-gamma. Nature **426**: 190-193.

Heximer SP, Watson N, Linder ME, Blumer KJ and Hepler JR (1997). RGS2/G0S8 is a selective inhibitor of Gqalpha function. Proc Natl Acad Sci U S A **94**: 14389-14393.

Hill JA and Olson EN (2008). Cardiac plasticity. N Engl J Med **358**: 1370-1380.

Ichiki T (2006). Role of cAMP response element binding protein in cardiovascular remodeling: good, bad, or both? Arterioscler Thromb Vasc Biol **26**: 449-455.

Illumina. Retrieved 15.12.16, from http://www.illumina.com/technology/next-generation-sequencing/sequencing-technology.html.

Iourgenko V, Zhang W, Mickanin C, Daly I, Jiang C, Hexham JM, Orth AP, Miraglia L, et al. (2003). Identification of a family of cAMP response element-binding protein coactivators by genome-scale functional analysis in mammalian cells. Proc Natl Acad Sci U S A **100**: 12147-12152.

Kach J, Sethakorn N and Dulin NO (2012). A finer tuning of G-protein signaling through regulated control of RGS proteins. Am J Physiol Heart Circ Physiol **303**: H19-35.

Kai H, Muraishi A, Sugiu Y, Nishi H, Seki Y, Kuwahara F, Kimura A, Kato H, et al. (1998). Expression of proto-oncogenes and gene mutation of sarcomeric proteins in patients with hypertrophic cardiomyopathy. Circ Res **83**: 594-601.

Kang M, Chung KY and Walker JW (2007). G-protein coupled receptor signaling in myocardium: not for the faint of heart. Physiology (Bethesda) **22**: 174-184.

Kanyo R, Price DM, Chik CL and Ho AK (2009). Salt-inducible kinase 1 in the rat pinealocyte: adrenergic regulation and role in arylalkylamine N-acetyltransferase gene transcription. Endocrinology **150**: 4221-4230.

Katoh Y, Takemori H, Horike N, Doi J, Muraoka M, Min L and Okamoto M (2004). Salt-inducible kinase (SIK) isoforms: their involvement in steroidogenesis and adipogenesis. Mol Cell Endocrinol **217**: 109-112.

Kehat I, Davis J, Tiburcy M, Accornero F, Saba-El-Leil MK, Maillet M, York AJ, Lorenz JN, et al. (2011). Extracellular signal-regulated kinases 1 and 2 regulate the balance between eccentric and concentric cardiac growth. Circ Res **108**: 176-183.

Ketsawatsomkron P, Keen HL, Davis DR, Lu KT, Stump M, De Silva TM, Hilzendeger AM, Grobe JL, et al. (2016). Protective Role for Tissue Inhibitor of Metalloproteinase-4, a Novel Peroxisome Proliferator-Activated Receptor-gamma Target Gene, in Smooth Muscle in Deoxycorticosterone Acetate-Salt Hypertension. Hypertension **67**: 214-222.

Kim H (2016). The transcription cofactor CRTC1 protects from aberrant hepatic lipid accumulation. Sci Rep **6**: 37280.

Koo SH, Flechner L, Qi L, Zhang X, Screaton RA, Jeffries S, Hedrick S, Xu W, et al. (2005). The CREB coactivator TORC2 is a key regulator of fasting glucose metabolism. Nature **437**: 1109-1111.

Koshman YE, Sternlicht MD, Kim T, O'Hara CP, Koczor CA, Lewis W, Seeley TW, Lipson KE, et al. (2015). Connective tissue growth factor regulates cardiac function and tissue remodeling in a mouse model of dilated cardiomyopathy. J Mol Cell Cardiol **89**: 214-222.

Koskivirta I, Kassiri Z, Rahkonen O, Kiviranta R, Oudit GY, McKee TD, Kyto V, Saraste A, et al. (2010). Mice with tissue inhibitor of metalloproteinases 4 (Timp4) deletion succumb to induced myocardial infarction but not to cardiac pressure overload. J Biol Chem **285**: 24487-24493.

Kovacs KA, Steullet P, Steinmann M, Do KQ, Magistretti PJ, Halfon O and Cardinaux JR (2007). TORC1 is a calcium- and cAMP-sensitive coincidence detector

involved in hippocampal long-term synaptic plasticity. Proc Natl Acad Sci U S A **104**: 4700-4705.

Kukurba KR and Montgomery SB (2015). RNA Sequencing and Analysis. Cold Spring Harb Protoc **2015**: 951-969.

Kurrasch DM, Huang J, Wilkie TM and Repa JJ (2004). Quantitative real-time polymerase chain reaction measurement of regulators of G-protein signaling mRNA levels in mouse tissues. Methods Enzymol **389**: 3-15.

Kuwahara K, Saito Y, Takano M, Arai Y, Yasuno S, Nakagawa Y, Takahashi N, Adachi Y, et al. (2003). NRSF regulates the fetal cardiac gene program and maintains normal cardiac structure and function. EMBO J **22**: 6310-6321.

Laugwitz KL, Moretti A, Lam J, Gruber P, Chen Y, Woodard S, Lin LZ, Cai CL, et al. (2005). Postnatal isl1+ cardioblasts enter fully differentiated cardiomyocyte lineages. Nature **433**: 647-653.

Le Lay J, Tuteja G, White P, Dhir R, Ahima R and Kaestner KH (2009). CRTC2 (TORC2) contributes to the transcriptional response to fasting in the liver but is not required for the maintenance of glucose homeostasis. Cell Metab **10**: 55-62.

Lenart L, Hodrea J, Hosszu A, Koszegi S, Zelena D, Balogh D, Szkibinszkij E, Veres-Szekely A, et al. (2016). The role of sigma-1 receptor and brain-derived neurotrophic factor in the development of diabetes and comorbid depression in streptozotocin-induced diabetic rats. Psychopharmacology (Berl) **233**: 1269-1278.

Levy D (1991). Clinical significance of left ventricular hypertrophy: insights from the Framingham Study. J Cardiovasc Pharmacol **17 Suppl 2**: S1-6.

Lewin G, Matus M, Basu A, Frebel K, Rohsbach SP, Safronenko A, Seidl MD, Stumpel F, et al. (2009). Critical role of transcription factor cyclic AMP response element modulator in beta1-adrenoceptor-mediated cardiac dysfunction. Circulation **119**: 79-88.

Li H, He C, Feng J, Zhang Y, Tang Q, Bian Z, Bai X, Zhou H, et al. (2010). Regulator of G protein signaling 5 protects against cardiac hypertrophy and fibrosis during biomechanical stress of pressure overload. Proc Natl Acad Sci U S A **107**: 13818-13823.

Liao Y, Ishikura F, Beppu S, Asakura M, Takashima S, Asanuma H, Sanada S, Kim J, et al. (2002). Echocardiographic assessment of LV hypertrophy and function in aortic-banded mice: necropsy validation. Am J Physiol Heart Circ Physiol **282**: H1703-1708.

Lichtman JH, Bigger JT, Jr., Blumenthal JA, Frasure-Smith N, Kaufmann PG, Lesperance F, Mark DB, Sheps DS, et al. (2008). Depression and coronary heart disease: recommendations for screening, referral, and treatment: a science advisory from the American Heart Association Prevention Committee

of the Council on Cardiovascular Nursing, Council on Clinical Cardiology, Council on Epidemiology and Prevention, and Interdisciplinary Council on Quality of Care and Outcomes Research: endorsed by the American Psychiatric Association. Circulation **118**: 1768-1775.

Liggett SB, Tepe NM, Lorenz JN, Canning AM, Jantz TD, Mitarai S, Yatani A and Dorn GW, 2nd (2000). Early and delayed consequences of beta(2)-adrenergic receptor overexpression in mouse hearts: critical role for expression level. Circulation **101**: 1707-1714.

Liu Y, Huang H, Zhang Y, Zhu XY, Zhang R, Guan LH, Tang Q, Jiang H, et al. (2014). Regulator of G protein signaling 3 protects against cardiac hypertrophy in mice. J Cell Biochem **115**: 977-986.

Livak KJ and Schmittgen TD (2001). Analysis of relative gene expression data using real-time quantitative PCR and the 2(-Delta Delta C(T)) Method. Methods **25**: 402-408.

Lonze BE and Ginty DD (2002). Function and regulation of CREB family transcription factors in the nervous system. Neuron **35**: 605-623.

Lopes LR and Elliott PM (2014). A straightforward guide to the sarcomeric basis of cardiomyopathies. Heart **100**: 1916-1923.

Lorenz K, Schmitt JP, Vidal M and Lohse MJ (2009). Cardiac hypertrophy: targeting Raf/MEK/ERK1/2-signaling. Int J Biochem Cell Biol **41**: 2351-2355.

Lorenz K, Stathopoulou K, Schmid E, Eder P and Cuello F (2014). Heart failure-specific changes in protein kinase signalling. Pflugers Arch **466**: 1151-1162.

Love MI, Huber W and Anders S (2014). Moderated estimation of fold change and dispersion for RNA-seq data with DESeq2. Genome Biol **15**: 550.

Lovelock JD, Baker AH, Gao F, Dong JF, Bergeron AL, McPheat W, Sivasubramanian N and Mann DL (2005). Heterogeneous effects of tissue inhibitors of matrix metalloproteinases on cardiac fibroblasts. Am J Physiol Heart Circ Physiol **288**: H461-468.

Lu Y, Day FR, Gustafsson S, Buchkovich ML, Na J, Bataille V, Cousminer DL, Dastani Z, et al. (2016). New loci for body fat percentage reveal link between adiposity and cardiometabolic disease risk. Nat Commun **7**: 10495.

Luppino FS, de Wit LM, Bouvy PF, Stijnen T, Cuijpers P, Penninx BW and Zitman FG (2010). Overweight, obesity, and depression: a systematic review and meta-analysis of longitudinal studies. Arch Gen Psychiatry **67**: 220-229.

Lygren B, Carlson CR, Santamaria K, Lissandron V, McSorley T, Litzenberg J, Lorenz D, Wiesner B, et al. (2007). AKAP complex regulates Ca2+ re-uptake into heart sarcoplasmic reticulum. EMBO Rep **8**: 1061-1067.

Maillet M, van Berlo JH and Molkentin JD (2013). Molecular basis of physiological heart growth: fundamental concepts and new players. Nat Rev Mol Cell Biol **14**: 38-48.

Maldonado R, Smadja C, Mazzucchelli C and Sassone-Corsi P (1999). Altered emotional and locomotor responses in mice deficient in the transcription factor CREM. Proc Natl Acad Sci U S A **96**: 14094-14099.

Mantamadiotis T, Lemberger T, Bleckmann SC, Kern H, Kretz O, Martin Villalba A, Tronche F, Kellendonk C, et al. (2002). Disruption of CREB function in brain leads to neurodegeneration. Nat Genet **31**: 47-54.

Mayr B and Montminy M (2001). Transcriptional regulation by the phosphorylation-dependent factor CREB. Nat Rev Mol Cell Biol **2**: 599-609.

Meylan EM, Breuillaud L, Seredenina T, Magistretti PJ, Halfon O, Luthi-Carter R and Cardinaux JR (2016). Involvement of the agmatinergic system in the depressive-like phenotype of the Crtc1 knockout mouse model of depression. Transl Psychiatry **6**: e852.

Mittmann C, Chung CH, Hoppner G, Michalek C, Nose M, Schuler C, Schuh A, Eschenhagen T, et al. (2002). Expression of ten RGS proteins in human myocardium: functional characterization of an upregulation of RGS4 in heart failure. Cardiovasc Res **55**: 778-786.

Montminy M. (2005) CREB target gene database. Retrieved 15.12.2016, from http://natural.salk.edu/CREB/.

Nadal-Ginard B and Mahdavi V (1989). Molecular basis of cardiac performance. Plasticity of the myocardium generated through protein isoform switches. J Clin Invest **84**: 1693-1700.

Najafi A, Sequeira V, Helmes M, Bollen IA, Goebel M, Regan JA, Carrier L, Kuster DW, et al. (2016). Selective phosphorylation of PKA targets after beta-adrenergic receptor stimulation impairs myofilament function in Mybpc3-targeted HCM mouse model. Cardiovasc Res **110**: 200-214.

Nantel F, Monaco L, Foulkes NS, Masquilier D, LeMeur M, Henriksen K, Dierich A, Parvinen M, et al. (1996). Spermiogenesis deficiency and germ-cell apoptosis in CREM-mutant mice. Nature **380**: 159-162.

Nichols CB, Chang CW, Ferrero M, Wood BM, Stein ML, Ferguson AJ, Ha D, Rigor RR, et al. (2014). beta-adrenergic signaling inhibits Gq-dependent protein kinase D activation by preventing protein kinase D translocation. Circ Res **114**: 1398-1409.

Nikolaev VO, Moshkov A, Lyon AR, Miragoli M, Novak P, Paur H, Lohse MJ, Korchev YE, et al. (2010). Beta2-adrenergic receptor redistribution in heart failure changes cAMP compartmentation. Science **327**: 1653-1657.

O'Connell TD, Rodrigo MC and Simpson PC (2007). Isolation and culture of adult mouse cardiac myocytes. Methods Mol Biol **357**: 271-296.

Okumura S, Vatner DE, Kurotani R, Bai Y, Gao S, Yuan Z, Iwatsubo K, Ulucan C, et al. (2007). Disruption of type 5 adenylyl cyclase enhances desensitization of cyclic adenosine monophosphate signal and increases Akt signal with chronic catecholamine stress. Circulation **116**: 1776-1783.

Perlmann T and Wallen-Mackenzie A (2004). Nurr1, an orphan nuclear receptor with essential functions in developing dopamine cells. Cell Tissue Res **318**: 45-52.

Quteineh L, Preisig M, Rivera M, Milaneschi Y, Castelao E, Gholam-Rezaee M, Vandenberghe F, Saigi-Morgui N, et al. (2016). Association of CRTC1 polymorphisms with obesity markers in subjects from the general population with lifetime depression. J Affect Disord **198**: 43-49.

Ravnskjaer K, Kester H, Liu Y, Zhang X, Lee D, Yates JR, 3rd and Montminy M (2007). Cooperative interactions between CBP and TORC2 confer selectivity to CREB target gene expression. EMBO J **26**: 2880-2889.

Reid BG and Flynn GC (1997). Chromophore formation in green fluorescent protein. Biochemistry **36**: 6786-6791.

Rudolph D, Tafuri A, Gass P, Hammerling GJ, Arnold B and Schutz G (1998). Impaired fetal T cell development and perinatal lethality in mice lacking the cAMP response element binding protein. Proc Natl Acad Sci U S A **95**: 4481-4486.

Ruehr ML, Russell MA and Bond M (2004). A-kinase anchoring protein targeting of protein kinase A in the heart. J Mol Cell Cardiol **37**: 653-665.

Rutledge T, Reis VA, Linke SE, Greenberg BH and Mills PJ (2006). Depression in heart failure a meta-analytic review of prevalence, intervention effects, and associations with clinical outcomes. Journal of the American College of Cardiology **48**: 1527-1537.

Sadoshima J and Izumo S (1993). Molecular characterization of angiotensin II--induced hypertrophy of cardiac myocytes and hyperplasia of cardiac fibroblasts. Critical role of the AT1 receptor subtype. Circ Res **73**: 413-423.

Sanchez-Fernandez G, Cabezudo S, Garcia-Hoz C, Beninca C, Aragay AM, Mayor F, Jr. and Ribas C (2014). Galphaq signalling: the new and the old. Cell Signal **26**: 833-848.

Schlossarek S, Singh SR, Geertz B, Schulz H, Reischmann S, Hubner N and Carrier L (2014). Proteasome inhibition slightly improves cardiac function in mice with hypertrophic cardiomyopathy. Front Physiol **5**: 484.

Schulte JS, Fehrmann E, Tekook MA, Kranick D, Fels B, Li N, Wehrens XH, Heinick A, et al. (2016). Cardiac expression of the CREM repressor isoform CREM-IbDeltaC-X in mice leads to arrhythmogenic alterations in ventricular cardiomyocytes. Basic Res Cardiol **111**: 15.

Screaton RA, Conkright MD, Katoh Y, Best JL, Canettieri G, Jeffries S, Guzman E, Niessen S, et al. (2004). The CREB coactivator TORC2 functions as a calcium- and cAMP-sensitive coincidence detector. Cell **119**: 61-74.

Shiojima I, Sato K, Izumiya Y, Schiekofer S, Ito M, Liao R, Colucci WS and Walsh K (2005). Disruption of coordinated cardiac hypertrophy and angiogenesis contributes to the transition to heart failure. J Clin Invest **115**: 2108-2118.

Shubeita HE, McDonough PM, Harris AN, Knowlton KU, Glembotski CC, Brown JH and Chien KR (1990). Endothelin induction of inositol phospholipid hydrolysis, sarcomere assembly, and cardiac gene expression in ventricular myocytes. A paracrine mechanism for myocardial cell hypertrophy. J Biol Chem **265**: 20555-20562.

Simpson P, McGrath A and Savion S (1982). Myocyte hypertrophy in neonatal rat heart cultures and its regulation by serum and by catecholamines. Circ Res **51**: 787-801.

Siryk-Bathgate A, Dabul S and Lymperopoulos A (2013). Current and future G protein-coupled receptor signaling targets for heart failure therapy. Drug Des Devel Ther **7**: 1209-1222.

Solaro RJ and Rarick HM (1998). Troponin and tropomyosin: proteins that switch on and tune in the activity of cardiac myofilaments. Circ Res **83**: 471-480.

Song C, Zhang S and Huang H (2015). Choosing a suitable method for the identification of replication origins in microbial genomes. Front Microbiol **6**: 1049.

Song Y, Altarejos J, Goodarzi MO, Inoue H, Guo X, Berdeaux R, Kim JH, Goode J, et al. (2010). CRTC3 links catecholamine signalling to energy balance. Nature **468**: 933-939.

Takimoto E, Koitabashi N, Hsu S, Ketner EA, Zhang M, Nagayama T, Bedja D, Gabrielson KL, et al. (2009). Regulator of G protein signaling 2 mediates cardiac compensation to pressure overload and antihypertrophic effects of PDE5 inhibition in mice. J Clin Invest **119**: 408-420.

TexasHeartInstitute. Retrieved 15.12.2016, from http://www.texasheart.org/HIC/Anatomy/anatomy2.cfm.

ThermoScientific. Retrieved 15.12.2016, from https://www.thermofisher.com/de/de/home.html.

Tilley DG (2011). G protein-dependent and G protein-independent signaling pathways and their impact on cardiac function. Circ Res **109**: 217-230.

Tokudome T, Kishimoto I, Horio T, Arai Y, Schwenke DO, Hino J, Okano I, Kawano Y, et al. (2008). Regulator of G-protein signaling subtype 4 mediates

antihypertrophic effect of locally secreted natriuretic peptides in the heart. Circulation **117**: 2329-2339.

Tsang S, Woo AY, Zhu W and Xiao RP (2010). Deregulation of RGS2 in cardiovascular diseases. Front Biosci (Schol Ed) **2**: 547-557.

Tsien RY (1998). The green fluorescent protein. Annu Rev Biochem **67**: 509-544.

Ungerer M, Bohm M, Elce JS, Erdmann E and Lohse MJ (1993). Altered expression of beta-adrenergic receptor kinase and beta 1-adrenergic receptors in the failing human heart. Circulation **87**: 454-463.

Uys GM, Ramburan A, Loos B, Kinnear CJ, Korkie LJ, Mouton J, Riedemann J and Moolman-Smook JC (2011). Myomegalin is a novel A-kinase anchoring protein involved in the phosphorylation of cardiac myosin binding protein C. BMC Cell Biol **12**: 18.

van Dijk EL, Auger H, Jaszczyszyn Y and Thermes C (2014). Ten years of next-generation sequencing technology. Trends Genet **30**: 418-426.

Wang Y (2007). Mitogen-activated protein kinases in heart development and diseases. Circulation **116**: 1413-1423.

Wang Y, Inoue H, Ravnskjaer K, Viste K, Miller N, Liu Y, Hedrick S, Vera L, et al. (2010). Targeted disruption of the CREB coactivator Crtc2 increases insulin sensitivity. Proc Natl Acad Sci U S A **107**: 3087-3092.

Wettschureck N, Rutten H, Zywietz A, Gehring D, Wilkie TM, Chen J, Chien KR and Offermanns S (2001). Absence of pressure overload induced myocardial hypertrophy after conditional inactivation of Galphaq/Galpha11 in cardiomyocytes. Nat Med **7**: 1236-1240.

Whelan RS, Konstantinidis K, Xiao RP and Kitsis RN (2013). Cardiomyocyte life-death decisions in response to chronic beta-adrenergic signaling. Circ Res **112**: 408-410.

Wilkins BJ and Molkentin JD (2004). Calcium-calcineurin signaling in the regulation of cardiac hypertrophy. Biochem Biophys Res Commun **322**: 1178-1191.

Wong W and Scott JD (2004). AKAP signalling complexes: focal points in space and time. Nat Rev Mol Cell Biol **5**: 959-970.

Xiao L, Pimental DR, Amin JK, Singh K, Sawyer DB and Colucci WS (2001). MEK1/2-ERK1/2 mediates alpha1-adrenergic receptor-stimulated hypertrophy in adult rat ventricular myocytes. J Mol Cell Cardiol **33**: 779-787.

Xie Z, Liu D, Liu S, Calderon L, Zhao G, Turk J and Guo Z (2011). Identification of a cAMP-response element in the regulator of G-protein signaling-2 (RGS2) promoter as a key cis-regulatory element for RGS2 transcriptional regulation by angiotensin II in cultured vascular smooth muscles. J Biol Chem **286**: 44646-44658.

Xing G, Zhang L, Russell S and Post R (2006). Reduction of dopamine-related transcription factors Nurr1 and NGFI-B in the prefrontal cortex in schizophrenia and bipolar disorders. Schizophr Res **84**: 36-56.

Xu Q, Ji XF, Chi TY, Liu P, Jin G, Gu SL and Zou LB (2015). Sigma 1 receptor activation regulates brain-derived neurotrophic factor through NR2A-CaMKIV-TORC1 pathway to rescue the impairment of learning and memory induced by brain ischaemia/reperfusion. Psychopharmacology (Berl) **232**: 1779-1791.

Xu W, Kasper LH, Lerach S, Jeevan T and Brindle PK (2007). Individual CREB-target genes dictate usage of distinct cAMP-responsive coactivation mechanisms. EMBO J **26**: 2890-2903.

Yan L, Vatner DE, O'Connor JP, Ivessa A, Ge H, Chen W, Hirotani S, Ishikawa Y, et al. (2007). Type 5 adenylyl cyclase disruption increases longevity and protects against stress. Cell **130**: 247-258.

Yin Z, Ren J and Guo W (2015). Sarcomeric protein isoform transitions in cardiac muscle: a journey to heart failure. Biochim Biophys Acta **1852**: 47-52.

Zaccolo M and Pozzan T (2002). Discrete microdomains with high concentration of cAMP in stimulated rat neonatal cardiac myocytes. Science **295**: 1711-1715.

Zhang W, Anger T, Su J, Hao J, Xu X, Zhu M, Gach A, Cui L, et al. (2006). Selective loss of fine tuning of Gq/11 signaling by RGS2 protein exacerbates cardiomyocyte hypertrophy. J Biol Chem **281**: 5811-5820.

9 Appendix

9.1 Curriculum vitae

<u>Personal data</u>	
Name	Karoline Morhenn
Date of birth	May 9th, 1987
Place of birth	Pittsburgh, Pennsylvania, USA
Nationality	German and US American
<u>Education</u>	
Since August 2013	PhD student Under supervision of Prof. Dr. med. Elke Oetjen Institute of Clinical Pharmacology and Toxicology University Medical Center, Hamburg-Eppendorf
October 2014 – September 2016	Graduate studies in molecular biology University of Hamburg, Center for Molecular Neurobiology (ZMNH), Hamburg
January 2013	Approbation
December 2012	3rd state examination
April 2011	2nd state examination
April 2007 – December 2012	Studies in Pharmacy Westfälische Wilhelms University, Münster
July 2006	Abitur and Baccalauréat Gymnasium Kreuzgasse, Cologne
<u>Scholarship</u>	
April 2014 – March 2015	Doctoral scholarship at the University of Hamburg
<u>Awards</u>	
April 2015	Second place for oral presentation, 12th Hamburger Studententagung

9.2 Conference participations

The presenting author is written in bold.

1. **K. Morhenn**, S. Schroeder, A. Pahl, S. Schlossarek, L. Carrier, T. Eschenhagen, J.-R. Cardinaux, S. Lutz, Z. Guo, E. Oetjen
   CRTC1 deficient mice show cardiac hypertrophy and decreased protein levels of RGS2.
   Poster presentation, 80th Annual Meeting of the Deutsche Gesellschaft für experimentelle und klinische Pharmakologie und Toxikologie (DGPT), March 31st – April 3rd, 2014

2. **K. Morhenn**, T. Quentin, S. Schroeder, A. Pahl, S. Schlossarek, L. Carrier, T. Eschenhagen, J.-R. Cardinaux, K. Lorenz, S. Lutz, W.H. Zimmermann, M. Steinmetz, A. Kaul, G. Hasenfuss, U. Laufs, Z. Guo, E. Oetjen
   Influence of increased levels of the transcriptional co-activator CRTC1 in cardiac hypertrophy.
   Poster presentation, Annual Meeting of the Deutsche Pharmazeutische Gesellschaft (DPhG), September 24rd – 26th, 2014

3. **K. Morhenn**, S. Schroeder, B. Geertz, T. Eschenhagen, J.-R. Cardinaux, S. Lutz, E. Oetjen
   Crtc1-deficient mice show cardiac hypertrophy and reduced cardiac function.
   Poster presentation, 81st Annual Meeting of the Deutsche Gesellschaft für experimentelle und klinische Pharmakologie und Toxikologie (DGPT), March 10th – 12th, 2015

4. **K. Morhenn**, S. Schroeder, A. Pahl, B. Geertz, T. Eschenhagen, S. Schlossarek, L. Carrier, J.-R. Cardinaux, S. Lutz, E. Oetjen
   Crtc1-deficient mice show cardiac hypertrophy and decreased protein levels of RGS2.
   Oral presentation, 81st Annual Meeting of the Deutsche Gesellschaft für Kardiologie (DGK), April 8th – 11th, 2015

5. **K. Morhenn**, B. Geertz, T. Eschenhagen, J.-R. Cardinaux, S. Lutz, E. Oetjen
***Crtc1*$^{-/-}$ Mäuse zeigen kardiale Hypertrophie und verminderte RGS2 Level.**
Oral presentation, 12th Hamburger Studententagung, April 28th, 2015

6. **K. Morhenn**, B. Geertz, T. Eschenhagen, J.-R. Cardinaux, S. Lutz, E. Oetjen
Crtc1-deficient mice show cardiac hypertrophy and reduced cardiac function.
Poster presentation, Annual Meeting of the Deutsche Pharmazeutische Gesellschaft (DPhG), September 23rd – 26th, 2015

7. **K. Morhenn**, T. Quentin, S. Schroeder, A. Pahl, M. Steinmetz, B. Geertz, T. Eschenhagen, S. Schlossarek, L. Carrier, J.-R. Cardinaux, W.H. Zimmermann, S. Lutz, E. Oetjen
CRTC1 - a Novel Player in Cardiac Hypertrophy.
Poster presentation, Annual Meeting of the American Heart Association, November 7th – 11th, 2015

8. **K. Morhenn**, T. Quentin, S. Schroeder, A. Pahl, M. Steinmetz, B. Geertz, T. Eschenhagen, S. Schlossarek, L. Carrier, J.-R. Cardinaux, W.H. Zimmermann, S. Lutz, E. Oetjen
CRTC1 – a Novel Player in Cardiac Hypertrophy.
Poster presentation, 3rd Young DZHK retreat, September 14th – 17th, 2016

9. **K. Morhenn**, B. Geertz, T. Eschenhagen, E. Oetjen
***Crtc1*-deficient mice show reduced cardiac function which is ameliorated by isoprenaline treatment.**
Poster presentation, Annual Meeting of the Deutsche Pharmazeutische Gesellschaft (DPhG), October 4th – 7th, 2016

10. **A. L. Gundler**, K. Morhenn, E. Oetjen
Distinct cardiac metabolic shifts in two mouse models of cardiac hypertrophy.
Poster presentation, Annual Meeting of the Deutsche Pharmazeutische Gesellschaft (DPhG), October 4th – 7th, 2016

11. **K. Morhenn**, T. Quentin, S. Schroeder, A. Pahl, M. Steinmetz, B. Geertz, T. Eschenhagen, S. Schlossarek, L. Carrier, J.-R. Cardinaux, W.H. Zimmermann, S. Lutz, E. Oetjen
    ***Crtc1*-deficient mice show cardiac hypertrophy and decreased cardiac function.**
    Poster presentation, Basic Science Meeting of the Deutsche Gesellschaft für Kardiologie (DGK), September 6th – 8th, 2016

Awards:

Second place for oral presentation, 12th Hamburger Studententagung, April 28th, 2015

9.3 EU-GHS Hazard (H) and Precaution (P) statements

According to the 8th ATP of the CLP regulation of May 19, 2016

H Codes	H Phrases
H225	Highly flammable liquid and vapor.
H226	Flammable liquid and vapor.
H228	Flammable solid.
H272	May intensify fire; oxidizer.
H280	Contains gas under pressure; may explode if heated.
H281	Contains refrigerated gas; may cause cryogenic burns or injury.
H290	May be corrosive to metals.
H300	Fatal if swallowed.
H301	Toxic if swallowed.
H302	Harmful if swallowed.
H310	Fatal in contact with skin.
H312	Harmful in contact with skin.
H314	Causes severe skin burns and eye damage.
H315	Causes skin irritation.
H317	May cause an allergic skin reaction.
H318	Causes serious eye damage.
H319	Causes serious eye irritation.
H330	Fatal if inhaled.
H331	Toxic if inhaled.
H332	Harmful if inhaled.
H334	May cause allergy or asthma symptoms or breathing difficulties if inhaled.
H335	May cause respiratory irritation.
H336	May cause drowsiness or dizziness.
H340	May cause genetic defects.
H341	Suspected of causing genetic defects.
H350	May cause cancer.
H351	Suspected of causing cancer.

H Codes	H Phrases
H360	May damage fertility or the unborn child.
H361	Suspected of damaging fertility or the unborn child.
H362	May cause harm to breast-fed children.
H370	Causes damage to organs.
H371	May cause damage to organs.
H372	Causes damage to organs through prolonged or repeated exposure.
H373	May cause damage to organs through prolonged or repeated exposure.
H300 + H310 + H330	Fatal if swallowed, in contact with skin or if inhaled.
H301 + H331	Toxic if swallowed or if inhaled.
H301 + H311 + H331	Toxic if swallowed, in contact with skin or if inhaled.
H302 + H332	Harmful if swallowed or if inhaled.
H312 + H332	Harmful in contact with skin or if inhaled.
H302 + H312 + H332	Harmful if swallowed, in contact with skin or if inhaled.
H400	Very toxic to aquatic life.
H410	Very toxic to aquatic life with long lasting effects.
H411	Toxic to aquatic life with long lasting effects.
H412	Harmful to aquatic life with long lasting effects.
H413	May cause long lasting harmful effects to aquatic life.

P Codes	P Phrases
P101	If medical advice is needed, have product container or label at hand.
P102	Keep out of reach of children.
P103	Read label before use.
P201	Obtain special instructions before use.
P202	Do not handle until all safety precautions have been read and understood.
P210	Keep away from heat, hot surfaces, sparks, open flames and other ignition sources. No smoking.
P233	Keep container tightly closed.
P234	Keep only in original packaging.
P240	Ground and bond container and receiving equipment.

P Codes	P Phrases
P260	Do not breathe dust/fume/gas/mist/vapors/spray.
P261	Avoid breathing dust/fume/gas/mist/vapors/spray.
P262	Do not get in eyes, on skin, or on clothing.
P264	Wash … thoroughly after handling.
P270	Do not eat, drink or smoke when using this product.
P272	Contaminated work clothing should not be allowed out of the workplace.
P273	Avoid release to the environment.
P280	Wear protective gloves/protective clothing/eye protection/face protection.
P282	Wear cold insulating gloves and either face shield or eye protection.
P284	[In case of inadequate ventilation] wear respiratory protection.
P305	IF IN EYES:
P308	IF exposed or concerned:
P310	Immediately call a POISON CENTER/doctor/…
P311	Call a POISON CENTER/doctor/….
P312	Call a POISON CENTER/doctor/… if you feel unwell.
P314	Get medical advice/attention if you feel unwell.
P315	Get immediate medical advice/attention.
P321	Specific treatment (see … on this label).
P330	Rinse mouth.
P338	Remove contact lenses, if present and easy to do. Continue rinsing.
P351	Rinse cautiously with water for several minutes.
P390	Absorb spillage to prevent material damage.
P391	Collect spillage.
P301+P310	IF SWALLOWED: Immediately call a POISON CENTER/doctor/….
P301+P312	IF SWALLOWED: Call a POISON CENTER/doctor/… if you feel unwell.
P302+P352	IF ON SKIN: Wash with plenty of water/…
P303+P361+P353	IF ON SKIN (or hair): Take off immediately all contaminated clothing. Rinse skin with water [or shower].
P304+P340	IF INHALED: Remove person to fresh air and keep comfortable for breathing.

P Codes	P Phrases
P305+P351+P338	IF IN EYES: Rinse cautiously with water for several minutes. Remove contact lenses, if present and easy to do. Continue rinsing.
P308+P313	IF exposed or concerned: Get medical advice/attention.
P332+P313	If skin irritation occurs: Get medical advice/attention.
P333+P313	If skin irritation or rash occurs: Get medical advice/attention.
P336+P315	Thaw frosted parts with lukewarm water. Do not rub affected area. Get immediate medical advice/attention.
P337+P313	If eye irritation persists: Get medical advice/attention.
P342+P311	If experiencing respiratory symptoms: Call a POISON CENTER/doctor/…
P362+P364	Take off contaminated clothing and wash it before reuse.
P370+P378	In case of fire: Use … to extinguish.
P403	Store in a well-ventilated place.
P405	Store locked up.
P403+P233	Store in a well-ventilated place. Keep container tightly closed.
P403+P235	Store in a well-ventilated place. Keep cool.
P410+P403	Protect from sunlight. Store in a well-ventilated place.
P501	Dispose of contents/container to …

10 Acknowledgement

I want to thank Elke Oetjen sincerely for her supervision and support during the last years. Without her great thoughts and ideas, her constructive criticism, her guidance, and her motivation, this thesis would not be as it is today. I am grateful she always had an open door and ear for my ideas and questions and I enjoyed the interesting discussions we had. I thank her not only for giving me the opportunity to attend various conferences and to share my research, but also for accompanying and supporting me. Also, I would like to thank her for providing weekly enzymes for keeping me healthy.

I want to thank Sabine Schröder for introducing me to the research laboratory work. It was always fun learning techniques from her and I appreciate the great working atmosphere she provided. The work for this thesis would have been more challenging without this “good soul” of the lab. Sabine also always had an open ear and provided solutions for work as well as life problems. Furthermore, thanks to her never ending candy supply, her cooking and baking skills, and her relaxed attitude, I never had to worry about losing weight due to stress. I want to thank Jorge Duque Escobar for making the last years at work fun and exciting. It was great and rewarding sharing a lab and attending conferences together with him. I would like to thank him for the constructive criticism and the time he invested in reading and correcting several of my abstracts and posters. Anna Gundler and Kyra Köster were two great additions to our small group. With their fun and joyful attitudes they helped me to stay in a good mood especially while writing my thesis. I want to thank them both for the effort of proof reading my work.

I want to thank Prof. Böger for giving me the opportunity to work on my PhD thesis at the Institute of Clinical Pharmacology and Toxicology.

Special thanks to my colleagues at the Institute of Clinical Pharmacology and Toxicology and the Institute of Experimental Pharmacology and Toxicology for creating such a wonderful research environment, for supporting my work, teaching me new techniques, and for never making it hard for me to go to work.

I want to thank my parents for supporting me and for pushing me to become what I am today. I especially want to thank Johannes Büttner for helping me in any way he could including the challenging task of proof reading my thesis.

Last but not least I am very grateful for the financial support of the German Center for Cardiovascular Research (DZHK) which financed part of my work for this thesis.

11 Declaration

I hereby declare that this dissertation submitted to the University of Hamburg entitled

The role of the transcription factor CRTC1 in the development of cardiac hypertrophy in mice

is my own original research work. It has been conducted under the supervision of Prof. Elke Oetjen at the Institute of Clinical Pharmacology and Toxicology, University Medical Center Hamburg-Eppendorf. All sources of information as well as the results obtained in collaboration with other investigators are indicated. This written version corresponds to the version on the electronic data storage device. The dissertation has not been submitted for any degree at any other university.

Hamburg, December 20th, 2016

(Karoline Morhenn)

Hiermit erkläre ich an Eides statt, die vorliegende, an der Universität Hamburg eingereichte Dissertation mit dem Titel

The role of the transcription factor CRTC1 in the development of cardiac hypertrophy in mice

selbst verfasst und keine anderen als die angegebenen Hilfsmittel benutzt zu haben. Die Dissertation wurde unter der Anleitung von Prof. Elke Oetjen am Institut für Klinische Pharmakologie und Toxikologie des Universitätsklinikums Hamburg-Eppendorf verfasst. Die eingereichte schriftliche Fassung entspricht der auf dem elektronischen Speichermedium. Ich versichere, dass diese Dissertation nicht in einem früheren Promotionsverfahren eingereicht wurde.

Hamburg, den 20. Dezember 2016

(Karoline Morhenn)